TECHNISCHE UNIVERSITÄT MÜNCHEN

Lehrstuhl für Analytische Lebensmittelchemie

Comprehensive Characterization of Dissolved Organic Matter by Using Chemical Fractionation and High Resolution Organic Structural Spectroscopy

Yan Li

Vollständiger Abdruck der von der Fakultät Wissenschaftszentrum Weihenstephan für Ernährung, Landnutzung und Umwelt der Technischen Universität München zur Erlangung des akademischen Grades eines

Doktors der Naturwissenschaften

genehmigte Dissertation.

Vorsitzender: Prof. Dr. Jürgen Geist

Prüfer der Dissertation: 1. apl. Prof. Dr. Philippe Schmitt-Kopplin

2. Prof. Dr. Michael Rychlik

3. Prof. Dr. Boris P. Koch

(Hochschule Bremerhaven)

Die Dissertation wurde am 15.02.2017 bei der Technischen Universität München eingereicht und durch die Fakultät Wissenschaftszentrum Weihenstephan am 29.05.2017 angenommen.

For my parents

For Dr. Ayer Yediler

Acknowledgements

Summary

Dissolved organic matter (DOM) is an essential participant in the global carbon cycle of all terrestrial ecosystems. However, its molecular compositions and structures remain largely ill-defined even today due to extreme molecular heterogeneity and polydispersity. This thesis focused on improving solid phase extraction (SPE) and SPE-based fractionation of freshwater and marine DOM. The obtained DOM fractions were extensively characterized by optical (UV and fluorescence) and NMR spectroscopy as well as by ultrahigh resolution FT-ICR mass spectrometry.

Suwannee River (SR) water was used to study the effects of critical SPE variables such as loading mass, concentration, flow rate and up-scaling on the extraction selectivity of the SPE sorbents. High-field NMR and FT-ICR mass spectra of eluates, permeates and wash fluids served to optimize DOM retention which reached 89% of DOC (dissolved organic carbon) at a DOM/sorbent ratio of 1:800.

A polarity-based stepwise SPE procedure with separate collection of aliquots of methanolic eluates produced molecularly distinct DOM fractions different from LC-based fractionation. Reduction of sample complexity improved spectral resolution, and analogous clustering according to fractions was obtained for fluorescence, NMR and mass spectra.

The molecular selectivity and leaching behavior of 24 SPE sorbents with SR and North Sea (NS) water under conditions of pH=2 sorption and methanolic elution produced higher DOC recovery in case of SR DOM. Analogous sorption mechanisms operated for both DOM materials and the molecular distinction reflected intrinsic properties of SR and NS DOM. The widely used HLB sorbent was found to leach.

From here, a phase-optimized solid phase extraction (POP-SPE) method was developed for SR DOM isolation which jointly used several complementary SPE cartridges in succession. POP SPE produced desirable overall DOM recovery and molecularly diverse fractions with superior spectral resolution.

Zusammenfassung

Gelöstes organisches Material (dissolved organic matter, DOM) ist ein wesentlicher Teilnehmer des globalen Kohlenstoffkreislaufes in allen terrestrischen Ökosystemen. Allerdings bleiben dessen molekulare Zusammensetzung und chemische Struktur aufgrund der extremen molekularen Heterogenität und Polydispersität bis heute weitgehend ungeklärt. Diese Arbeit konzentrierte sich auf die Verbesserung der Festphasenextraktion (SPE) und die SPE-basierte Fraktionierung von Süß- und Seewasser DOM. Die erhaltenen DOM-Fraktionen wurden durch optische (UV- und Fluoreszenz-) und NMR-Spektroskopie sowie durch ultrahochauflösende FT-ICR-Massenspektrometrie umfassend charakterisiert.

Suwannee River (SR) Wasser wurde verwendet, um die Auswirkungen von kritischen SPE-Variablen wie Beladung, Konzentration, Durchfluss und Aufwärtsskalierung auf die Extraktionsselektivität des SPE-Sorbens zu untersuchen. Hochfeld-NMR- und FT-ICR-Massenspektren von Eluaten, Permeaten und Waschflüssigkeiten dienten zur Optimierung der DOM-Retention, die 89% des DOC (gelöster organischer Kohlenstoff) bei einem DOM / Sorbentverhältnis von 1:800 erreichte.

Ein polaritätsbasiertes schrittweises SPE-Verfahren mit separater Sammlung von Aliquots an methanolischem Eluat erzeugte molekular unterschiedliche DOM-Fraktionen, die sich von einer Fraktionierung auf LC-Basis unterscheiden. Die Verminderung der Probenkomplexität verbesserte die spektrale Auflösung und es wurde ein analoges Clustering nach Fraktionen für Fluoreszenz-, NMR- und Massenspektren erhalten.

Die molekulare Selektivität und die Stabilität von 24 SPE-Sorbentien mit SR und Nordsee (NS) Wasser unter Bedingungen von Sorption bei pH = 2 und methanolischer Elution ergab eine höhere DOC-Ausbeute im Falle von SR DOM, was bei gleichartigem Trennmechanismus die Bedeutung der intrinsischen Eigenschaften von DOM widerspiegelt. Das weit verbreitete HLB-Sorbens ist unter diesen Trennbedingungen nicht stabil.

Ausgehend hiervon wurde für die SR-DOM-Isolation eine phasenoptimierte Festphasenextraktion (POP SPE) entwickelt, die mehrere hintereinandergeschaltete komplementäre SPE-Kartuschen verwendete. POP SPE produzierte eine sehr gute Gesamt-DOM-Rückgewinnung; die isolierten, molekular verschiedenen Fraktionen zeigten durchwegs verbesserte spektrale Auflösung bezogen auf das unfraktionierte Ausgangsmaterial.

Publications

1. <u>Yan Li</u>, Mourad Harir, Marianna Lucio, Basem Kanawati, Kirill Smirnov, Ruth Flerus, Boris P. Koch, Philippe Schmitt-Kopplin, Norbert Hertkorn **(2016)**. Proposed guidelines for solid phase extraction of Suwannee River dissolved organic matter. *Analytical Chemistry* (88), 6680-6688.

2. <u>Yan Li</u>, Mourad Harir, Marianna Lucio, Michael Gonsior, Boris P. Koch, Philippe Schmitt-Kopplin, Norbert Hertkorn **(2016)**. Comprehensive structure-selective characterization of dissolved organic matter by reducing molecular complexity and increasing analytical dimensions. *Water Research* (106), 477-487.

3. Chloé Roullier-Gall, Daniel Hemmler, Michael Gonsior, <u>Yan Li</u>, Maria Nikolantonaki, Alissa Aron, Christian Coelho, Philippe Schmitt-Kopplin, Regis Gougeon **(2017)**. Sulfites and the wine sulfur metabolome. *Food Chemistry* (237), 106-113.

4. <u>Yan Li</u>, Mourad Harir, Jenny Uhl, Basem Kanawati, Marianna Lucio, Kirill Smirnov, Boris P. Koch, Philippe Schmitt-Kopplin, Norbert Hertkorn **(2017)**. How representative are dissolved organic matter (DOM) extracts? A comprehensive study of sorbent selectivity for DOM isolation. *Water Research* (116), 316-323.

5. <u>Yan Li</u>, Mourad Harir, Basem Kanawati, Michael Gonsior, Boris P. Koch, Philippe Schmitt-Kopplin, Norbert Hertkorn **(2017)**. Insights into dissolved organic matter compositions and structures by phase-optimized solid phase extraction. *Analytical Chemistry*. To be submitted.

Contents

List of figures

List of tables

List of abbreviations

AI: aromaticity index

APCI: atmospheric pressure chemical ionization

APPI: atmospheric pressure photoionization

CDOM: chromophoric dissolved organic matter

CE: capillary electrophoresis

CI: chemical ionization

COSY: correlation spectroscopy

CRAM: carboxylic-rich alicyclic molecules

DBE: double bond equivalent

DEPT: distortionless enhancement by polarization transfer

DESI: desorption electrospray ionization

DOC: dissolved organic carbon

DOM: dissolved organic matter

EEM: excitation-emission matrix

EI: electron ionization

ESI: electrospray ionization

FT-ICR: Fourier transformation ion cyclotron resonance

GC: gas chromatography

HILIC: hydrophilic interaction liquid chromatography

HMBC: heteronuclear multiple bond correlation

HSQC: heteronuclear single quantum coherence

IC: ion chromatography

IHSS: International Humic Substances Society

IP: ion trap

JRES: J-resolved spectroscopy

LC: liquid chromatography

LDI: laser desorption/ionization

MALDI: matrix-assisted laser desorption/ionization

MS: mass spectrometry

NOM: natural organic matter

PARAFAC: parallel factor analysis

POP: phase-optimized

RO/ED: reverse osmosis / electrodialysis

SEC: size exclusion chromatography

SPE: solid phase extraction

STOCSY: statistical total correlation spectroscopy

TOCSY: total correlation spectroscopy

TOF: time of flight

UF: ultrafiltration

Chapter 1

General Introduction

1 General Introduction

1.1 Introduction to DOM

1.1.1 Definition of DOM

Natural organic matter (NOM) refers to organic materials in water, soil or sediment derived from the activities of plants and animals (other than humans) in the environment (Brezonik and Arnold, 2011). A fraction of NOM that passes through the filter (pore size: 0.1-1.0 μm, mostly 0.45 μm) is defined as dissolved organic matter (DOM), and the fraction that is retained on the filter is called particulate organic matter (POM) (Kördel et al. 1997, Mopper et al. 2007, Nebbioso and Piccolo 2013). The definition of DOM is quite operational, rather than according to its chemical structures, due to its molecular heterogeneity and polydispersity (Hertkorn et al. 2007). Moreover, DOM can not only be dissolved but also be colloidal.

1.1.2 Structures of DOM

DOM is a mixture of organic compounds with abiotic and biotic origin such as lignins, tannins, carboxylic-rich alicyclic molecules (CRAM), black carbon, carbohydrates, lipids, peptides to name a few. The general properties of these key classes of DOM constituents are listed in Table 1-1.

Lignins are the second most abundant terrestrial biopolymer, consisting ~ 30% of the organic carbon in the biosphere (Boerjan et al. 2003). Biologically, lignins bind cellulose, hemicellulose and pectin components, and facilitate water conduction for plant's vascular tissue. Chemically, lignins are cross-linked phenolic polymers, rendering them certain optical characteristics, for example, absorption of ultraviolet radiation and possessing fluorescent properties (Fichot et al. 2016). The compositions of lignins vary among plant species. Generally, they are hydrophobic as well as aromatic, and contain small amounts of incomplete or modified monolignols. They have become widely used biomarkers for terrestrial DOM in the ocean (Hernes and Benner 2003).

Besides lignins, tannins are the second most abundant group of plant phenolics (Melone et al. 2013a, b). These polyhydroxyphenols are the secondary metabolites of plants and display two main biological activities. Tannins bind proteins, basic compounds, pigments, large molecular weight compounds and metal ions and they possess pronounced antioxidative quality (Melone et al. 2013a, b). Tannins are typically divided into four chemical groups: hydrolysable tannins

(galloyl esters and derivatives), ellagitannins (esters of hexahydrodiphenic acid), catechin tannins and condensed tannins (oligomeric and polymeric proanthocyanidin) (Melone et al. 2013a, b). Generally, tannins are highly oxygenated, with the atomic O/C ratios regularly exceeding 0.67.

Carboxylic rich alicyclic molecules (CRAM) incorporate the major components of terrestrial and marine DOM (Hertkorn et al. 2006, Simpson et al. 2007), and are comprised of the carboxylated and fused alicyclic structures with a **C**OX: C**C**H ratio of 1:2 to 1:7 (Hertkorn et al. 2006). CRAM distribute in the compositional section with O/C ratios of ~0.3-0.6 and H/C ratios: ~0.7-1.6. CRAM originate from biomolecules with structural similarities to sterols and hopanoids, and actively involved in ecosystem processes such as complexation with metals, aggregation and formation of marine gels (Hertkorn et al. 2006).

Carbohydrates make up one of the most abundant DOM pools, e.g. with ~ 10-70% of OM in planktonic exudates (Engbrodt and Kattner 2005). In marine DOM, they account for up to 50% of the total components in surface water whereas less than 30% in deep water (Benner et al. 1992). Chemically, they are constituted of polyhydroxy aldehydes and ketones, usually with a hydrogen–oxygen atom ratio of 2:1, and cover the elemental section with H/C ratios of ~1.5-2.4 and O/C ratios of ~ 0.67-1.2. There are typically four chemical groups of carbohydrates: monosaccharides, disaccharides, oligosaccharides and polysaccharides. They serve diverse functions in DOM activities such as storage of energy, structural components, important component of coenzymes, backbone of the genetic molecule, formation of mucilaginous aggregates and so on. Furthermore, the proportions of certain neutral sugars, in particular glucose and the deoxysugars, can be used as indicator of the diagenetic state of the extracted DOM. For example, a low molar ratio (fucose + rhamnose) / (arabinose + xylose) in deep sea extractable DOM can imply a high contribution of material modified by microorganisms (Engbrodt and Kattner 2005, Hunag et al. 2003).

Lipids account for an appreciable portion of DOM pool as well as ~ 3-20% biogenic carbon. They consist of structurally heterogeneous groups of hydrophilic and hydrophobic small molecules such as fatty acids, glycerolipids, glycerophospholipids, sphingolipids, saccharolipids, polyketides, sterol lipids and prenol lipids. They play a significant role in the DOM pool like storing energy, signaling, and acting as structural components of cell membranes. Chemically, they are highly saturated and less oxygenated (H/C ratios: 1.5-2.0, O/C ratios: 0-0.3). In DOM studies, they have been widely employed as biomarkers for

terrigenous and planktonic POM/DOM in various aquatic and sedimentary environments (Bourguet et al. 2009, Mannino and Harvey 1999).

Amino acids, another significant contributor to the DOM pool, contain amide, amine and carboxyl functional groups, along with aliphatic side-chains. They actively participate in comprising proteins, neurotransmitter transport and biosynthesis. Moreover, they have been widely applied as molecular indicators for bioavailable DOM in marine and groundwater systems (Benner and Kaiser 2010).

Table 1-1 Characteristics of the main groups of compounds in DOM.

Name	Structure	Quantity	Origin	Function	Molecular information
Lignin	Cross-linked phenolic polymer	~ 30% of the organic carbon in the biosphere	Plants	Binding cellulose, hemicellulose and pectin component, and facilitates water conduction for plant's vascular tissue	Indicator for terrigenous/plant-derived DOM
Tannin	Hydrolysable tannin (galloyl esters & derivatives); ellagitannins (esters of hexahydrodiphenic acid); catechin tannin; condensed tannin (oligomeric and polymeric proanthocyanidin)	Second largest polyphenols (after lignin)	Plants	Binding proteins, basic compounds, pigments, large molecular weight compounds and metallic ions; antioxidant activities	Highly oxygenated; O/C ratio > 0.67, H/C ratio: ~0.6-1.4
CRAM	Carboxylic-rich alicyclic molecules, with structural similarities to sterols and hopanoids	Main component in terrestrial and marine DOM	Biomolecules	Constituting a strong ligand for metal binding, promote aggregation and marine gel formation thereby affecting the bioavailability of nutrients and trace metals.	Comprised of a complex mixture of carboxylated and fused alicyclic structures with a **C**OX: **C**CH ratio of 1:2 to 1:7; O/C ratio: ~0.3-0.6, H/C ratio: ~0.7-1.6
Carbohydrates	Polyhydroxy aldehydes and ketones; usually with a hydrogen–oxygen atom ratio of 2:1; four chemical groups: monosaccharides, disaccharides, oligosaccharides, and polysaccharides.	Abundant biopolymers, 10-70% of OM in plankton cells	Plants and microorganism	Storage of energy; structural components; important component of coenzymes; backbone of the genetic molecule; formation of mucilaginous aggregates	H/C ratio: 1.5-2.4, O/C ratio: ~ 0.67-1.2; neutral sugar composition (in particular glucose and the deoxysugars) is indicative of the diagenetic state of the extracted DOM, lowest molar ratio (fucose + rhamnose)/(arabinose + xylose) in deep sea extractable DOM, indicating a high contribution of material modified by microorganisms

Name	Structure	Quantity	Origin	Function	Molecular information
Lipids	Hydrophilic and hydrophobic small molecules, such as fatty acids, glycerolipids, glycerophospholipids, sphingolipids, saccharolipids, and polyketides; sterol lipids and prenol lipids	A small portion of DOM; 3-20% of biogenic carbon	Microorganism	Storing energy, signaling, and acting as structural components of cell membranes	Highly saturated & less oxygenated (H/C ratio: 1.5-2.0, O/C ratio: 0-0.3); biomarkers for terrigenous and planktonic POM/DOM in various aquatic and sedimentary environments
Amino acids	Containing amine and carboxyl functional groups, along with a side-chain	Small portion of DOM	Microorganism	Comprising proteins; neurotransmitter transport and biosynthesis	Molecular indicator for bioavailable DOM in marine and groundwater system; key source of nitrogen

1.1.3 DOM from different origin

The global carbon cycle distributes distinct DOM across ecosystems (Battin et al. 2009, Bianchi 2011). The concentrations and qualities of DOM from different origin play a significant role in the ecosystem in terms of DOM mobility, degradability and bioavailability (Hedges et al. 1997). The DOM origin commonly provides a rough estimation of its concentrations and consitituents, which the subsequent experiemal designs highly rely on. The general concentrations (average or the range) of DOM samples from different origin (Kördel et al. 1997) are shown in Fig. 1-1.
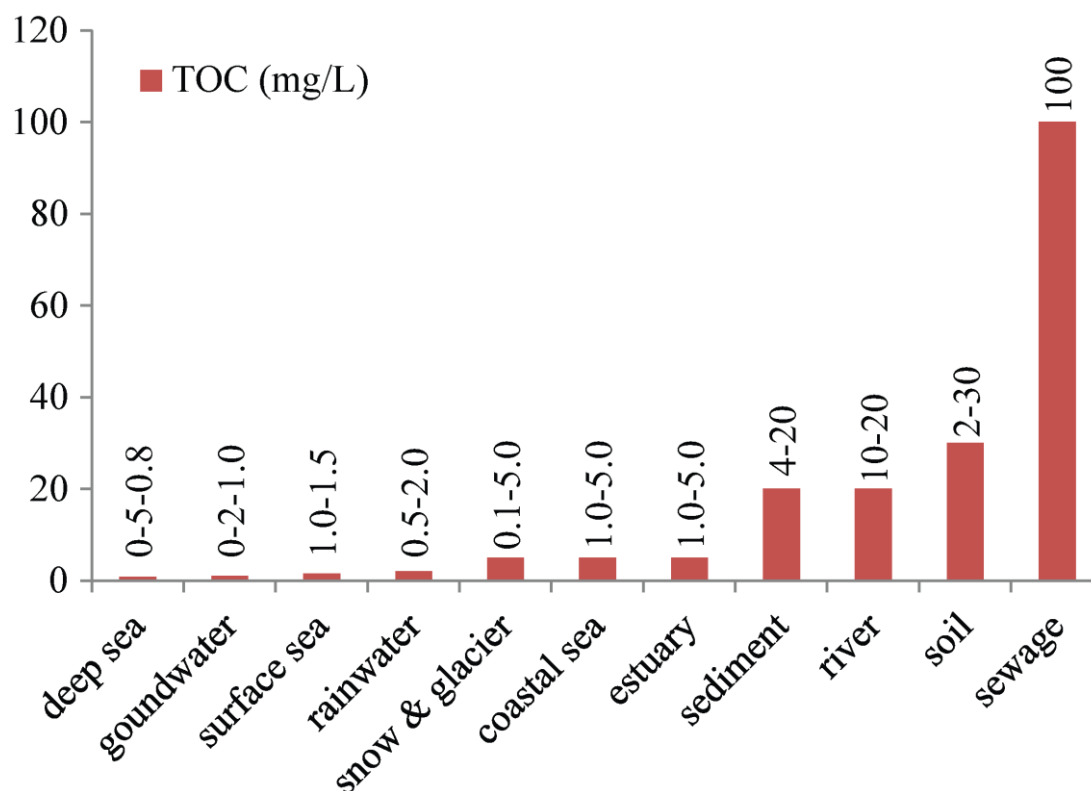
Fig. 1-1 Approximate concentrations of DOM in ecosystems, adapted from Kördel et al. 1997.

Generally, groups of compounds such as lignins, tannins, carbohydrates, amino acids, lipids and aromatics are constituents in DOM, but their quantities vary significantly in different DOM systems. For example, Nordic Lake DOM contained larger amounts of carbohydrates and amino acids than Suwannee River DOM (http://humicsubstances.org/sugar.html and http://humicsubstances.org/aminoacid.html). The detailed general molecular characteristics of different DOM samples are summarized in Table 1-2.

Table 1-2 Molecular characteristics of DOM from different origin.

DOM type	Abundant compounds	Key structural and molecular characteristics
Freshwater DOM	CRAM, aliphatics, lignin, amino acids, tannins	Aliphatic in nature, N-containing compounds, high aromaticity, relativelg high unsaturation
Marine DOM (surface)	Carbohydrate-related substructures, oxygenated aliphatics and acetate derivatives, CRAM, peptides, lipids	Fewer methyl esters, higher DBE than freshwater DOM, more S-containg compounds
Marine DOM (deep)	Carboxylic acids and ketones, C-based aliphatics, CRAM, black carbon	More molecularly diverse than surface marine DOM, black sulfur, larger molecular weight
Sedimentary DOM	Lignins, tannin, black carbon, peptides, amino acids, aliphatic compounds	Highly unsaturated compounds, N-containing compounds (S-containing compounds in early digenetic region), DBE: 8.40-8.95
Soil DOM	Lignins, black carbon, lipids, carbohydrates	O/C: 0.4 (0.28-0.47), H/C: 1.50 (1.30-1.74), DBE: 6.35 (3.89-7.85), enriched of N-, S-containing compounds, lowest unsaturation than other DOM
Groundwater DOM	Lignins, aromatics, amino acids, terpenoid	Smaller molecular weight, highly aliphatic, small fractions of bioavailble DOM and bacterial-derived DOM, deplete in oxygen-containing functional groups, 5% of aromatic carbon

1.1.3.1 Freshwater DOM

Frshwater DOM is formed as a product of autochthonous production/degradation (self-production of microorganism/flora/fauna, metabolism, and natural decay) and allochthonous input (leaching of plants and soils, and discharge by human beings) in rivers and lakes (Kördel et al. 1997). Approximately 0.4 Pg C/year of the terrestrial and freshwater DOM is transported into marine system via discharge (Hedges et al. 1997). Thus, these DOM are not only essential to the global carbon and other elements cycles, but also crucial to the biogeochemical balance of their specific ecosystem.

The main structural components in freshwater DOM consist of aliphatics (linear terpenoids), CRAM, carbohydrates, peptides, lipids and small amounts of aromatics (Sleighter and Hatcher 2008). Considerable variance is observed in structures among freshwater DOM of different origin such as rivers, estuaries, lakes, and mangroves, e.g. lignins, tannins, lipids and aromatics, especially those highly oxygenated tannins (O/C ratio: 0.67-1.0; H/C ratio: 0.6-0.8) are depleted in coastal DOM (Sleighter and Hatcher 2008).

Lakes are reported to be shaped by precipitation, inflow and outflow of tributories, water residence time and temperature, but its DOM commonly includes lipids, peptides, carbohydrates, lignins, tannins and N-, S-containing compounds (Kellerman et al. 2014, Kellerman et al. 2015, Goldberg et al. 2015, Zhang et al. 2014). The oxidized aromatic compounds are preferentially removed during organic matter degradation whereas rather saturated aliphatics and N-containing compounds more resistant to degradation are more likely to persist in aquatic systems (Kellerman et al. 2014, 2015). Moreover, certain N-containing components (proteinaceous materials) in relatively cold high-elevation lakes are found to be rather refractory with 100-200 year residence time and those autochthonous proteins can accumulate over a long time period. Seasonal shifts in the compositions and structures of lake DOM are also observed. For example, more proteins are produced in spring or summer time (Goldberg et al. 2015). A systematic study of DOM during and after cyanobacterial bloom (summer to fall) in Taihu lake demonstrated the loss of H**C**-O units (commonly carbohydrates) and aliphatic oxygenated groups and an increase in carbon bound methyl, methylene and methine carbon as well as the reduction in molecular diversity. The seasonal DOM transformation resulted in the smaller molecules, increased abundance of CHNO compounds, and rapid processing or vanishing of simple carbohydrates and amino acids type compounds in the metabolic pathways (Zhang et al. 2014).

DOM in wetlands with different sources is found to share many molecular features, such as analogous fluorescence properties, main structures of aliphatics, CRAM, carbohydrates, peptides and aromatics, and the common groups of lignins, tannins, lipids and N-containing compounds. Regardless of the similarity, each sample differs in compositions due to specific environmental drivers or specific biogeochemical processes (Hertkorn et al. 2016). Generally, the averaged elemental ratios (H/C ratio: 1.01-1.09, O/C ratio: 0.53-0.56) in wetland DOM shift to be more oxygenated and less saturated compared with lake DOM (H/C ratio: 1.08-1.16, O/C ratio: 0.42-0.43) (Koch et al. 2005).

1.1.3.2 Marine DOM

Marine DOM is one of the largest pools of the reduced carbon on earth with 694 Pg C (Hansell 2013, Moran et al. 2016). Most marine DOM has four main sources: the transportation by river and wind, production by the decay of dead organisms, excretion by algae/plants and excretion by marine animals (Kördel et al. 1997). Due to molecular diversity and the corresponding reactivity, marine DOM is classified into five fractions based on the radiocarbon dating lifetime. More detailed information is shown in Table 1-3 (Hansell 2013).

Table 1-3 General properties of five fractions in marine DOM, adapted from Hansell 2013 and Moran et al. 2016.

Fraction	Lifetime (year)	Presence	Quantity (Pg C)	Molecular information and structural groups
Labile DOM	~0.001	Surface, deep	<0.2	Monocarboxylic acids, dicarboxylic acids, glycerols, fatty acids, sulfonates, N-containing metabolites
Semi-labile	~1.5	Upper 1000m	6±2	Carbohydrates, amino acids, neutral sugars, amino sugars
Semi-refractory	~20	Upper 1000m	14±2	Carbohydrates, amino acids, neutral sugars, amino sugars
Refractory	~16,000	Everywhere	630±32	Small molecules (m/z: 200-800), CRAM, tannins
Ultra-refractory	~40,000	Everywhere	>12	CRAM, polycyclic aromatic compounds

Molecular insights into refractory marine DOM have become possible after correlation of the mass spectrometry-derived (MS-derived) molecular database of marine DOM with radiocarbon dating (Flerus et al. 2012, Lechtenfeld et al. 2014). The observed radiocarbon derived processing of marine DOM correlated negatively with higher molecular masses (m/z) and lower H/C ratios. Furthermore, this approach enabled modeling of average elemental

compositions of the slowest degrading fractions in the DOM pool. The molecular formulae of the most persistent compounds covered a narrow range: H/C ratio at 1.17±0.13, O/C ratio 0.52±0.10 as well as molecular weights at 360±28 and 497±51 m/z (Flerus et al. 2012, Lechtenfeld et al. 2014). Based on the previous results, molecular transformation of marine DOM by microorganisms was investigated for a relatively short (70 days) and a rather long (2 years) term (Koch et al. 2014). Using glucose as substrate, the molecular characteristics of DOM after short term microbial incubation were different from those of the refractory marine DOM, and those after long term incubation showed the similarity with this microbial-derived marine organic matter (Koch et al. 2014). In addition to the molecular information and the formation of refractory marine DOM, a rough quantification of refractory marine DOM together with the compositional relationships was also possible. Marine DOM was shown to be degraded faster with larger molecular size, and it was estimated that the production rates of the small, refractory marine DOM ranged at 0.11-0.14 Gt/year carbon and ~0.005 Gt/year for dissolved orgniac nitrogen in the deep ocean (Walker et al. 2016).

However, due to non-ambiguous distinction of structural groups among the marine DOM fractions as well as operation problems (Hansell 2013), the two terms of surface (<25 m) and deep (>2400 m) marine DOM are applied more widely in the studies. In general, the five fractions are present in both surface and deep marine DOM, but vary significantly in proportions. There are less than 25% of carbohydrates, amino acids, lipids and amino sugars in deep marine DOM whereas these compounds constitute high percentage (25-50%) in the surface marine DOM (Koch et al. 2005). More detailed properties of surface and deep marine DOM are shown in Table 1-4 (Hedges et al. 1997).

Table 1-4 Differences between surface and deep marine DOM, adapted from Hedge et al. 1997.

Sample	C/N ratio	$\Delta^{14}C$ (‰)	$\delta^{13}C$ (‰)	$\delta^{15}N$ (‰)
Surface	16.5±0.7	-263±23	-21.7±0.2	+7.9±0.8
Deep	18.6±0.6	-546±14	-21.7±0.3	+8.1±0.6

Detailed comparison of open ocean surface and deep marine DOM (the South Atlantic Ocean) by NMR spectroscopy and MS presented the structural differences occurred mainly in five groups (Hertkorn et al. 2013). First, oxygenated aliphatics declined from surface to deep, and

they declined for methine, methylene and methyl carbon. Second, fewer methyl esters were found in surface marine DOM than at the fluorescence maximum at 48 depth, probably as a result of direct exposure to sunlight. In addition, the carbon-based aliphatics, CRAM as well as other carboxylic acids and ketones increased from surface to deep. The molecular diversity of marine DOM and the average molecular weights slightly increased with depth. Certain rather aliphatic CHOS and CHNOS molecular series were exclusively observed in the surface DOM whereas the unsaturated and rather oxygenated CHO and CHNO series were enriched in the deep (Hertkorn et al. 2013). Aromatic CHOS molecules (black sulfur) were solely detected in abyssal marine DOM near the ocean floor at 5446m depth. Nevertheless, the surface and deep marine DOM still share more than 50% of common molecular formulae, and those shared molecular compositions covered in analogous sections of H/C and O/C ratios as computed for the refractory DOM (Hertkorn et al. 2013).

Along gradient from riverine to marine waters (from land to sea), the DOM was found to become more aliphatic and less oxygenated but a considerable proportion of common formulae remained (Sleighter and Hatcher 2008). Marine DOM was found to share ~1/3 of the formulae with terrestrial DOM, which might be attributed to the presence of refractory DOM or arise from isomers with different chemical structures at the same formulae (Koch et al. 2005, Sleighter and Hatcher 2008).

1.1.3.3 Groundwater DOM

Groundwater DOM has the important origin from surface plant litter and soils, and it serves as a carbon and energy source for heterotrophic metabolism and drives the bioremediation of many pollutants (Shen et al. 2014).

Lignin phenols, as biomarkers of plant-derived DOM, were relatively deplete in groundwater DOM with low concentrations, indicative of substantial removal of plant-derived compounds during transportation (Shen et al. 2014). Biotic transformation was observed in plant-derived DOM in groundwater system, and depletion of oxygen resulted in decrease of aromatic compounds and carbohydrates together with increase of aliphatics (Einsiedl et al. 2007). By using certain amino acids (e.g. glycine) as indicators of bioavailable DOM and specific amino acids (e.g. D-enantiomers) as biomarkers of bacterial-derived DOM, groundwater DOM was reported to contain a small bioavailable fraction and a small bacterial-derived fraction (Shen et al. 2014). Compared to surface DOM, it exhibited lower molecular weights. After linking

the hydrology with composition and bioactivity of groundwater DOM, a conceptual regional chromatography model was applied to groundwater systems demonstrating a selective removal and differential retention of DOM during transport from surface to ground waters. The DOM sorption processes were rather complex and were highly related to the molecular properties such as molecular size, hydrophobicity, charge and so on. For instance, large and hydrophobic molecules like lignins were retained longer through soil columns whereas the small and hydrophilic molecules such as amino acids and carbohydrates eluted faster to the groundwater (Shen et al. 2014).

1.1.3.4 Sediment DOM

Sediment DOM generally refers to pore water organic matter and water extractable organic matter, and is a heterogeneous mixture of organic compounds with a wide range of activities and molecular size (Chen and Hur 2015). The coastal and continental margin sediments are reported to have an integrated dissolved organic carbon flux of 0.19 Gt C/year, which is comparable to the assumed carbon burial rate of 0.16 Gt C/year (Chen and Hur 2015, Schmidt et al. 2009, Schmidt et al. 2011).

DOC values of inland sediment DOM were found to be higher than those from the coastal areas, whereas no significant differences were observed in aromaticity and apparent molecular weights (Chen and Hur 2015). According to fluorescence index, inland sediment DOM indicated mixed sources whereas the costal sediment DOM showed characteristics of a marine end-member. Compared to riverine DOM, coastal pore water DOM was reported to exhibit a decreased molecular diversity, a higher aliphacity with a mean O/C ratio of 0.5 and mean H/C ratio of 1.26, and lower unstauration with DBE of 8.40-8.95. A higher abundance of N-containing compounds derived from terrestrial sources was also observed and was subject to considerable microbial activity (Schmidt et al. 2009, Schmidt et al. 2011). Furthermore, after implantation of mathematical models, N-containing compounds in sediment DOM could be deduced to be produced by certain transformations such as hydrolysis, deamination, oxidation and hydration, and methylation and dehydration. Interestingly, S-containing compounds (mainly containing one sulfur atom) were found in early digenetic process although in different sediment ecosystem (Schmidt et al. 2009, Schmidt et al. 2011, Seidel et al. 2014).

1.1.3.5 Soil DOM

Soil DOM refers to DOM found in soil solution, and it represents the most labile fraction of soil organic matter. It is dominated by lignins, and rich in amino acids, lipids, carbohydrates and black carbon. In general, soil DOM showed average O/C ratios of 0.28-0.47 (mean 0.40), average H/C ratios of 1.30-1.74 (mean 1.50) and molecular weights of 380-417 Da (mean 395 Da) (Ohno et al. 2010). The DBE values were in the range of 3.89-7.85 with the mean of 6.35, which were lower than those of sediment, marine and freshwater DOM. Compared with plant extracts, soil DOM was marked by increase in lignins and carbohydrates and decrease in amino acids, which might be attributed to microbial uptake of N-containing organic matter and release of water soluble lignins and carbohydrates during decomposing plant biochemical compounds (Ohno et al. 2010).

1.1.4 Functions of DOM

DOM plays a significant role in ecosystem with diverse functions, namely, interaction with elements and bacterial metabolism, being electron acceptors and involvement in photodegradation.

1.1.4.1 Interactions with elements

a. Interations with sulfur. Marine dissolved organic sulfur (DOS) consititues a large sulfur servior and is actively involved in marine biogeochemical cycles (Ksionzek et al. 2016). During photochemical transformation of marine DOM, many sulfur-containing compounds can be formed, for instance, dimethyl sulfide, dimethylsulfoniopropionate, carbonyl sulfide, dimethyl sulfoxide, dimethyl disulfide, carbon disulfide, methane thiol, cysteine, glutathione, phytochelatins and methionine (Mopper and Kieber 2002).

b. Interactions with chloride. Chloride is the most abundant ion in marine waters. Transformations of marine chloride to non-volatile organochlorine through biological and abiotic pathways were observed. The organochlorine was revealed to present primarily in concentrated aliphatic forms consistent with lipid chlorination, along with a more diffuse aromatic fraction (Leri et al. 2015). In addition, organochlorine was also observed during chlorination along the water treatment, and the organochlorine mainly contained one or two chloride atoms (Zhang et al. 2012).

c. Interactions with iron species. Iron is an important micronutrient for plants and mircroorganisms in the ecosystem, and is found to be strongly associated with DOM. The ferric iron could be stabilized by DOM as small iron oxide colloids (able to pass a 0.45 µm dialysis membrane), which affects its bioavailability (Peiffer et al. 1999). In addition, positive correlation of DOM and iron concentration was observed, and the coupling of DOM with iron fluxes could imply that DOM exports partially was caused by increasing activities in iron reduction (Knorr 2013).

1.1.4.2 Interactions with bacterial metabolism

a. DOM production from microbial degradation. Microorganisms metabolized terrigenous DOM in brown-water streams at the cost of low carbon use efficiency and shifted its composition (from fluorescence and absorbance) towards less aromatic and low molecular weight compounds (Fasching et al. 2014). In addition, microbial DOM generated from exometabolites by marine bacteria exhibited a large proportion of refractory molecules (CRAM), and showed a dominant role for bacteria in shaping the refractory nature of marine DOM (Lechtenfeld et al. 2015).

b. Modification by bacterial metabolism. Phosphate limitation greatly influenced both the amount and the composition of the secreted DOM molecules by heterotrophic bacteria. Under phosphate limitation, the composition of the exo-metabolome changed during bacterial growth, showing an increase in highly unsaturated, phenolic and polyphenolic compounds, while under phosphate surplus conditions the secreted DOM molecules were mainly peptides and highly unsaturated compounds. (Romano et al. 2014).

1.1.4.3 Involvement in photodegradation

a. DOM photoproducts. DOM photoproducts were classified into four groups: low molecular-weight carbonyl compounds with MW<200; carbon gases; unidentified bleached organic matter and N-, P- containing compounds (Moran and Zepp 1997). A bacterial assay experiment showed that the photoproducts could simulate biomass production or activities by 1.5- to 6- fold. DOM photoproducts were found to meet large proportions of the bacterial carbon and nitrogen demands (Moran and Zepp 1997). In addition, polyols were found during photo-transformation of DOM in oligotrophic surface ocean, and they accounted for 2% of total molecular signatures in ^{1}H NMR spectra (Gonsior et al. 2014).

b. Molecular alteration of DOM compounds. Selective photodegradation of DOM molecules was observed with application of multiple analytical approaches. Under oxygen atmosphere, structures of lignic and lipidic origin were most photolabile in comparison with carbohydrates, alkylbenzenes, or N-containing structures that accumulated in the system. Under nitrogen atmosphere the acids remained fairly stable. Under UV/Vis irradiation indirect photolysis were suggested to be the major pathway in DOM degradation (Schmitt-Kopplin et al. 1998). Similar results were also found by other authors (Stubbins et al. 2010). Aromatic compounds were found to be most photoactive, with 90% being lost upon irradiation. The photoproduced DOM pool was enriched of aliphatic compounds and a small number of aromatics (including condensed aromatics). The refractory condensed aromatics were removed significantly whereas CRAM actually shifted towards more refractory regions instead of getting removed (Stubbins et al. 2010).

1.2 Isolation techniques of DOM

DOM isolation is an essential and error-prone step, which has a significant effect on both overall recovery and the molecular composition and structure. Different isolation methods have been applied for DOM, and those methods normally are based on the solubility, charge, molecular weight, polarity and so on (Minor et al. 2014, Perminova et al. 2009, Sandron et al. 2015). More recently, studies have shown that selective isolation of DOM provides more detailed information of the structures than studying the complex bulk materials (Koch et al. 2008, Woods et al. 2012). A general summary of DOM isolation methods is listed in Table 1-5 and more detailed decriptions can be found in Chapter 3.

Table 1-5 Summary of DOM isolation techniques.

Technique	Mechanism	Advantage	Drawbacks	DOC recovery	Specific DOM characteristics
UF	Separation through a semipermeable membrane by force	Large volumes and fast speed; least chemical alteration	Highly dependent on experimental procedures and equipment; membrane fouling; further desalting for marine DOM needed	Marine samples: 8-55%; freshwaters: up to 80%	Only high molecular weight fraction of DOM retained; reduction in the recovery of high molecular weight compounds at increased salinity
RO/ED	RO is similar to UF, but uses the applied force to overcome osmotic pressure. ED removes salts through ion-exchange membranes under the influence of an applied electric potential difference	Large volumes and fast speed; high DOC recovery	High time and cost requirement; harsh chemical conditions	Oceanic water: 70-75%; freshwater: ~90%	For marine DOM, a relatively lower proportion of carbohydrate carbon and a relatively greater proportion of alkyl carbon is reocvered; C/N ratios are most representative of authentic water
SPE	Based on the solute partition coefficient between sorbent and aqueous phases	Facile and flexible; low cost	Relatively harsh chemical condition; side reactions	Marine DOM: ≤65%; freshwater DOM: ~40-90%	Highly sorbent selective
RP LC	Based on differential partitioning between the mobile and stationary phases	Specific fractionation according to polarity of analytes and selectivity of columns	Low volumes	Not measured	O/C ratios abd double bond equivalents (DBE) decreased whereas H/C ratios increased with separation.
CE	According to ionic mobility and/or partitioning into an alternative phase via non-covalent interactions or gradients in conductivity and pH	Low injection volumes, reduced complexity, improved spectra resolution	Artefacts from separation conditions and instrumental constrains	Not measured	Larger molecules deteriorating into smaller components
SEC	According to hydrodynamic molecular size	Reduced complexity, improved spectra resolution	Not particularly accurate; potential artefact; lack of standard calibration of analytes	Not measured	Aquatic DOM with molecular weight 0.55-7.13 kDa

Technique	Mechanism	Advantage	Drawbacks	DOC recovery	Specific DOM characteristics
HILIC	Normal-phase HPLC with a polar stationary phase but utilizes partial aqueous mobile phase	Improved resolution; more detailed structural information revealed	Large consumption of organic solvents; interactions of DOM with sorbents	Not measured	Good for polar retention; selective
IC	Based on the affinity of ions and polar molecules to the ion exchanger	Quantification of certain groups of compounds	Strict sample pretreatment; highly selective	Limited recovery	Better for polar compounds such as lipids and carbohydrates in DOM
GC	Based on interaction of gaseous compounds with the column	Quantification and identification of certain groups of compounds; possible access to library if coupled with certain mass analyzers	Proper sample pretreatment and operation conditions required; selective towards small volatile molecules; chemical derivatization is required	Not measured	Volatile compounds and easily derivatised into volatile species; lignins, PAHs
Passive sampling	Membrane with anion exchange resin	A range of temporal and spatial experiment and "average" signals of sample	Impossible for short time period sampling	72-89%	Larger proportions of aromatics and extraction of carbohydrates
RO/ED with SPE	Combination of RO/ED and SPE process	Increased DOC recovery	Higher cost and more labor intensive	Up to 98% for marine DOM	More representative nature of DOM

1.3 Characterization approaches of DOM

The chemically-diverse DOM samples require multi-level complementary analytical approaches for their comprehensive characterization; on the other hand, complementary analysis of DOM samples generates large data sets, and their joint assessment enables in-depth elucidation of DOM characteristics (Hertkorn et al. 2007). Common DOM characterization approaches are listed in Table 1-6. Up to date, comprehensive DOM characterization has enabled remarkable distinctions of e.g. freshwater, marine, atmospheric and extraterrestrial DOM with measurement of FT-ICR MS and NMR spectroscopy ((Hertkorn et al. 2013, 2016, Schmitt-Kopplin et al. 2010a, b), and as well merged the DOM molecular features with interconnected optical properties with structural spectroscopy (Kellerman et al. 2015, Hertkorn et al. 2016).

Table 1-6 Comprehensive characterization approaches of DOM.

DOM isolation / characterization method	General capability	Specific utility in DOM characterization	Drawbacks
Elemental analysis	abundance of elemental composition; elemental ratios	Fundamental bulk parameters; evaluation of MS-derived results	Not in-depth
Isotope analysis	Isotope abundance	Tracing the DOM and apparent ages (^{14}C)	No in-depth resolution of molecular diversity
Optical spectroscopy	Optical signals	Quick, sensitive & powerful tool for rough estimate of origin, content and chemical environment	Highly selective towards sp^2 carbon chemical environment
FT-ICR mass spectrometry	Detection of molecular formulas	Sensitive; elucidation of CHO, CHOS, CHNO and CHNOS molecular formulas based on excellent mass accuracy and mass resolution	Selective in ionization
NMR spectroscopy	In depth structural analysis of NOM	Multinuclear and multidimensional NMR spectroscopy of NOM fractions defines close-range atomic orders of DOM molecules	Insensitive
Mathematical data evaluation: statistical total correction spectroscopy (STOCSY)	Correlations within and across methods	enables testable cross correlation between NMR, MS, and separation techniques	Indirect correlations in polydisperse DOM; individual methods see different aspects of molecular structures

1.4 Objectives of the thesis

DOM occurs in all ecosystems and carries biological and biogeochemical signatures (Battin 2009), but its decisive role in the global carbon and other element cycles is still not well understood due to its polydispersity and molecular heterogenuiety (Hertkorn et al. 2007).

At present, DOM isolation by means of SPE represents a fair compromise between field work capability and acceptable yield in the range of 40-60 % of DOC recovery, depending on DOM source (Dittmar et al. 2008). Meanwhile the low-resolutin methods are not robust enough to resovle DOM bulk parameters (Ritchie and Perdue 2003).

The remarkably different molecular signatures, however, can be deduced by high resolution separation and high-performance organic structural spectroscopy (Gasper et al. 2010, Hertkorn et al. 2007, Woods et al. 2011). High resolution separation has provided complexity-reduced DOM fractions, providing more improved resolution than bulk materials. Modern high resolution organic structural spectroscopy, especially FT-ICR MS and NMR, has demonstrated the outstanding molecular diversity of DOM obtained from various sources such as freshwater, marine and atmosphere (Einsiedl et al. 2007, Hertkorn et al. 2006, Schmitt-Kopplin et al. 2010).

The main objective of the thesis is to develop a comprehensive approach of DOM characterization using chromatographic and spectroscopic techniques with the following specific goals (workflow of this thesis shown in Fig. 1-2):

1. Improving DOM isolation techniques to extract fractions more presentative of original samples (high DOC recovery as well as considerable molecular information).

2. In-depth isolation of DOM with SPE and to be followed by spectroscopic analysis of the structure-selective fractions.

3. In-depth characterization of DOM fractions by applying complementary instrumental analysis such as high resolution FT-ICR mass spectrometry, optical and NMR spectroscopy.

4. Statistical total correlation spectroscopy (STOCSY) for joint mathematical classification of mass, optical and NMR spectra and bidirectional statistical correlation, statistical correlation spectroscopy within and across methods.
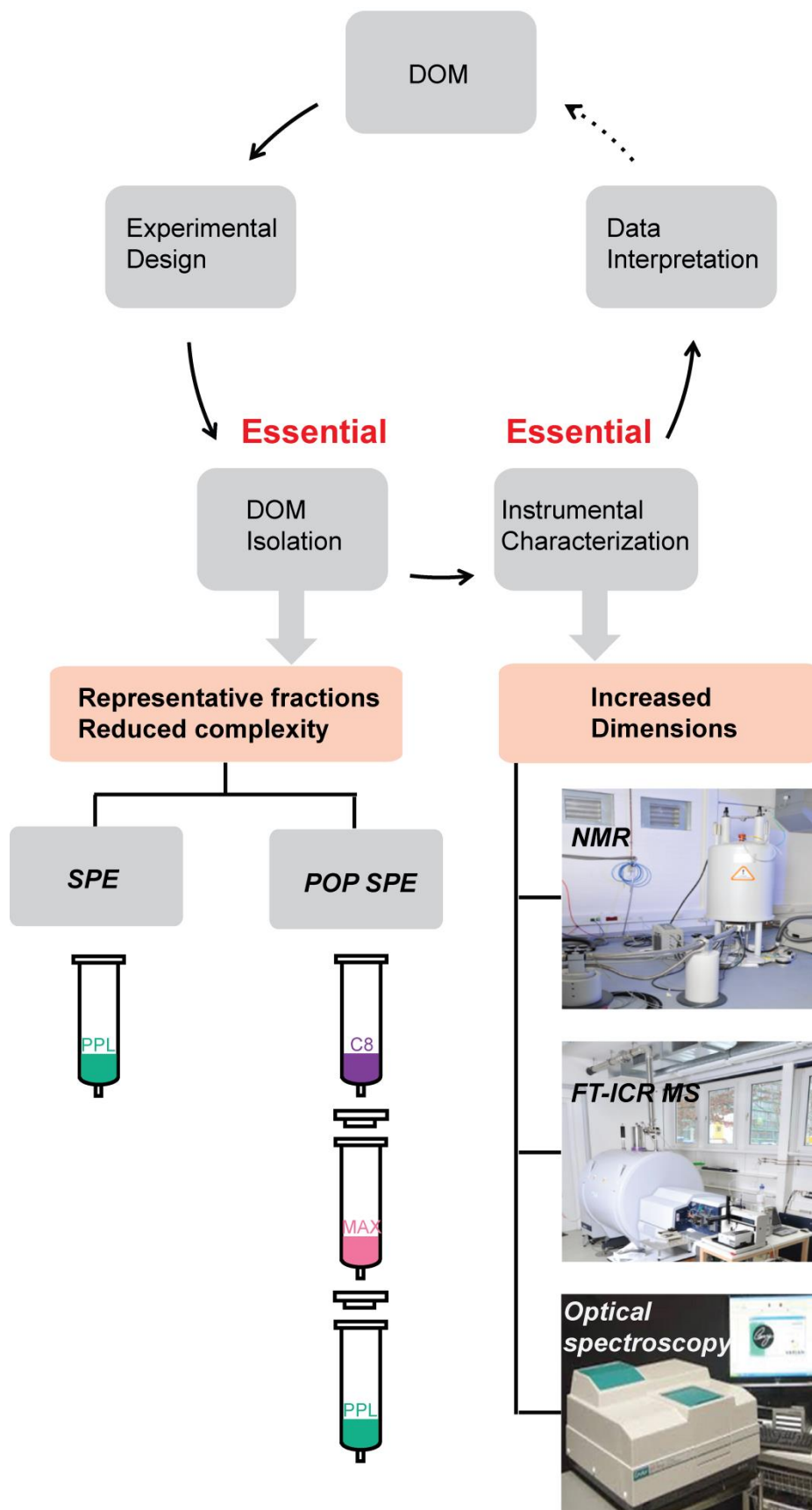
Fig. 1-2 Workflow of this thesis.

1.5 References

Battin, T.J., Luyssaert, S., Kaplan, L.A., Aufdenkampe, A.K., Richter, A. and Tranvik, L.J. (2009) The boundless carbon cycle. Nat Geosci 2(9), 598-600.

Benner, R. and Kaiser, K. (2010) Biological and photochemical transformations of amino acids and lignin phenols in riverine dissolved organic matter. Biogeochemistry 102(1-3), 209-222.

Bianchi, T.S. (2011) The role of terrestrially derived organic carbon in the coastal ocean: a changing paradigm and the priming effect. Proc Natl Acad Sci U S A 108(49), 19473-19481.

Boerjan, W., Ralph, J. and Baucher, M. (2003) Lignin biosynthesis. Annu Rev Plant Biol 54, 519-546.

Benner, R., Pakulski, J.D., McCarthy, M., Hedges, J.I. and Hatcher, P.G.. (1992) Bulk chemical characteristics of dissolved organic matter in the ocean. Science 255, 1561–1564.

Bourguet, N., Gouty, M., Ghiglione, J.-P., Pujo-Pay, M., Mével, G., Momzikoff, A., Mousseau, L., Guigue, C., Garcia, N., Raimbault, P., Pete, R., Oriol, L. and Lefèvre, D. (2009) Lipid biomarkers and bacterial lipase activities as indicators of organic matter and bacterial dynamics in contrasted regimes at the DYFAMED site, NW Mediterranean. Deep-Sea Res PT II 56, 1454-1469.

Brezonik, P.L. and Arnold, W.A. (2011) Water chemistry: an introduction to the chemistry of natural and engineered aquatic systems. Oxford University Press. ISBN: 9780199730728.

Chen, M. and Hur, J. (2015) Pre-treatments, characteristics, and biogeochemical dynamics of dissolved organic matter in sediments: A review. Water Res 79, 10-25.

Dittmar, T., Koch, B., Hertkorn, N. and Kattner, G. (2008) A simple and efficient method for the solid-phase extraction of dissolved organic matter (SPE-DOM) from seawater. Limnol and Oceanogr-Meth 6(6), 230-235.

Einsiedl, F., Hertkorn, N., Wolf, M., Frommberger, M., Schmitt-Kopplin, P. and Koch B. P. (2007) Rapid biotic molecular transformation of acids in a karst aquifer. Geochim Cosmochim Ac 71, 5474-5482.

Engbrodt, R. and Kattner G. (2005) On the biogeochemistry of dissolved carbohydrates in the Greenland Sea (Arctic). Org Geochem 36, 937-948.

Fasching, C., Behounek, B., Singer, G.A. and Battin, T.J. (2014) Microbial degradation of terrigenous dissolved organic matter and potential consequences for carbon cycling in brown-water streams. Sci Rep 4, 4981.

Fichot, C.G., Benner, R., Kaiser, K., Shen, Y., Amon, R.M.W., Ogawa, H. and Lu, C.-J. (2016) Predicting Dissolved Lignin Phenol Concentrations in the Coastal Ocean from Chromophoric Dissolved Organic Matter (CDOM) Absorption Coefficients. Front Mar Sci 3, 7.

Flerus, R., Lechtenfeld, O.J., Koch, B.P., McCallister, S.L., Schmitt-Kopplin, P., Benner, R., Kaiser, K. and Kattner, G. (2012) A molecular perspective on the ageing of marine dissolved organic matter. Biogeosciences 9(6), 1935-1955.

Goldberg, S.J., Ball, G.I., Allen, B.C., Schladow, S.G., Simpson, A.J., Masoom, H., Soong, R., Graven, H.D. and Aluwihare, L.I. (2015) Refractory dissolved organic nitrogen accumulation in high-elevation lakes. Nat Commun 6, 6347.

Gonsior, M., Hertkorn, N., Conte, M.H., Cooper, W.J., Bastviken, D., Druffel, E. and Schmitt-Kopplin, P. (2014) Photochemical production of polyols arising from significant photo-transformation of dissolved organic matter in the oligotrophic surface ocean. Mar Chem 163, 10-18.

Hansell, D.A. (2013) Recalcitrant dissolved organic carbon fractions. Ann Rev Mar Sci 5, 421-445.

Hedges, J.I., Keil, R.G. and Benner, R. (1997) What happens to terrestrial organic matter in the ocean? Org Geochem 27(5-6), 195-212.

Hernes, P.J. and Benner, R. (2003) Photochemical and microbial degradation of dissolved lignin phenols: Implications for the fate of terrigenous dissolved organic matter in marine environments. J Geophys Res 108(C9), 3291.

Hertkorn, N., Benner, R., Frommberger, M., Schmitt-Kopplin, P., Witt, M., Kaiser, K., Kettrup, A. and Hedges, J.I. (2006) Characterization of a major refractory component of marine dissolved organic matter. Geochim Cosmochim Ac 70 (12), 2990-3010.

23

Hertkorn, N., Harir, M., Koch, B.P., Michalke, B. and Schmitt-Kopplin, P. (2013) High-field NMR spectroscopy and FTICR mass spectrometry: powerful discovery tools for the molecular level characterization of marine dissolved organic matter. Biogeosciences 10(3), 1583-1624.

Hertkorn, N., Harir, M., Cawley, K.M., Schmitt-Kopplin, P. and Jaffé, R. (2016) Molecular characterization of dissolved organic matter from subtropical wetlands: a comparative study through the analysis of optical properties, NMR and FTICR/MS. Biogeosciences 13(8), 2257-2277.

Huang, C.-C., Guo, L., Santschi, P. H., Alvarado-Quiroz, N. and Haye, J. M. (2003) Distribution of carbohydrate species in the Gulf of Mexico. Mar Chem, 81, 119-135.

Kellerman, A.M., Dittmar, T., Kothawala, D.N. and Tranvik, L.J. (2014) Chemodiversity of dissolved organic matter in lakes driven by climate and hydrology. Nat Commun 5, 3804.

Kellerman, A.M., Kothawala, D.N., Dittmar, T. and Tranvik, L.J. (2015) Persistence of dissolved organic matter in lakes related to its molecular characteristics. Nat Geosci 8(6), 454-457.

Knorr K.-H. (2013) DOC-dynamics in a small headwater catchment as driven by redox fluctuations and hydrological flow paths-are DOC exports mediated by iron reduction/oxidation cycles? Biogeosciences 10, 891-904.

Koch, B.P., Witt, M., Engbrodt, R., Dittmar, T. and Kattner, G. (2005) Molecular formulae of marine and terrigenous dissolved organic matter detected by electrospray ionization Fourier transform ion cyclotron resonance mass spectrometry. Geochim Cosmochim Ac 69(13), 3299-3308.

Koch, B.P., Kattner, G., Witt, M. and Passow, U. (2014) Molecular insights into the microbial formation of marine dissolved organic matter: recalcitrant or labile? Biogeosciences 11(15), 4173-4190.

Kördel, W., Dassenakis, M., Lintelmann, J. and Padberg, S. (1997) The importance of natural organic material for environmental processes in waters and soils (Technical Report). Pure Appl Chem 69(7), 1571-1600.

Ksionzek, K.B., Lechtenfeld, O.J., McCallister, S.L., Schmitt-Kopplin, P., Geuer, J.K., Geibert, W. and Koch, B.P. (2016) Dissolved organic sulfur in the ocean: Biogeochemistry of a petagram inventory. Science 354(6311), 456-459.

Lechtenfeld, O.J., Kattner, G., Flerus, R., McCallister, S.L., Schmitt-Kopplin, P. and Koch, B.P. (2014) Molecular transformation and degradation of refractory dissolved organic matter in the Atlantic and Southern Ocean. Geochim Cosmochim Ac 126, 321-337.

Lechtenfeld, O.J., Hertkorn, N., Shen, Y., Witt, M. and Benner, R. (2015) Marine sequestration of carbon in bacterial metabolites. Nat Commun 6, 6711.

Leri, A.C., Mayer, L.M., Thornton, K.R., Northrup, P.A., Dunigan, M.R., Ness, K.J. and Gellis, A.B. (2015) A marine sink for chlorine in natural organic matter. Nat Geosci 8(8), 620-624.

Mannino, A. and Harvey, R. (1999) Lipid composition in particulate and dissolved organic matter in the Delaware Estuary: sources and diagenetic patterns. Geochim Cosmochim Ac, 63, 2219-2235.

Melone, F., Saladino, R., Lange, H. and Crestini, C. (2013a) Tannin structural elucidation and quantitative (3)(1)P NMR analysis. 1. Model compounds. J Agric Food Chem 61(39), 9307-9315.

Melone, F., Saladino, R., Lange, H. and Crestini, C. (2013b) Tannin structural elucidation and quantitative (3)(1)P NMR analysis. 2. Hydrolyzable tannins and proanthocyanidins. J Agric Food Chem 61(39), 9316-9324.

Minor, E.C., Swenson, M.M., Mattson, B.M. and Oyler, A.R. (2014) Structural characterization of dissolved organic matter: a review of current techniques for isolation and analysis. Environ Sci Process Impacts 16(9), 2064-2079.

Mopper, K. and Kieber, D.J. (2002) Photochemistry and the cycling of carbon, sulfur, nitrogen and phosphorus. In book: Biogeochemistry of Marine Dissolved Organic Matter, Edition: 1st, Chapter: 9, Publisher: Academic Press, Editors: Dennis A. Hansell, Craig A. Carlson, pp.455-507. DOI: 10.1016/B978-012323841-2/50011-7.

Mopper, K., Stubbins, A., Ritchie, J.D., Bialk, H.M. and Hatcher, P.G. (2007) Advanced instrumental approaches for characterization of marine dissolved organic matter: extraction

techniques, mass spectrometry, and nuclear magnetic resonance spectroscopy. Chem Rev 107(2), 419-442.

Moran, M.A. and Zepp, R.G. (1997) Role of photoreactions in the formation of biologically labile compounds from dissolved organic matter. Limnol Oceanogr 42(6), 1307-1316.

Moran, M.A., Kujawinski, E.B., Stubbins, A., Fatland, R., Aluwihare, L.I., Buchan, A., Crump, B.C., Dorrestein, P.C., Dyhrman, S.T., Hess, N.J., Howe, B., Longnecker, K., Medeiros, P.M., Niggemann, J., Obernosterer, I., Repeta, D.J. and Waldbauer, J.R. (2016) Deciphering ocean carbon in a changing world. Proc Natl Acad Sci U S A 113(12), 3143-3151.

Nebbioso, A. and Piccolo, A. (2013) Molecular characterization of dissolved organic matter (DOM): a critical review. Anal Bioanal Chem 405(1), 109-124.

Ohno, T., He, Z., Sleighter, R.L., Honeycutt, C.W. and Hatcher, P.G. (2010) Ultrahigh resolution mass spectrometry and indicator species analysis to identify marker components of soil- and plant biomass- derived organic matter fractions. Environ Sci Technol 44(22), 8594-8600.

Peiffer, S., Walton-Day, K. and Macalady, D. L. (1999) The interaction of natural organic matter with iron in a wetland (Tennessee Park, Colorado) receiving acid mine drainage. Aquat Geochem 5, 207-223.

Perminova, I.V., Konstantinov, A.I., Kunenkov, E.V., Gaspar, A., Schmitt-Kopplin, P., Hertkorn, N., Kulikova, N.A. and Hatfield, K. (2009) Separation technology as a powerful tool for unfolding molecular complexity of natural organic matter and humic substances. DOI: 10.1002/9780470494950.ch13.

Ritchie, J.D. and Perdue, E.M. (2003) Proton-binding study of standard and reference fulvic acids, humic acids, and natural organic matter. Geochim Cosmochim Ac 67(1), 85-96.

Romano, S. Dittmar, T., Bondarev, V., Weber, R. J. M., Viant, M. R. and Schulz-Vogt, H. N. (2014) Exo-metabolome of *pseudovibrio sp.* FO-BEG1 analyzed by ultra-high reolution mass spectrometry and the effect of phosphate limitation. PLOS ONE 9(5): e96038.

Sandron, S., Rojas, A., Wilson, R., Davies, N.W., Haddad, P.R., Shellie, R.A., Nesterenko, P.N., Kelleher, B.P. and Paull, B. (2015) Chromatographic methods for the isolation,

separation and characterisation of dissolved organic matter. Environ Sci Process Impacts 17(9), 1531-1567.

Schmidt, F., Elvert, M., Koch, B.P., Witt, M. and Hinrichs, K.-U. (2009) Molecular characterization of dissolved organic matter in pore water of continental shelf sediments. Geochimi Cosmochim Ac 73(11), 3337-3358.

Schmidt, F., Koch, B.P., Elvert, M., Schmidt, G., Witt, M. and Hinrichs, K.U. (2011) Diagenetic transformation of dissolved organic nitrogen compounds under contrasting sedimentary redox conditions in the Black Sea. Environ Sci Technol 45(12), 5223-5229.

Schmitt-Kopplin, P, Hertkorn, N., Schulten, H.-R., Kettrup, A. (1998) Structural changes in a dissolved soil humic acid during photochemical degradation processes under O_2 and N_2 atmosphere. Environ. Sci. Technol. 32, 2531-2541.

Schmitt-Kopplin, P., Gelencser, A., Dabek-Zlotorzynska, E., Kiss, G., Hertkorn, N., Harir, M., Hong, Y. and Gebefugi, I. (2010a) Analysis of the unresolved organic fraction in atmospheric aerosols with ultrahigh-resolution mass spectrometry and nuclear magnetic resonance spectroscopy: organosulfates as photochemical smog constituents. Anal Chem 82(19), 8017-8026.

Schmitt-Kopplin, P., Gabelica, Z., Gougeon, R.D., Fekete, A., Kanawati, B., Harir, M., Gebefuegi, I., Eckel, G. and Hertkorn, N. (2010b) High molecular diversity of extraterrestrial organic matter in Murchison meteorites reveal 40 years after its fall. Proc Natl Acad Sci U S A 107(7), 2763-2768.

Seidel, M., Beck, M., Riedel, T., Waska, H., Suryaputra, IG.N.A., Schnetger, B., Niggemann, J., Simon, M. and Dittmar, T. (2014) Biogeochemistry of dissolved organic matter in an anoxic intertidal creek bank. Geochim Cosmochim Ac, 140, 418-434.

Shen, Y., Chapelle, F.H., Strom, E.W. and Benner, R. (2014) Origins and bioavailability of dissolved organic matter in groundwater. Biogeochemistry 122(1), 61-78.

Sleighter, R.L. and Hatcher, P.G. (2008) Molecular characterization of dissolved organic matter (DOM) along a river to ocean transect of the lower Chesapeake Bay by ultrahigh resolution electrospray ionization Fourier transform ion cyclotron resonance mass spectrometry. Mar Chem 110(3-4), 140-152.

Stubbins, A., Spencer, R.G.M., Chen, H., Hatcher, P.G., Mopper, K., Hernes, P.J., Mwamba, V.L., Mangangu, A.M., Wabakanghanzi, J.N. and Six, J. (2010) Illuminated darkness: Molecular signatures of Congo River dissolved organic matter and its photochemical alteration as revealed by ultrahigh precision mass spectrometry. Limnol Oceanogr 55(4), 1467-1477.

Walker, B.D., Beaupré, S.R., Guilderson, T.P., McCarthy, M.D. and Druffel, E.R.M. (2016) Pacific carbon cycling constrained by organic matter size, age and composition relationships. Nat Geosci 9, 888-891.

Woods, G.C., Simpson, M.J. and Simpson, A.J. (2012) Oxidized sterols as a significant component of dissolved organic matter: evidence from 2D HPLC in combination with 2D and 3D NMR spectroscopy. Water Res 46(10), 3398-3408.

Zhang, H., Zhang, Y., Shi, Q., Ren, S., Yu, J., Ji, F., Luo, W., Yang, M. (2012) Characterization of low molecular weight natural organic matter along the treatment trait of a waterworks using Fourier transform ion cyclotron resonance mass spectrometry. Water Res. 46, 5197-5204.

Zhang, F., Harir, M., Moritz, F., Zhang, J., Witting, M., Wu, Y., Schmitt-Kopplin, P., Fekete, A., Gaspar, A. and Hertkorn, N. (2014) Molecular and structural characterization of dissolved organic matter during and post cyanobacterial bloom in Taihu by combination of NMR spectroscopy and FTICR mass spectrometry. Water Res 57, 280-294.

Chapter 2

Materials and Methods

2 Materials and Methods

2.1 Sample preparation

DOM Samples were taken in Suwannee River in May 2012 as described by Green et al. (Green et al. 2015), and in June 2012 in the Southern North Sea (54.1757 N / 7.8977 E; RV Heincke, Expedition HE 426 II). Water samples were immediately filtered after collection with 0.47 μm GF/F glass fiber (Whatman, precombusted at 450 ^{o}C) and adjusted to pH 2 (concentrated HCl, Merck) prior to SPE. The SPE experiments were done according to our previous developed protocol (Li et al., 2016). The SPE extracts were kept at -25°C in the dark prior to further analysis (Flerus et al., 2011).

2.2 DOC measurement

DOC was determined by high temperature catalytic oxidation and subsequent non-dispersive infrared spectroscopy and chemiluminescence detection (TOC-VCPN, Shimadzu). Final DOC concentrations are average values of triplicate measurements. If the standard variation or the coefficient of variation exceeded 0.1 μM or 1 %, respectively, up to two additional analyses were performed and outliers were eliminated. After each batch of five samples, one reference standard (DOC-DSR, Hansell Research Lab, University of Miami, USA), one ultrapure water blank and one potassium hydrogen phthalate standard were measured. The limit of detection (3σ of the blank) and quantitation (9σ of the blank) was 7 and 21 μmol C L^{-1}, respectively. The accuracy was ±5 % (Flerus et al., 2012). Samples (100 μL of methanol eluates – equivalent to 1 mL SR water and 50 mL NS water, and 500 μL water solutions of permeate and wash) were evaporated and re-dissolved in 1 mL ultrapure water for analysis.

2.3 High-field FT-ICR MS analysis

High-field FT-ICR mass spectra of DOM solutions were acquired by a 12 T Bruker Solarix mass spectrometer (Bruker Daltonics, Bremen, Germany) and an Apollo II electrospray ionization (ESI) source in negative ionization mode. Samples were diluted in methanol to ~5 μg/mL DOC, and then injected into the electrospray source at a flow rate of 120 μL/h with a nebulizer gas pressure of 138 kPa and a drying gas pressure of 103 kPa. Spectra were first externally calibrated based on clusters of arginine in methanol (5 μg/mL), and internal calibration was systematically performed using specific DOM reference mass list, reaching accuracy values lower than 500 ppb. The spectra were acquired with a time domain of 4 Mega words over a mass range of m/z 150-1000 amu, and 500 scans were accumulated for each

mass spectrum. Elemental formulae were computed for each peak in a batch mode by using custom-built software (Tziotis et al., 2011). Final elemental formulae were generated and categorized into groups containing CHO, CHNO, CHOS and CHONS molecular series which were used to reconstruct the group-selective mass spectra (CHO and CHNO series were assigned in the second study due to the limited sulfur content in SR DOM). The computed average values for H, C, N and O (atom %) and the H/C, O/C and C/N ratios as well as DBE, DBE/C, mass-to-charge (m/z) and aromaticity were based upon intensity weighted averages of mass peaks with assigned molecular formulae.

2.4 NMR analysis

^{1}H NMR detected spectra of eluates were acquired with a 800 MHz Bruker Avance III spectrometer ($B_0 = 18.7$ T) at 283 K with 0.05-2 mg of solid obtained by evaporation of original methanol-h4 solution, dissolved in approx. 110-150 µL CD_3OD (Merck. 99.95% 2H) solution with a 5 mm z-gradient ^{1}H/^{13}C/^{15}N/^{31}P QCI cryogenic probe (90° excitation pulses: [13]C ~ [1]H ~ 10 µs; $B_0 = 18.7$ T) with Bruker standard pulse sequences in sealed 2.0 or 2.5 mm Bruker MATCH tubes. Detailed parameters of NMR have been described by Hertkorn et al. (Hertkorn et al., 2013, 2016). ^{1}H NMR chemical shift reference of HD_2OD was 3.3 ppm. ^{1}H NMR spectra were recorded with solvent suppression with pre-saturation and 1 ms spin-lock (*noesypr1d*), 5 s acquisition time (aq), 5 s relaxation delay (d1), typically 512-2048 scans, and 1 Hz exponential line broadening. A phase sensitive, gradient enhanced TOCSY NMR spectrum with solvent suppression (*dipsi2etgpsi19*) was acquired for an acquisition time of 1 s, a mixing time of 100 ms, and a relaxation delay of 1 s (spectral width of 9615.4 Hz, 16 scans, 1523 increments; computation to a 16384×2048 matrix).

^{13}CNMR spectra used *cpmg_cpd_d5* for T2 relaxation; 14 s relaxation delay; typically 30000-65000 scans) with an acquisition time of 1s and an exponential line broadening of 12.5Hz. ^{13}C DEPT NMR spectra (distortionless enhanced polarization transfer) were acquired with aq = 1 s and d1 = 2 s. The NMR section integrals were obtained by using Bruker AMIX software (version 3.9.4) with a bucket resolution of 0.01 ppm chemical shifts for ^{1}H NMR and 1 ppm chemical shift for ^{13}C NMR, and with exclusion of methanol and water.

2.5 Optical spectroscopy

SPE extracts were dried and re-dissolved in Milli-Q water at the original concentrations and then diluted to achieve raw absorbance of less than 0.4 at 300 nm. The dilution factor was

used to calculate the initial fluorescence intensity. The dilution was necessary to be able to correct for inner filtering effects and to not exceed the linear range of fluorescence response. Absorbance and EEM spectra were recorded simultaneously using a Horiba Aqualog fluorometer at excitation wavelengths from 240 to 500 nm (3 nm increments) and an emission range between 230 to 600 nm (~3 nm increments). The fluorescence was then corrected for Raleigh scattering and inner filter effects. The raw fluorescence intensity was then normalized to a 1 ppm Starna quinine sulfate reference cell (Gonsior et al., 2013).

2.6   Statistical analysis

The R package "pvclust" (RStudio, Version 0.98.978) was used to apply hierarchical cluster analysis (HCA) via multiscale bootstrap resampling. HCA of the eluates was based on Euclidean distance and Ward's linkages. Two types of p-values were calculated for each cluster: approximately unbiased (au) and bootstrap (bp) p-values. Clusters with au larger than 95% were marked by red rectangles. The ^{1}H NMR section integrals were obtained by using Bruker AMIX software (version 3.9.4) with a bucket resolution of 0.01 ppm chemical shift, and with exclusion of methanol and water. EEM fluorescence spectroscopy data were pretreated into one-dimensional data set, and then analyzed as well with the R package "pvclust". HCA of the FT-ICR MS data was obtained with Hierarchical Clustering Explorer, and the principal component analysis (PCA) was performed using the software SIMCA-P9.0.

2.7   References

Flerus, R., Koch, B.P., Schmitt-Kopplin, P., Witt, M. and Kattner, G. (2011) Molecular level investigation of reactions between dissolved organic matter and extraction solvents using FT-ICR MS. Mar Chem 124(1-4), 100-107.

Flerus, R., Lechtenfeld, O.J., Koch, B.P., McCallister, S.L., Schmitt-Kopplin, P., Benner, R., Kaiser, K. and Kattner, G. (2012) A molecular perspective on the ageing of marine dissolved organic matter. Biogeosciences 9(6), 1935-1955.

Gonsior, M., Schmitt-Kopplin, P. and Bastviken, D., 2013. Depth-dependent molecular composition and photo-reactivity of dissolved organic matter in a boreal lake under winter and summer conditions. Biogeosciences 10(11), 6945-6956.

Green, N.W.; Mclnnis, D.; Hertkorn, N.; Maurice, P.A. and Perdue E.M. (2015) Suwannee River natural organic matter: isolation of the 2R101N reference sample by reverse osmosis. Environ Eng Sci 32, 1-7.

Hertkorn, N., Harir, M., Koch, B.P., Michalke, B. and Schmitt-Kopplin, P. (2013) High-field NMR spectroscopy and FTICR mass spectrometry: powerful discovery tools for the molecular level characterization of marine dissolved organic matter. Biogeosciences 10(3), 1583-1624.

Hertkorn, N., Harir, M., Cawley, K.M., Schmitt-Kopplin, P. and Jaffé, R. (2016) Molecular characterization of dissolved organic matter from subtropical wetlands: a comparative study through the analysis of optical properties, NMR and FTICR/MS. Biogeosciences 13(8), 2257-2277.

Li, Y., Harir, M., Lucio, M., Kanawati, B., Smirnov, K., Flerus, R., Koch, B.P., Schmitt-Kopplin, P. and Hertkorn, N. (2016) Proposed Guidelines for Solid Phase Extraction of Suwannee River Dissolved Organic Matter. Anal Chem 88(13), 6680-6688.

Tziotis, D., Hertkorn, N. and Schmitt-Kopplin, P. (2011) Kendrick-analogous network visualisation of ion cyclotron resonance Fourier transform mass spectra: Improved options for the assignment of elemental composition and the classification of organic molecular complexity. Eur J Mass Spectrom 17(4), 415-421.

Chapter 3

Review of the Relevant Literature

3 Review of the Relevant Literature

3.1 Isolation of DOM

3.1.1 Physical isolation

3.1.1.1 Ultrafiltration (UF)

UF is one of the most widely applied methods for DOM isolation; UF employs semimembranes to separate compounds with different molecular size. During UF of DOM, high molecular weight fraction (typically m/z of 1k Da) is retained on the semipermeable membrane whereas small molecules together with salts and ions are penetrated through the membrane by force (pressure or concentration gradients) (Perminova et al. 2009).

UF normally allows for processing of large volumes of waer with a fast flow rate and large surface area of membranes, rendering it suitable for large scale sample pretreatment. Another advantage of UF is that its application does not require any chemical pretreatment of samples and therefore chemical alterations of DOM are limited. It is reported that by using UF DOC recoveries reached at the range of 8-55% for marine DOM and up to 80% for freshwater DOM (Minor et al. 2014, Sandron et al. 2015).

The limitations of UF reside in the following aspects (Minor et al. 2014, Perminova et al. 2009, Sandron et al. 2015). First and the most important one is that DOM fraction only with high molecular weights is extracted, leaving the small DOM molecules passing through the membrane. Second, significant variance of DOM fractionation and DOC recovery is regularly observed which highly depends on the experimental procedures and equipment applied. Additionally, membrane fouling is also a problem. When marine DOM is subjected to UF treatment, an additional desalting step is needed afterwards. Increase in salinity was found to have an effect of reducing the recovery of high molecular weight compounds by UF (Kruger et al. 2011).

3.1.1.2 Reverse osmosis / electrodialysis (RO/ED)

RO, quite similar to UF, concentrates DOM using an applied force to overcome osmotic pressure, and consecutive ED removes salts through ion-exchange membranes under the influence of an applied electric potential difference. When RO is coupled with ED, DOM fractions with satisfactory DOC recovery as well as largely decreased salt content are obtained (Minor et al. 2014, Sandron et al. 2015).

This technique can be performed to process large volumes at fast speeds, which is beneficial for large-scaleDOM isolation. The greatest advantage of RO/ED compared with UF alone is that salts are considerably removed, which makes it an appropriate pretreatment before applying to advanced structural spectroscopy, especially in the case of marine DOM isolation (Minor et al. 2014, Sandron et al. 2015). RO/ED has showed the capacity to isolate DOM efficiently, with ~ 90% DOC recovery for freshwater DOM and an average of 75% DOC recovery for marine DOM (Minor et al. 2014, Sandron et al. 2015). The obtained isolated samples showed the consistent UV-visible absorbance spectra and molar C/N ratios similar to the original marine samples, indicating no bias for/against these two properties (Chen et al. 2014, Tfaily et al. 2012). Compared with UF isolated samples, RO/ED samples contained a relatively lower proportion of carbohydrate carbon and a relatively greater proportion of alkyl carbon (Serkiz and Perdue 1990, Koprivnjak et al. 2009).

However, RO/ED is currently more expensive than other isolation methods; in addition, a chemically harsh condition at pH 12 (0.01 M NaOH) is needed to remove adsorbed organic matter, which might cause the degradation of certain molecules (Sandron et al. 2015).

3.1.2   Chemical isolation

3.1.2.1   Solid phase extraction (SPE)

For more than three decades SPE has been and still is the most extensively applied method for DOM isolation due to the low cost and flexible usage. SPE works based on the solute partition coefficient between sorbents and aqueous phases, and therefore is highly influenced by the physical and chemical properties of the sorbents and solutes (Minor et al. 2014, Sandron et al. 2015). In practice, SPE isolation of DOM follows a chronology of five steps. First, SPE sorbents are conditioned to the respective optimal conditions. Second, DOM samples are loaded on the sorbents, and some molecules are retained on the sorbents whereas the others pass through the sorbents under the given experimental conditions. Third, the sorbents with adsorbed DOM are washed with certain solvents to get rid of impurities. Fourth, the sorbents are dried. Finally, the retained DOM is eluted with certain organic solvents such as methanol, acetonitrile or acetone to isolate these operational defined DOM fractions (Li et al. 2016a).

There are mainly two modes of SPE operation for DOM isolation, namely, simultaneous elution of DOM molecules with a desired wide range of properties by a single solvent, and stepwise selective fractionation of DOM molecules using different sorbents/eluting solvents

or successive collection of individual fractions with limited quantities of solvents. Due to ease of operation and less chemical changes/solvents involved, the first category has been the most applied SPE method. (This paragraph was adapted from Li et al. 2016a ©copyright ACS publication)

Since the 1980s, scientists have investigated different types of SPE sorbents to improve DOC recovery (Thurman and Malcolm 1981). The classical XAD and improved DAX resins were the first generation sorbents for DOM isolation, which enabled a recovery of hydrophobic acids in the range from 19-90% (Perdue and Ritche 2003, Thurman and Malcolm 1981). These were substituted by the second generation of silica-based sorbents as a result of laborious works and commercial availability (Kim et al. 2003, Kruger et al. 2011, Tfaily et al. 2012). More recently, polymer-based sorbents have been widely utilized owing to their stability at wide pH ranges and easy to follow extraction procedures. In particular, the sorbent of functionalized styrene-divinylbenzene copolymer (PPL) (Dittmar et al. 2008) capable to extract hydrophobic and certain polar compounds like phenols showed both appreciable DOM recovery as well as adequate depiction of intrinsic DOM molecular diversity inherent to different sources such as river, ground, lake and sea water (Dittmar et al. 2008). In comparison with classical XAD-2 resins, which are also styrene divinylbenzene polymers polymers, contemporary PPL resin features larger specific surface area (600 versus 300 m^2/g), and proprietary functionalization for improved retention of polar compounds such as phenols. Compared with silica-based sorbent C18 and classical XAD-8 resin, PPL resin isolated representative DOM components with abundance of aliphatic groups, and was recommended for DOM extraction from natural waters (Perminova et al. 2014). (This paragraph was adapted from Li et al. 2016a ©copyright ACS publication)

With increasing focus on the molecular composition of the obtained SPE extracts instead of merely evaluating DOC recovery, the DOM extraction selectivity of the SPE cartridges with respect to certain DOM compounds has drawn awareness, and DOM extracts obtained with different functionalized SPE sorbents have been compared (Minor et al. 2014, Sandron et al. 2015). While PPL was reported to retain higher proportions of nitrogen-containing compounds from both fresh- and marine waters (Dittmar et al. 2008, Perminova et al. 2014, Zherebker et al. 2016), C18 had shown affinity to more saturated molecules in arctic marine DOM and distinct DOM from oligotrophic Lake Superior (Perminova et al. 2014, Li and Minor 2015); on the other hand, HLB could not completely elute freshwater DOM

compounds with high molecular weights (Raeke et al. 2016). (This paragraph was adapted from Li et al. 2016c ©copyright Elsevier)

The second category is still attractive because of the well classified individual fractions and the rather representative overall DOM fractions. Typically, XAD series (XAD-2, 4, 7 and 8) were applied first, and later diethylaminoethylcellulose (DEAE cellulose) came into use (Imai et al. 2001, He and Hur 2015), and more recently new materials such as certain polymer-based sorbents and ion exchangers were tested. With this method, DOM sample could be extracted into six fractions based on polarity and charge: hydrophobic base, hydrophobic acid, hydrophobic neutral, hydrophilic base, hydrophilic acid and hydrophilic neutral. A novel SPE method for DOM fractionation used polymer-based materials nonpolar ENV, cation exchanger Strata X-C and anion exchanger Strata X-AW in sequence, and used different eluting solvents like methanol, HCl and NaOH. After stepwise eluting and correction, 57-64% of total DOC recovery was obtained with hydrophobic acids, hydrophobic neutrals, hydrophilic acids and hydrophilic neutrals accounting for large proportions of total DOC (Ratpukdi et al. 2009).

One new modification tried to combine the first and second SPE categories: two different online SPE sorbents embracing different sorption mechanisms (nonpolar PPL and activated carbon Hypercarb) were coupled in sequence, then the normal SPE procedure was performed, finally the two sorbents were separated and eluted individually. This new method obtained considerably higher overall DOC recoveries than using only a single PPL cartridge, showing the potential as an improved SPE method, especially recommendable for high carbohydrates contained DOM samples (Swenson et al. 2014).

Comparisons of SPE and RO/ED on DOM isolation have been made based on DOC recovery, molecular composition, time and costs (Green et al. 2014, Li et al. 2016a). SPE with PPL, SPE with XAD and RO/ED were applied for isolation of surface and deep marine DOM on large scale (Green et al. 2014). The DOC recovery obtained by the three methods showed the pattern: RO/ED > SPE with PPL >> SPE with XAD; SPE with XAD selectively extracted carbon-enriched compounds whereas RO/ED isolates was most representative of the original samples; SPE with PPL was the most economical in terms of initial costs, operator costs and running costs (Green et al. 2014). In the case of isolating Suwannee River water sample, RO/ED produced a slightly higher DOC recovery than SPE with PPL cartridge (RO/ED: 94.2% and PPL: 89%), and these two extracts contained distinctive structural and molecular

information (Li et al. 2016a). Although a rather satisfactory overall congruence of the extracts was observed with respect to NMR line shape distribution, RO/ED extract was more representative of original sample by NMR results. However, RO/ED extract was distinct from original water and SPE extracts in FT-ICR MS analysis, which might be caused by the molecules of low and large molecular weights (m/z: 150-250 and 650-730). SPE extract was found to discriminate against two groups of molecules, namely, the highly oxygenated compounds with O/C ratios > 0.9 and more saturated region of lipids (Li et al. 2016a).

3.1.2.2   Reversed-phase liquid chromatography (RP LC)

Based on differential partitioning between the mobile and stationary phases, RP LC fractionates the polydisperse and heterogeneous DOM into different groups of fractions according to polarity, molecular weight and degree of unsaturation (Sandron et al. 2015). In the RP LC system, the analogous nonpolar C18 columns were chosen although different DOM samples and mobile phases were applied (Koch et al. 2008, Stenson A. 2008). Generally, the polar fractions elute first whereas the nonpolar fractions last. After isolation, the obtained fractions can be further measured at online or offline mode by advanced structural spectroscopy such as FT-ICR MS or NMR spectroscopy, and have revealed improved resolution and more detailed compositional/structural characteristics. It is noteworthy that the mobile phase and eluting solvents chosen in the RP LC system should be amenable to the subsequent instrumental analysis (Koch et al. 2008, Simpson et al. 2004, Stenson et al. 2008).

With water-acetonitrile as gradient mobile phase, co-eluting occurred and DOM samples were eluted out within the first 10 min, indicative of the poor separation. After adding ion pair reagent, the chromatograms were improved to a great extent with most compounds eluting out gradually during 10-27 min. 105 fractions were collected and subjected to NMR characterization. The early rather polar fractions presented high proportions of aliphatics, CRAMs, carbohydrates and considerable amounts of aromatics (Simpson et al. 2004).

 Later, it was observed that RP LC-based fractionation was quite selective and complicated, and O/C ratios, molecular weights and carbon skeletons were involved in defining the elution sequence. For instance, higher O/C ratios, lower molecular weights, and carbon-skeletons more densely covered with hydroxl, carboxy and/or carbonyl groups were found in earlier fractions (Stenson 2008). Moreover, a buffer-free RP LC model for DOM fractionation was

developed and the rather resolved UV and fluorescence data of the separated peaks were observed (Koch et al. 2008). In the chromatogram, the early and late peaks were well resolved while the second and third fractions still had overlaps which were subjected to 2-dimensional (2-D) separation prior to mass spectrometry. A general trend was observed in this study that with the decrease in polarity, the O/C ratios and unsaturation (DBE values) decreased as well whereas the H/C ratio increased continuously. No ambiguous trends in molecular weights were observed, which might be attributed to the non-continual effects of the 2-D separation on the mass spectrometry (Koch et al. 2008).

It summarizes that RP LC fractionation of DOM is a polarity-based separationin which due to the molecular complexity of DOM O/C ratios, H/C ratios, unsaturation, carbon-skeletons, molecular weights and others show influences on the fractionation sequence.

3.1.2.3 Capillary electrophoresis (CE)

CE separates compounds according to ionic mobility and/or partitioning into an alternative phase via non-covalent interactions, and it can also concentrate samples through gradients in conductivity and pH (Schmitt-Kopplin and Kettrup 2003, He et al. 2014, Gaspar et al. 2010). CE has the simplicity in the setup of the instrument and requires only a small volume of samples. Compared with chromatography, CE has different techniques of injection into the capillary as well as the different means by which the sample is driven through the column by electroosmosis instead of hydrodynamic pumping (Perminova et al. 2009, Schmitt-Kopplin and Kettrup 2003). Among different CE techniques, capillary zone electrophoresis (CZE) is the basic and the mostly referred separation, and it is highly affected by the separation buffer pH and the electroosmotic flow. Free-flow electrophoresis (FFE) is one CZE method, which has been successfully applied to NOM and metabolic analysis (Gaspar et al. 2010, Perminova et al. 2009).

As is known, NOM is a complex mixture of anionic polyelectrolytes in aquatic solution and covers a wide range of electrophoretic mobilities. CZE-separated FFE produced different Suwannee River NOM fractions with low molecular weights and an unresolved hump across the entire mass range in the electropherogram, and also demonstrated high contribution of low molecular weight fractions at higher mobility together with a superimposition of low molecular weight signals at low mobility in the mass spectra (Schmitt-Kopplin and Kettrup 2003). Based on the success of this approach, FFE were tried to obtain 96 fractions of

Suwannee River fulvic acid in a preparative scale, and then the fractions were further subjected to FT-ICR MS measurement (Gaspar et al. 2010). The fractions changed from with relatively low O/C ratios, high H/C ratios and low molecular weights to those with higher O/C ratios, lower H/C ratios and higher molecular weights when proceeding from lower to higher electrophoretic mobility. Moreover, low aromatic indices together with low proportions of oxygen atoms at the low mobility regions were observed whereas two different groups were found at high mobility regions: compounds deplete in oxygen atoms with high aromaticity index and low molecular weights; components saturated with heteroatoms with low aromaticity index and large molecular weights. Interestingly, the constituents present in low mobility regions showed average H/C and O/C ratios typtical of CRAMs, and were suggested that CRAMs with open aliphatic chains showed lower mobility region while those with alicyclic geometry showed relatively higher mobility (Gaspar et al. 2010).

In addition, different CE methods have also been developed for complex mixtures. Counterbalance CE uses the reversed electroosmosmotic flow with low pH and high concentration buffer, applied on NOM fractionation for the first time (Cottrell et al. 2013). After optimizing the operation conditions such as buffer concentration, pH, stacking, organic modifier, capillary length and temperature, an electropherogram comprised up to hundreds of peaks superimposed on the hump was observed. Eight Suwannee River NOM fractions were collected and analyzed by optical spectroscopy. UV absorbance at 254 nm presented the classic Gaussian distribution of the eight fractions with fraction 4 and 5 accounting for the majority. Fluorescence spectra showed the main four NOM peaks (A, C, M and T) with peak A consisting of ~ 50% of the total fluorescence in all fractions except fraction 4 (Cottrell et al. 2013).

Capillary electrokinetic fractionation separates samples under the influence of a homogeneous electrical field where only compounds with moderate mobilities between leading electrolyte and terminating electrolyte can be identified, a potential for fractionation of complex samples (He et al. 2014). Four different groups of standards were investigated and showed the predictable pH-depending behaviors for the structure features: carboxylic groups got ionized at low pH with enhancement at pH 4; phenolic groups at high pH with enhancement at pH 10; in the mixed profile of carboxylic groups and phenolic groups, the first enhancement caused by carboxylic acids and the second one by phenolic acids; sulfonic groups were ionized all over the pH range. This established method was further applied to two real red wine samples

from different vintages, and showed the selectivity to fractionate sulfur-containing compounds at pH 1.66 (He et al. 2014).

3.1.2.4 Size exclusion chromatography (SEC)

SEC separates mixtures of compounds according to differences in molecular size, and is used for the determination as well as quantification of the distribution of molecular weights in the samples. In a SEC system, compounds first pass through a SEC column which functions as a sieve and then elute at different rates according to molecular size: molecules with larger size require less time or elution volume to get eluted whereas the small molecules need large time or elution volume (Perminova et al. 2009). However, SEC is not based on molecular size alone, and many factors influence the fractionation such as stationary phase, ionic strength, buffer pH, concentration of the sample, hydrophobicity and organic modifiers (Hoque et al. 2003, Perminova et al. 2009).

As one of the most widely applied methods in the fractionation of humic substances and NOM, plenty of researches have worked on SEC. Perminova et al. summarized the size of the common materials (eg. NOM and humic substances, peptides, virus, bacteria, sugars and so on), conversion scale between molecular size and weight based on dextran scale, and the separation scale of different isolation methods. SEC turned out to be a suitable technique for DOM isolation due to its wide coverage of mass range (100-100000 Da) with NOM and humic subastances at the range of ~100-100000 Da (Perminova et al. 2009). They illustrated the mechanism of SEC, non-exclusion effects such as ionic exclusion and sorption in detail and summarized the averaged molecular weights of DOM, NOM and humic substances from different environments. In general, the molecular weights of different samples followed this pattern: Suwannee River fulvic acid, aquatic HS, aquatic DOM < Suwannee River humic acid, soil fulvic acid, soil solution humic substances and coal humic acid < bottom sediment humic substances, soil humic acid and peat humic substances. This work suggested that SEC provides meaningful estimation of the trends in molecular weights of DOM, NOM and humic substances (Perminova et al. 2009).

But there are some uncertainties needed to take into consideration. The concentration of the electrolytes can influence the elution volumes: the higher the concentration (before reaching a complete suppression of ion-exclusion interactions), the greater in the shifts of the elution volumes to larger values. The changes in buffer pH have a significant effect on SEC. For

instance, at pH 4.2, the strong carboxylic groups dissociated, resulting in the early eluting at the void volume of the column. Generally, the elution volumes shifted to larger values with the decrease of pH. As the pH reached ~ 2, one broad diffuse peak could be observed, indicative of a strong specific sorption of humic substances on the column (Hoque et al. 2003).

SEC is capable to generate more homogeneous DOM fractions whose structures are significantly altered based on size. According to the NMR results, the early SEC fractions were enriched with carbohydrates and aromatics; the middle fractions were abundant of CRAMs; the late fractions exhibited strong signals of aliphatics (Woods et al. 2010).

3.1.2.5 Hydrophilic interaction liquid chromatography (HILIC)

HILIC is a normal-phase HPLC with a polar stationary phase but utilizes high percentage of organic solvents as mobile phase, a separation suitable for polar compounds (Sandron et al. 2015). In the HILIC system, the compounds are retained on the polar stationary phase according to the mechanism of partition or ion exchange, and get eluted with the increase of their hydrophilicity: the hydrophobic compounds elute first whereas the hydrophilic ones elute out last (Woods et al. 2011, Woods et al. 2012). During HILIC process, many factors may influence the separation such as hydrogen-bonding, dipole-dipole interaction and hydrophobic retention (Sandron et al. 2015)

HILIC has been applied for the first time to separate a polydisperse and highly heterogeneous mixture of DOM. 80 fractions of Suwannee River DOM were collected after 60 runs in order to get sufficient amount for NMR measurement as well as for fluorescence spectroscopy. The isolated fractions showed a much better improved resolution in NMR spectra with numerous sharp peaks which indicated the presence of the individual compounds. They differed from fraction to fraction structurally and showed the patterns of the functional groups as follows: the aromatic groups were found most abundant in mid-polar fractions, slightly different from the previous studies; CRAMs and aliphatics varied in the earliest and latest fractions, but in general showed the trend that decreased with the hydrophilicity; carbohydrates increased with the hydrophilicity as expected. Those fractions were also measured by fluorescence spectroscopy, classified according to relative proportions of certain fluorescent peaks/components, and further statistically associated with NMR functional groups. The fractions demonstrated the variability across the polarity gradient in fluorescence data:

quinone-influenced signals were most abundant in hydrophobic fractions while amino acid-type fluorescence were most prominent in hydrophilic fractions. After the association analysis, the most hydrophobic fractions were discovered to be enriched of CRAMs and aliphatics which also carried the majority of the fluorescence signals, whereas the hydrophilic materials were highly correlated with carbohydrates together with high contributions from amino acid fluorescence (Woods et al. 2011).

Proceeding from these, a two-dimensional (2-D) HILIC/HILIC system were developed for DOM isolation. In this system, two highly orthogonal HILIC columns were chosen, and the first dimension was run for long periods of time (~ 2h) with high percentage of organic solvent as mobile phase (95% acetonitrile) whereas the second dimension was run for short time (3.4 min) to avoid diffusion with 50% acetonitrile. 126 fractions with 70 replicates were obtained and subjected to extensive 1-D ^{1}H NMR measurement, and certain fractions were subjected to multidimensional NMR measurement for in-depth elucidation of the structures. Most of the fractions were found to contain large amount of highly oxidized sterols. Furthermore, the hydrophobic and hydrophilic fractions probably shared the similar structural backbone, but the hydrophilic fractions contained higher proportions of COOH or OH groups (Woods et al. 2012).

However, according to the previous study of DOM isolation by RP LC, a relatively large proportion of hydrophobic molecules are present in DOM, which indicates HILIC might not be capable to separate those components in a satisfactory manner. Overall, HILIC is an appropriate separation method for DOM, and can be used as a complementary to RP LC.

3.1.2.6 Ion exchange chromatography (IC)

IC separates compounds based on the affinity of ions and polar molecules to the ion exchange resin; IC is especially used for isolation of polar compounds in DOM such as lipids, amino acids and carbohydrates. Due to the requirement of the system (low salinity levels), pretreatment of DOM samples is necessary (Sandron et al. 2014)

Neutral sugars have been separated and purified from marine DOM samples, and further measured by radiocarbon analysis for an improved interpretation of global carbon cycling. After acid hydrolysis, marine DOM was separated by an anion exchange column to obtain carbohydrates which were then purified by two cation exchange columns to get neutral sugars. Those neutral sugars were further purified by two amino functionalized columns to get

individual sugar compounds for compound-specific radiocarbon analysis (Repeta and Aluwihare 2006).

Recently, a more facile IC separation method of neutral sugars has been developed with the utilization of pulsed amperometric detection (Sandron et al. 2014). The IC system was applied on artificial DOM with an anion exchange column and pulsed ampeometric detection, and then on the marine and freshwater DOM (DOM samples were pretreated with SPE process using PPL cartridges). Peaks corresponding to certain neutral sugars were present, but with low intensity (slightly higher than the baseline) (Sandron et al. 2014). This low intensity might be attributed to the inappropriate sample pretreatment. It is known that SPE of DOM samples with PPL cartridges discriminates against carbohydrates, which implied that certain sugar compounds in that study were not or poorly extracted by SPE.

3.1.2.7 Gas chromatography (GC)

GC separates molecules based on interactions of volatile compounds with the columns, and is suitable for certain compounds which are volatile or can be derivatised into volatiles (Sandron et al. 2015). Due to the complexity and the presence of large polyfunctional molecules in DOM samples, sample pretreatment like CuO-oxidation and chemical reduction is applied first to make the large-size and polydisperse DOM molecules degraded into species amenable for GC, and then derivation processes are performed to protect and derivatise DOM's functional groups with acidic protons such as COOH, OH, NH and SH (Arakawa and Aluwihare 2015).

The most widely application of GC for DOM is the separation of lignins and tannins, and if coupled with mass spectrometry, structures of lignins could be characterized. Normally, the DOM samples are pretreated by CuO-oxidation first, and then derivatised prior to GC (Sandron et al. 2014). A new GC method was recently developed for DOM separation and characterization by using 2-D GC×GC and coupled to mass spectrometry. This advanced method provided unsurpassed chromatographic resolution, and has enabled the separation of homologous molecules along predictable trajectories in 2-D retention time spaces which could further complement the information of mass spectra and aid in molecular interpretation. With this method, some novel compounds (e.g. lignin-derived cyclobutane photodimers) were discovered which escaped detection by previous methods, and the sterically constained

benzene polycarboxylic acid isomers were found to be strongly retained on the second chromatographic dimension (Ball and Aluwihare 2014).

Another application of GC in the assessment of DOM molecular structures referred to the distinction of the carbon backbone, and was used for characterization of the functional group when coupled to mass spectrometry as well (Arakawa and Aluwihare 2015). After pretreatment by selective chemical reduction and derivation procedure, DOM samples were separated into different backbone structures by GC. A new method with 2-D GC×GC coupled with mass spectrometry was capable to separate DOM comprehensively with improved chromatographic resolution. It showed that reduced compounds corresponded to alicyclic hydrocarbons in the size range from C10 to C17, and cyclic terpenoids were the only biomolecular class with contiguous, alicyclic carbon backbones of this size.

3.1.3   Combination of physical and chemical isolation

Combination of SPE and RO/ED has been applied to surface and deep marine DOM, and it has been also compared with the individual isolation methods (Green et al. 2014). There, the samples were extracted by SPE with PPL cartridge first and then the wastes from SPE process were subject to RO/ED. This combined technique enabled high DOC recovery (98% for deep marine DOM and 101% for the surface one), and was representative of original water samples in terms of C/N ratios.

Passive sampling was also been applied on DOM isolation, which was consisted of a molecular weight selective membrane and an anion exchange resin. ~ 72-89% of DOC recovery for Lake Ontario was obtained by this method, with the structural groups extremely similar to the fraction isolated by the same anion exchange resin. However, the carbohydrate groups were discriminated against by this method when compared with the original Suwannee River RO sample, which might be attributed to the selectivity of this anion exchange resin. In general, it was cost-effective, easy use, and allowed for a range of temporal and spatial experiments that would be very difficult or impossible to perform using conventional approaches. The most fundamental difference between this method and the others resided in the time scale that the DOM information provided by passive sampling was rather integrative (with 1-2 weeks of time period) whereas other isolation methods provided a "snapshot" of DOM in time (Lam and Simpson 2006).

3.2 Characterization of DOM

3.2.1 Bulk analysis

3.2.1.1 Elemental analysis

The determination of H, C, O, N, S and P gives the percentages of the elemental compositions and relevant elemental ratios. It is the most fundamental bulk information for DOM characterization (Kördel et al. 1997). The first function of elemental analysis is to check the reliability of the results obtained by other measurement such as highly advanced structural spectroscopy. For example, a general assessment of the FT-ICR MS measurement is possible by comparing the FT-ICR MS-derived H/C and O/C ratios with the original elemental ratios of the same sample (Li et al. 2016a). The second function of elemental analysis is to obtain rough estimates of the changes in DOM samples by checking different samples. For instance, variations in elemental ratios and elemental compositions are common among DOM from different sources or occur after certain chemical/physical treatments (Kördel et al. 1997).

3.2.1.2 Titration

The acid-base properties of DOM are of great significance, as it moderates the acid-base balance in the natural waters and complexes formation with other elements or organic compounds in the environment. The functional groups of carboxylic acids and phenolic groups are widely measured and reported for the general acid-base properties, which are obtained by the indirect titration or direct titration. Indirect titration has the advantages of simplicity to use and no additional acidity involved whereas direct titration provides more detailed information about the thermodynamics of the proton-binding (Driver and Perdue 2015, Ritchie and Perdue 2003). These parameters serve as instrumental information on which further studies such as SPE and RP LC highly rely on.

The content of carboxylic groups in IHSS samples showed the order as follows: terrestrial fulvic acids > aquatic fulvic acids > Suwannee River NOM > aquatic humic acids > terrestrial humic acids; the content of phenols was higher in aquatic samples than the terrestrial samples, whereas it was rather similar in fulvic acids and humic acids (Ritchie and Perdue 2003). The carboxylic contents were found to be much higher than phenolic contents, with approximately ratio of 4:1. Moreover, the Suwannee River NOM sample showed the $\log K$ for carboxylic groups of ~4 and $\log K$ for phenolic groups of ~10, with average $\log K$ for proton-binding at 4.02 (Driver and Perdue 2015). This explains well the necessity for pH adjustment to pH=2

during SPE of Suwannee River NOM by hydrophobic sorbents: DOM molecules can retain on the SPE sorbents very well under pH conditions which are by 2 units lower than the significant log$K$ (Li et al. 2016a).

3.2.1.3 Isotope analysis and radiocarbon analysis

Isotope analysis identifies the isotope signatures in the chemical compounds, and can be used to trace the sources and understand the dynamic cycling processes in DOM studies. The two major isotopes used in DOM studies are ^{13}C and ^{15}N, whose ratioes may be altered by biological and geophysical processes (Guo and Sun 2009).

Carbon has three natural isotopes ^{12}C, ^{13}C and ^{14}C, with the abundance of 98.89%, 1.11% and 10^{-10} %, respectively. $\delta^{13}C$ isotope is widely used in DOM studies for trace the origin based on the assumption that DOM from different origin has a distinct $\delta^{13}C$ isotope value. A general trend is observed for DOM with different sources: the value ranges from -35‰ to -25‰ for terrestrial derived DOM; it is in the range of -18‰ and -8‰ for marsh macrophytes; and intermediate for the marine phytoplankton (Guo and Sun 2009). The variation in the values is mainly attributed to the isotope fractionation during carbon metabolism in the plants in which ^{13}C commonly becomes progressively enriched as well as the isotope composition in different source materials.

Nitrogen has two natural isotopes ^{14}N and ^{15}N, with the abundance of 99.63% and 0.37%, respectively. $\delta^{15}N$ isotope is used for tracing and distinguishing nitrogen sources and monitoring certain nitrogen-dependent biogeochemical processes such as nitrification and microbial processes. Generally, the $\delta^{15}N$ values range from -10‰ to 20‰ in different DOM samples (Guo and Sun 2009).

The radioactive ^{14}C with a half-life of 5730±40 years is used to determine the apparent age in organic materials by radiocarbon dating method. It serves as a proxy for DOM ages with the time scale of ~50,000 years based on the assumption that negligible exchange of organic carbon is involved in the studied ecosystem. The radiocarbon values typically are -263±23‰ and -546±14‰ for marine surface and deep DOM, respectively (Guo and Sun 2009). However, due to the complexity of the ecosystem, it is advisable to measure the compound-specific radiocarbon analysis for the better representation of the age of the DOM source (Guo and Sun 2009). For instance, individual sugar compounds were isolated and collected in

marine DOM for the compound-specific radiocarbon analysis so as to understand the role of carbohydrates in the cycling system (Repeta and Aluwihare 2006).

3.2.2 Optical spectroscopy

3.2.2.1 UV-visible spectroscopy

The application of UV-visible spectroscopy provides the rough estimates of DOM concentration, sources and certain functional groups. It boasts the advantages of low cost, ease of use and satisfactory reliability at high sensitivity, rendering it one of the most widely used techniques in DOM characterization. But it is highly selective to the chromophoric DOM instead of the overall DOM pool, and can be easily affect by ion strength and pH changes (Minor et al. 2014). Two absorbance indices are extensively applied in DOM studies.

The specific UV absorbance ($SUVA_{254}$) measures the absorbance at the wavelength of 254 nm at normalized DOM concentrations. It has been used as an indictor of the relative aromaticity in DOM samples, in which a higher $SUVA_{254}$ value is associated with greater aromatic content (Weishaar et al. 2003). $SUVA_{254}$ also correlates to the hydrophobicity or hydrophilicity in DOM samples: hydrophilic fractions were associated with low $SUVA_{254}$ (< 3) whereas hydrophobic fractions of supposedly higher aromaticity were associated with low $SUVA_{254}$ (> 4) (Weishaar et al., 2003).

The specific absorption slope ratio (S_R) is a ratio of UV spectral wavelength sections at 275-295 and 350-400 nm (Weishaar et al., 2003). Lower S_R roughly correlates to larger molecular weight and higher aromaticity in DOM (Weishaar et al., 2003). Generally, large S_R associates to marine DOM (ranging from ~1.7 for coastal DOM and up to ~4.6 for photobleached offshore DOM), whereas smaller values (S_R < 1) were recorded for terrestrial DOM (Helms et al., 2008).

3.2.2.2 Fluorescence spectroscopy

Fluorescence spectroscopy measures the fluorescence properties in DOM samples. Similar to UV-visible spectroscopy, it is efficient as well as powerful to collect DOM information like rough quantification of the concentration, characterization of certain functional groups and monitoring the reactivity, but only works on chromophoric DOM (Minor et al. 2014). Excitation-emission matrix fluorescence (EEM), as one of the most widely applied technique in the structure assessment of DOM, acquires a range of emission spectra from the excitation

spectra. EEM spectra provide rich information in terms of fluorescence indices and fluorescence peaks (Jaffé et al. 2014). The general characteristics of fluorescence indices together with UV indices are listed in Table 3-1.

The fluorescence index (FI) is used as a proxy for DOM sources (Fasching et al., 2014). FI values ranging near 1.7-2.0 is reported to represent DOM with low aromaticity (12-17%) whereas lower FI in the range of 1.3-1.5 indicates DOM of higher aromaticity (McKnight et al. 2001).

The freshness index (β/α) is a measure of fresh microbially produced DOM (Fasching et al. 2014). The β/α value >1 suggests a predominantly autochthonous origin or freshly released DOM, while β/α < 1 may indicate low production of, or aged DOM (Huguet et al. 2009).

The humification index (HIX) is another proposed indicator of DOM humification degree, where high values denote extensive humic character and unsaturation derived from terrigenous sources (Huguet et al. 2009, Ohno 2002).

Fluorescence peaks in EEM spectra can be related to the DOM sources and components, like protein-like materials or phytoplankton-derived materials. There are generally seven fluorescence peaks in EEM spectra, each corresponding to specific DOM characteristics, more detailed information is available in Table 3-2. The fluorescence peaks are traditionally used by 'peak picking' method, and nowadays extensively applied together with the statistical method parallel factor analysis (PARAFAC) (Murphy et al. 2013, Stedmon and Bro 2008). EEM with PARAFAC model quantifies the fluorescence peaks (or chemical components) into defined proportions which can be further statistically associated with other spectroscopic results such as NMR and FT-ICR MS, and has been successfully perform to access the environmental dynamics (Jaffé et al. 2014, Kellerman et al. 2015, Woods et al. 2011). However, the PARAFAC model only works under certain conditions which meet its assumptions: changes in the concentration of an analyte only influence its fluorescence intensity (not shape); a linear dependence between fluorescence and concentration is assumed; components are unique with respect to their concentration profile, emission spectra and excitation spectra; individual components do not influence each other (Murphy et al. 2013). The properties of EEM spectra can be found in Table 3-3.

Table 3-1 Characteristics of optical indices.

Terminology	Description	Characteristics
$SUVA_{254}$	Specific UV absorbance	Indicate the relative aromaticity
S_R	Specific absorption slope ratio	Roughly depends on molecular weight and relative aromaticity of DOM
FI	Fluorescence index	A proxy for DOM sources and aromaticity
β/α	Freshness index	A measure of fresh microbially produced DOM
HIX	Humification index	Proposed indicator of DOM humification degree

Table 3-2 Characteristics of fluorescence peaks, adapted from http://or.water.usgs.gov/proj/carbon/EEMS.html.

Fluorescence peak	Excitation/emission wavelength (nm)	Properties
A	260/450	Classical peak, humic-like
B	270/306	Tyrosine like-protein like, associated with autochthonous organic matter
C	340/440	Classical peak, humic-like, terrestrial, wide spread
D	390/510	Soil fulvic acid
F	370/460	In-situ fluorescence that is highly correlated to DOC (dissolved organic matter) concentrations
M/N	300/390	Humic like, possibly marine, possible microbial reprocessing, more labile humic acids
T	270/340	Tyrosine-like, protein-like, associated with autochthonous organic matter

Table 3-3 Excitation-emission matrix fluorescence (EEM) spectra.

EEM	Characteristics
Suitable compounds	Compounds containing several combined aromatic groups, or planar/cyclic molecules with several n- or π- bonds
Capabilities	Rough estimate of origin, concentration, presence and proportions of certain structural groups, molecular weights and chemical environment
Advantages	Fast, sensitive, widely applied
Limitations	Variable (affected by pH, concentration, operation conditions such as filter type and sample pretreament, chemical environment); no detailed structural information

3.2.3 Mass spectrometry (MS)

mass spectrometry
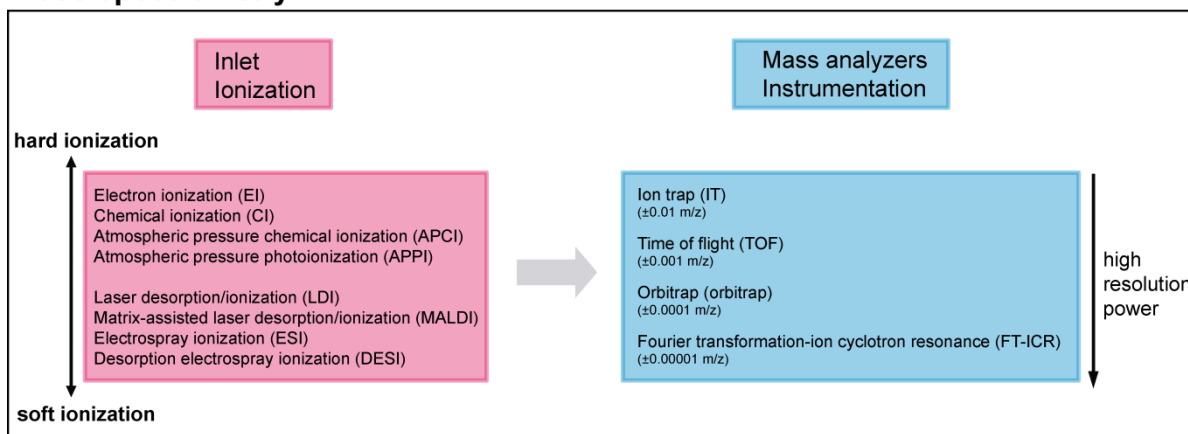
data visualization
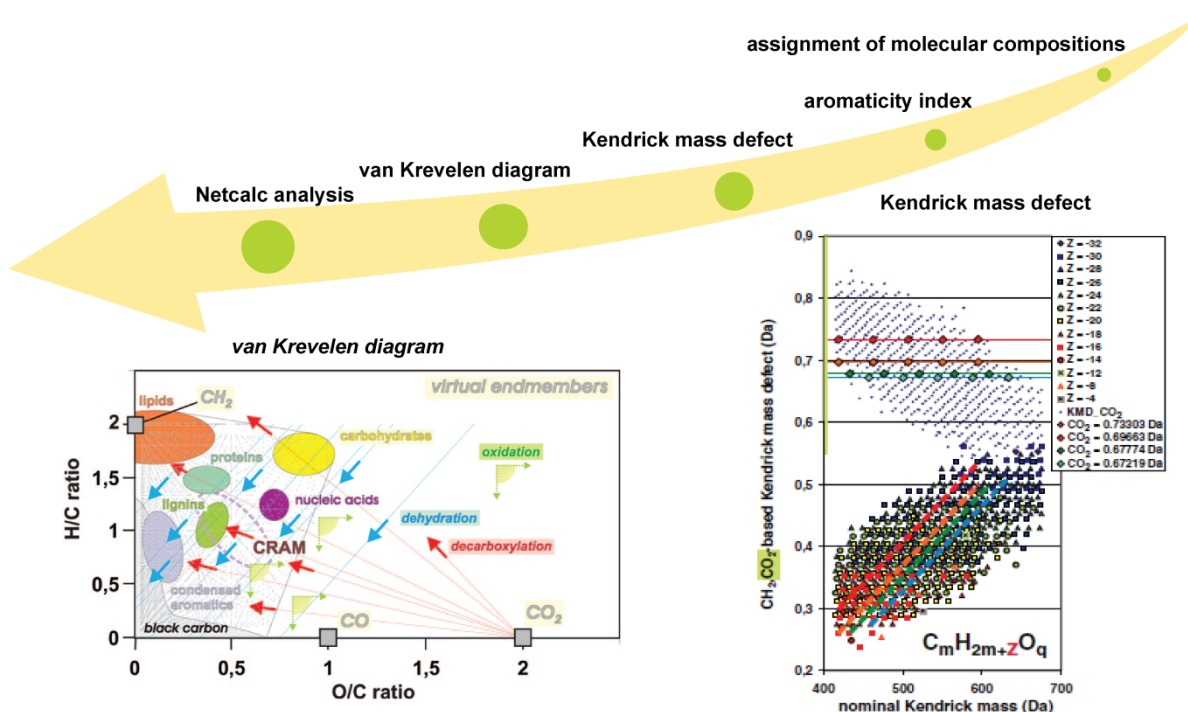
Fig. 3-1 Current available approaches for DOM characterization by mass spectrometry, adapted from Gross 2011, Hertkorn et al. 2006, 2008 and Kujawinski 2011.

3.2.3.1 Characteristics of ionization modes

Mass spectrometry (MS) generates ions from inorganic/organic compounds with appropriate methods and separates those ions according to the mass-to-charge (m/z) and detects them qualitatively and quantitatively by their m/z and abundance. The application of MS in DOM studies provides the information on molecular weights and chemical composition which can be further interpreted into different groups of compounds (Gross 2011, Kujawinski 2011,

Mopper et al. 2007, Nebbioso and Piccolo 2013). A general workflow of DOM characterization by MS can be found in Fig. 3-1.

Before applying DOM samples into the MS instrument, it is necessary to know the basic functions of different ionization modes. Nowadays, plenty of ionization modes are available. A general summary of the properties of the different ionization modes is listed in Table 3-4.

Electron ionization (EI), as the classical ionization method, ionizes the gaseous neutrals with a beam of energetic electrons with an energy of 10-60 eV shooting on them (Gross 2011). EI is suitable for low to medium polarity, non-ionic organic compounds with the molecular weight up to 1,000 amu, which should also be non-thermo-labile and volatile. Generally, it has been applied to a wide variety of different groups of molecules such as aliphatics, aromatic hydrocarbons and their derivatives, heterocycles, flavones, steroids, terpenes and so on. Moreover, EI spectra are usually measured at standard conditions and highly reproducible, allowing for the use of EI mass spectral databases available for mass peak assignment. It is a hard ionization technique, requiring high energy to get wanted molecules ionized, and in certain conditions molecular ions are too weak or absent due to the fragmentation (Gross 2011).

Chemical ionization (CI) is a soft ionization method in MS and generates ions based on ion-molecule interactions, in which gaseous molecules interact with ions (Gross 2011). The distinct mechanism of CI requires bimolecular processes to generate ions, which implies that enough ion-molecule collisions have to be induced. Thus the sensitivity of CI highly depends on the experiment conditions like the reagent gas, pressure, temperature of the ion source and the nature of the samples. In general, the molecules applicable for EI can be also analyzed by CI, and CI is commonly suitable for organic compounds with the mass range from 80 to 1200 amu (Gross 2011).

Atmospheric pressure chemical ionization (APCI) generates ions based on ion-molecule reactions at atmospheric pressure instead of in a vacuum, and a corona discharge-powered plasma is applied for ionization (Gross 2011). The neutral molecules are heated for vaporization prior to ionization. Although high temperature up to ~500 $^{\circ}$C is used for vaporization, it is still softer than the traditional CI. Typically, non-thermolabile, moderately polar and semi-volatile samples are suitable for atmospheric pressure photoionization (APPI), and the mass range of APPI can reach to 1,000 amu.

Atmospheric pressure photoionization (APPI), as an alternative or a complement for APCI, generates ions based on ion-molecule reactions at atmospheric pressure with UV light source to replace the corona plasma (Gross 2011). The energy of UV photons and the ionization energies of the molecules are essential and can affect the APPI initiation. In the APPI process, ions are actively generated from neutrals. This mode is applicable to semi-volatile, low- to medium-polar compounds with the molecular weight up to 1,000 amu. This ionization mode shows certain drawbacks: inefficient ion production, mixed ion formation, addition of dopants, and ionization depending on the dopant type.

Laser desorption/ionization (LDI) gets samples evaporated and ionized by using laser irradiation (Gross 2011). It can be applied to analyse organic/inorganic salts, molecules with large conjugated π-electron systems and UV-absorbing polymers. It can also be applied to samples at low mass range. In LDI, the range up to m/z 10^5 can be employed for the detection of ions. Recently, LDI has showed good sensitivity for N-containing aromatic species, polycyclic aromatic hydrocarbons, shale oils, ship diesel and Suwannee River DOM (Ruger et al. 2015). However, ions in LDI mode get produced depending on the polarity of analytes, ionization energy and impurities; fragmentation may occur.

Matrix-assisted laser desorption/ionization (MALDI) uses a suitable matrix material to which is intimately mixed with the samples. This mixture is then subjected to laser pulses which initiate vaporization followed by soft ionization (Gross 2011). MALDI spectra provide singly or doubly charged ions which can be interpreted easily. Compared with LDI, MALDI is softer, resulting in exclusion of detailed MS/MS information. Similar to LDI, MALDI generates ions depending on many parameters such as the polarity of analytes, ionization energy, matrix type and impurities. In general, the samples can be measured by MALDI should be either neutral or ionic with no/few salts. Theoretically, MALDI could detect unlimited high mass range; the common practical upper mass limit is near m/z 3×10^5. In order to attentuate the interference resulting from matrix ions, analyte molecules should have m/z > 3×10^3. So far MALDI has been successfully applied to proteins, peptides, carbohydrates and other large biomolecules, which occur in DOM as well.

Electrospray ionization (ESI), the most employed ionization method in MS, generates ions directly from the infused solution by applying to a conductive capillary high voltage (> kV) (Gross 2011). Unlike the ionization methods described above which actively create ions, ESI is more like a method of ion transfer. In ESI mode, analytes are present in the volatile sample

solution, and then get ionized during and after transfer into the gas phase, which renders it as a rather soft ionization process. Due to its softness, intact molecular ions are obtained. Generally, ESI is applicable for small polar molecules, medium polar compounds with the mass range of 10 to 10^3 amu, ionic metal complexes and large molecules like proteins. In ESI mode, the detected m/z can reach up to 3×10^3 amu. Its wide application range of analytes acceptance of both polarity and mass renders it compatible with different separation techniques such as LC, GC and IC. However, ESI has certain drawbacks like susceptibility to contaminants, relatively low ion currents, complex spectra due to production of cluster ions, and multiply charged ion signals.

In desorption electrospray ionization (DESI) mode, an electronically charged plume is directed on the sample surface, and then ions are withdrawn and transported through air to the mass analyzer (Gross 2011). DESI allows the analytes to be measured without sample preparation, as the greatest advantage of this technique, which makes it possible for high-throughput analysis. The analytes subjected to DESI mode should meet two requirements: soft surface of samples and the surface exposed to electrospray plume. DESI serves well for polar and non-polar compounds with low to moderate mass range, and typically m/z can reach up to 1×10^3 amu. The intrinsic limitation of DESI is that the detection of the analytes highly depends on the matrix applied and DESI performace is critically affected by many parameters in terms of angle, gas flow rate, liquid flow rate, temperature and salts.

Different ionization mode in MS has been applied on characterization of DOM/humic substances and the corresponding comparisons among them are also available. LDI was applied to Suwannee River fulvic acid, and showed ions essentially distributed at every m/z value in the range of 200-700 m/z with the absence of ions at high mass range. This phenomenon was attributed to the complexity of DOM compounds and the potential fragmentation occurred during LDI mode. Due to the polydispersity of DOM compounds together with the complexity in the ion formation, the general assumption that compounds get equally ionized and that the ions represent parent ions instead of fragmentation ions might not be applicable on LDI mode. (Fievre et al. 1997)

ESI showed the limitations on the fractions of Suwannee River fulivc acid and humic acid with large molecular weight. When the compounds are above 1000 amu, their intact ions were not observed (Reemtsma 2009, These and Reemtsma 2003). A systematic study compared ESI, APCI and APPI in both positive and negative modes on Suwannee River fulvic acid at

m/z of 200-1000 amu. Generally, larger number of detected peaks as well as the assigned formulae was obtained in negative mode than in positive mode, rendering negative mode predominately applied in MS of DOM for future studies (Hertkorn et al. 2008). The number decreased in the order: APCI > ESI > APPI in negative mode, whereas it showed the pattern: APPI > APCI > ESI in positive mode. The obtained orders were derived from the theoretical expectation that ESI ionizes a wide range of compounds while APCI and APPI are applicable for less polar and smaller molecules. This behavior clearly indicated that high selectivity in ionization modes occurred in the case of polydisperse and molecular heterogenueous DOM. Interestingly, APCI shared approximately half of the negative ions with both ESI and APPI. Moreover, ESI was found to be more selective for the compounds with high O/C ratios (0.3-0.75), APPI more selective for aromatic compounds, and APCI emphasized components with relatively smaller O/C ratios (0.2-0.4) (Hertkorn et al. 2008).

MALDI was competent to measure small moieties (m/z: 200-1200) and macromolecules together with aggregates formed within DOM (m/z: 1200-15000) (Wang et al. 2014). Compared with ESI at 200-800 m/z range, MALDI preferentially ionized more unsaturated and aromatic DOM constituents with lower O/C ratios (< 0.5) whereas ESI was selective for more polar compounds with higher O/C ratios. In MALDI mode, compounds with aromatic structures, moderate O/C ratios (0.25-0.7) and lower H/C ratios were liable to form even m/z ions while those with higher H/C ratios were more likely to form odd m/z ions. Furthermore, approximately half of molecules identified by MALDI belonged to aromatic groups which could get ionized by MALDI as they were liable to absorb electrons (Cao et al. 2015).

Table 3-4 Characteristics of ionization modes.

Ionization mode	Mechanism	Advantages	Drawback	Suitable sample	m/z
EI	A beam of electrons is shot on gaseous neutrals	Oldest and best characterized approach; reproducible spectra; libraries available	High energy required; molecular ions may be weak or absent for many compounds due to fragmentation	Non-thermolabile, volatile, Low- to medium-polar, non-ionic organic compounds	Low to moderate, $\leq 1\times10^3$ amu
CI	Gaseous compounds interact with ions and based on ion-molecule reactions	Simple mass spectra and reduced fragmentation (compared to EI)	Results depend on reagent gas type, pressure and nature of sample	Non-thermolabile, volatile	Low to moderate, $\leq 1\times10^3$ amu
APCI	Ion-molecular reactions occurring at atmospheric pressure for analyte subjected to a corona discharge	Actively generates $[M+H]^{+\cdot}$ ions from neutrals	Neutrals need to be transferred to the gas phase through heated source prior to ionization	Non-thermolabile, moderately polar, semi-volatile samples	Low to moderate; $\leq 1\times10^3$ amu
APPI	Ion-molecular reactions occurring at atmospheric pressure for analytes subjected to photoionization UV light	Actively generates ions from neutrals	Inefficient ion production; mixed ion formation. Dopants are needed; ionization is affected depending on the dopant type	Non-thermolabile, low- to medium-polar, semi-volatile samples	Low to moderate; $\leq 1\times10^3$ amu
LDI	Sample evaporated and ionized by the laser irradiation	Alternative to MALDI; no interference with matrix ions	Fragmentation may occur; ionization depending on the polarity of analytes, ionization energy and impurities	Organic/inorganic salt; molecules with large conjugated π-electron systems	Low to high; $\leq 1\times10^5$ amu
MALDI	Sample mixed with a suitable matrix material; radiation by a pulsed laser and get ionized softly	Singly and doubly charged ions; easy interpretation of mass spectra	No MS/MS details due to soft ionization; ionization can depend on the polarity of analytes, ionization energy, matrix type and impurities	Proteins, peptides, large biomolecules	Medium to high; 3×10^3 to 3×10^5 amu
ESI	Highly charged droplets are generated directly from the infused solution	Intact molecular ions; compatible with separation techniques	Sensitive to contaminants; relatively low ion currents; complex spectra due to production of cluster ions; multiply charged ion signals	Charged, polar compounds	Low to high, $\leq 3\times10^3$ amu
DESI	An electronically charged mist is directed on the sample surface, and ions are withdrawn and transported through air to mass analyzer	Without sample preparation and pre-treatment; ambient conditions; high-throughput analysis	Ionization vulnerable to many parameters: angle, gas flow rate, liquid flow rate, temperature, salt	Polar and nonpolar; soft-surface	Low to moderate, $\leq 1\times10^3$ amu

3.2.3.2   Characteristics of mass analyzers

Different mass analyzers have been applied in mass spectrometry of DOM samples, and a general description of those mass analyzers is listed in Table 3-5.

Ion trap (IP) separates ions by selected ejection time from a voltage trap. It provides a mass of resolution ~ 10^2 to 10^3 amu and a mass accuracy up to 10^{-2} amu, applicable for samples within the range up to 10^4 m/z (Gross 2011).

Time-of-flight (TOF) analyzes ions of different m/z dispersed in time during their flight along a field-free drift path of known length. Within the specific dimensions provided, the lighter ions arrive earlier at the detector and vise versa (Gross 2011). Theoretically, the flight time is proportional to $(m/z)^{1/2}$ according to the equation shown below:

$$t = \frac{s}{\sqrt{\frac{2ezU}{mi}}}$$

(s: a distance; e: electron charges; z: integer number; U: voltage; m_i: ionic mass)

TOF allows for large m/z range (up to 10^5 amu), relatively high resolution (up to 10^4), desirable mass accuracy within 10^{-3} amu and possible tandem MS^n experiment. TOF is also inexpensive and rather simple to operate, making it a widespread and accessible method.

The Orbitrap (orbitrap) analyzer measures the power absorption from axial oscillation in inhomogeneous electric fields, separates ions by trapping frequency, and employs image current detection of ion oscillations and Fourier transformation of time-domain transient signals into frequency domains. In an orbitrap, the frequency of axial oscillations ω_z can be denoted as

$$\omega_z = \sqrt{k\left(\frac{q}{mi}\right)}$$

(k: the field curvature; q: ionic charge; m_i: ionic mass)

It shows that the frequency ω_z depends on the field curvature, ionic charge and ionic mass, independent of the velocity. Here, the frequency is proportional to $(q/m)^{1/2}$.

The resolving power R can be calculated as

$$R = \frac{m}{\Delta m} = \frac{1}{2\Delta \omega z} \sqrt{\frac{kq}{m}}$$

It suggests that orbitrap offers good resolving power at both low and high m/z values (low: 50-250 m/z; high: 800-2000 m/z). Overall, orbitrap serves well for the compounds within the mass range of 10^4 amu, exhibits the resolution as high as 10^5 amu, and reaches the mass accuracy to 10^{-4} amu (Gross 2011).

Fourier Transfer Ion Cyclontron Resonance (FT-ICR) analyzes trapped ions in a strong homogeneous magnetic field (Lorenz force), separates them by cyclotron frequency, and employs image current detection and Fourier transformation of transient signals (Marshall et al. 1998, Nikolaev et al. 2016). In a FT-ICR mass spectrometer, the cyclotron frequency f_c can be denoted as

$$f_c = \frac{qB}{2\pi mi}$$

(B: magnetic field; q: ionic charge; m_i: ionic mass)

Thus, the cyclotron frequency is proportional to the magnetic field B and (q/m), independent of velocity (Marshall et al. 1998, Nikolaev et al. 2016). The magnetic field B is crucial to the FT-ICR system. It correlates positively with resolving power and scan speed, and its square associates with upper mass limit, ion trapping time, ion energy as well as number of trapped ions. However, there are other parameters jointly influence the resolution and accuracy such as ICR cell and operation conditions (Gross 2011, Marshall et al. 1998, Kido Soule et al. 2010).

Different from orbitrap, the resolving power R of FT-ICR increases linearly with magnetic field B, and is proportional to q/m. FT-ICR mass spectrometry outperforms orbitrap mass

spectrometry at relatively moderate mass range. In general, FT-ICR boasts an overwhelmingly high mass resolution and mass accuracy (R: 10^6; $\Delta m < 10^{-5}$ amu), and is suitable for analytes up to m/z ~ 10^4 (Gross 2011, Marshall 1998).

Due to its ultra-high resolution together with its exceptional mass accuracy, FT-ICR MS has been dominatingly applied in MS for DOM molecular characterization. It offers thousands of discrete molecular masses with high accuracy which allows for the precise assignment of the elemental formulas. However, FT-ICR mass spectrometers are expensive, limiting their accessibility. Other mass analyzers on the other hand show the potential for DOM molecular characterization. When DOM samples get selectively fractionated into mixtures with reduced complexity, TOF is capable to achieve fairly resolved mass peaks. For instance, following defunctionalization and coupling with GC, TOF has been successfully performed on the characterization of alicyclic terpenoids in Suwannee River fulvic acids in DOM samples (Arakawa and Aluwihare 2015).

Orbitrap demonstrates the ability to characterize the CHO compounds below 250 Da in a complex mixture and most major ionizable molecules in DOM (exception of sulfur- and phosphorus-containing compounds) (Hawkes et al. 2016). As expected, fewer mass peaks and molecular formulas were obtained by orbitrap, as well as lower resolution. Orbitrap was found to detect ions in 100-200 m/z range with highest intensity whereas FT-ICR produced low intensity mass peaks at both low and high masses with a maximum ion abundance detected around an intermediate mass (400-600 m/z) (Remucal et al. 2012). This distinct distribution of ions in these two mass analyzers can be probably explained by their resolution equations mentioned above. Thus, orbitrap is an attractive and alternative in terms of relatively satisfactory performance and low cost, and is advised to be used as an alternative for FT-ICR in case of small DOM molecules without heteroatoms (except oxygen).

Table 3-5 General characteristics of mass analyzers.

Mass analyzer	Mechanism	Mass range (m/z)	Resolution	Accuracy (amu)
IT	Selected ejection time	10^4	$10^2\text{-}10^3$	10^{-2}
TOF	Arrival time of flights	10^5	10^4	10^{-3}
Orbitrap	Trapping frequency	10^4	10^5	10^{-4}
FT-ICR	Cyclotron frequency	10^4	10^6	10^{-5}

3.2.3.3 MS-derived data analysis and visualization

Once the MS measurement is finished, data analysis is necessary so that meaningful information can be drawn from it. MS-derived data analysis and visualization includes employment of formula assignment, Kendrick mass defect (KMD) analysis, van Krevelen diagram vidualization, aromaticity index computation and application of Netcalc analysis. Detailed properties of these tools of data analysis and visualization are listed in Table 3-6.

For the measured mass spectra, certain steps should be taken in order to obtain an aumbiguously reliable formula assignment. Generally, the core elements for DOM molecular composition are restricted to C, H, O, N, S, P and ^{13}C based mass peaks on the actual elemental analysis, and acknowledgement of these restrictions will attenuate the likelihood of false assignment to some extent. Then, the assigned formulae are examined by different chemical rules, namely, double bond equivalents (DBE), nitrogen rules and conservative thresholds for molecular ratios. In addition, other optional applications can also be helpful, for example, sorting the molecular formulas into homogenous series as well as calculation of isotope ratios and predicted carbon number of intense mass peaks (Koch et al. 2007).

Once the accurate formulae are assigned, two basic tools can be implemented to visualize the mass data. KMD analysis is applied for the recognition of homogenous series in a plot which is consisted of KMD as the y-axis and the nominal Kendrick mass as x-axis. Basically, compounds with the same constitution of heteroatoms and number of rings plus double bonds but different counts of groups have identical KMD. The mass scale of CH_2 is defined as 14.000 Da, and its corresponding IUPAC mass is 14.015650 Da. The CH_2-based Kendrick mass is defined as Kendrick mass = $(14.000/14.015650) \times$ IUPAC mass.

$$KMD = \text{Nominal Kendrick mass} - \text{Kendrick mass}$$

The common van Krevelen diagram is consisted of H/C ratios vs. O/C ratios. It provides assessment of different molecular groups together with certain chemical reactions, and the adapted version even offers information about the distribution of heteroatom-containing (N, S, P…) compounds in DOM (Hertkorn et al. 2008, Kim et al. 2003, Mopper et al. 2007, Schmitt-Kopplin et al. 2010). It is noteworthy that this plot provides the rough estimates of the molecular compositions, which is not sufficient enough to assign to unumbigous classes (Fig. 3-2). For example, the lignins and CRAMs overlap in the same region. Furthermore, there are no strict boundaries among different molecular classes of compounds in van Krevelen diagrams (Hertkorn et al. 2006, Minor et al. 2014, Kim et al. 2003).
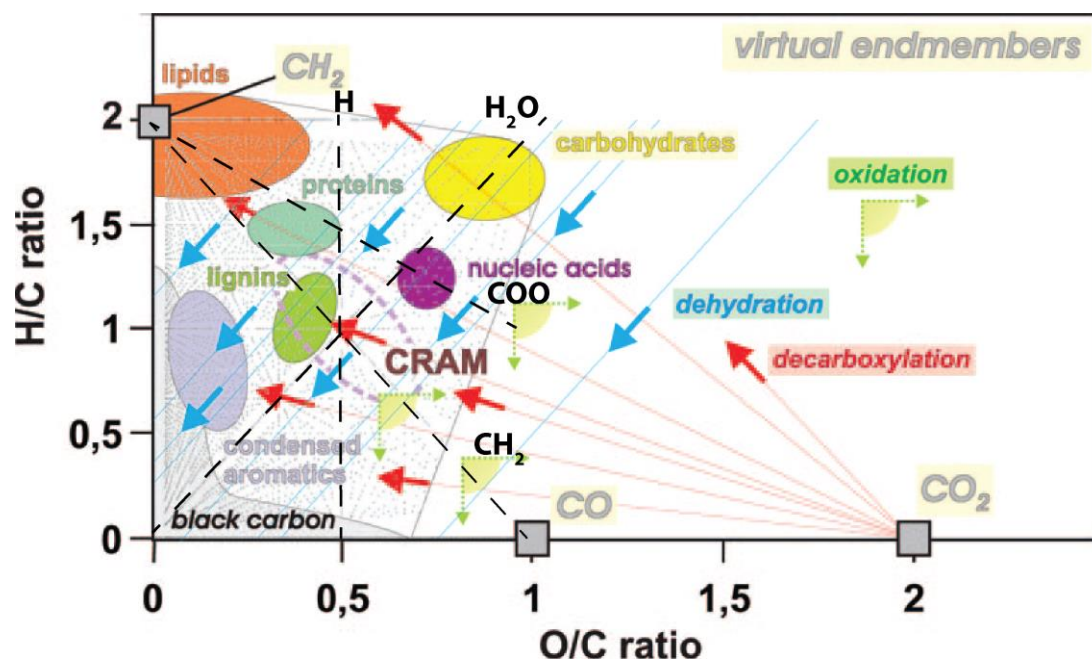
Fig. 3-2 Van Krevelen diagram of groups of various compounds and the lines indicative of chemical reactivities, adapted from Hertkorn et al. 2008.

Certain structural estimates can be deduced from extreme elemental ratios such as strongly hydrogen-deficient molecules. As an example, the aromaticity index (AI) or a modified AI can be calculated from molecular formulas as below (Koch and Dittmar 2006):

$$AI = \frac{1 + C - O - S - 0.5H}{C - O - S - N - P}$$

62

$$AI_{mod} = \frac{1 + c - 0.5O - S - 0.5H}{C - 0.5O - S - N - P}$$

The aromaticity index is proposed as criteria for assignment of aromatic compounds with threshold over 0.5 and condensed aromatics with the value over 0.67. Moreover, AI is easily implemented into van Krevelen diagram which facilitates the visualization of DOM molecular composition. However, AI is applicable for aromatics with few alkyl chains, but underestimates the values on aromatics with long alkyl chains. A modified version termed aromaticy equivalent (X_c) was proposed, which offers a constant value for each proposed core structure regardless of the degree of alkylation (Yassine et al. 2014). Threshold values of $X_c \geq$ 2.5000 and $X_c \geq$ 2.7143 were employed as unambiguous minimum criteria for the presence of aromatics and condensed aromatics, respectively.

Different visualization approaches (e.g. Netcalc analysis) enable improved assignment of elemental composition, classification of functional groups and even the reaction pathways. Kendrick-analogous networks are consisted of compositional networks (based on elemental composition) and functional networks (based on selected functional group equivalents), complementary to KMD plot and van Krevelen diagrams. By using the methods of formula assignment, the networks not only offer larger proportions of reliable molecular composition but also remove false annotations (Tziotis et al. 2011).

Table 3-6 General tools used for MS-derived data visualization.

Terminology	Functions	Description
Aromaticity Index (AI)	Indicative of aromatic compounds	AI ≥ 0.5, indicative of aromatic compounds; AI ≥ 0.67, indicative of condensed aromatics
Kendrick mass defect (KMD) plot	Presentation of homologous series	Compounds with the same constitution of heteroatoms and number of rings plus double bonds but different numbers of KMD groups have identical Kendrick mass defect
Van Krevelan diagram	General groups of compounds based on elemental H/C vs. elemental O/C ratios	Presentation of different groups of compounds For example, lipids, CRAM, lignin, tannin, carbohydrates, black carbon…
Netcalc analysis	Networks of MS data	Compositional networks based on elemental compositions and functional networks based on selected functional group equivalents

3.2.4 Magnetic nuclear resonance (NMR) spectroscopy

NMR is a technique that detects the spinning frequency of magnetic atomic nuclei which are placed in the homogeneous magnetic field and got irradiated by radiofrequency of several hundreds of MHz (Claridge 2016, Simpson 2012). Observation of the NMR signals requires the samples to be NMR-active, in other words, the samples should have magnetically active nuclides such as ^{1}H, ^{2}D, ^{13}C, ^{15}N, ^{19}F and ^{31}P. Generally, the magnetically active nuclides have (2I+1) spin states for a spin with the magnetic quantum number I. The effects of static field on the magnetic moment enable a percession around the applied field, referred to as Larmor procession. The direction of the motion is determined by the sign of gyromagnetic ratio γ, a unique constant for each NMR-active nuclide, which shows the number of rotations (per second) per unit of applied magnetic field. NMR occurs when two requirements are fulfilled. The first condition should be the required energy (ΔE), which can be described as below.

$$\Delta E = h\gamma B_o / 2\pi$$

(h: Planck's constant; γ: gyromagnetic ratio; B_o: magnetic field in tesla)

For a nuclear spin, near half of the spins align with the magnetic moment parallel to the applied magnetic field with the other near half antiparallel to the field, resulting in parallel (the α state, generally lower energy) and antiparallel (the β state) states. The difference in spin population between these two states can be described by Boltzmann equation:

$$N_\alpha / N_\beta = \exp(\Delta E / kT)$$

(N_α the number of spins at α state; N_β: the number of spins at β state; ΔE: the energy difference between α and β states; k: Boltzmann constant; T: temperature in Kelvin)

According to this equation, certain approaches can be taken to perturb the Boltzmann distribution: using higher magnetic field B_o; choosing an NMR-active nuclide with larger gyromagnetic ratio γ; and decreasing the temperature T.

The second condition to make NMR occur is that the frequency matches that of the Larmor precession for resonance conditions (Claridge 2016, Simpson 2012). If the frequency of applied radio frequency is well tuned to the Larmor frequency, the net magnetization can be tipped to different angles. The maximum signal intensities can be obtained at 90° or 270° pulse angle, whereas no/few signals at 180° or 360° pulse angle. After excitation, relaxation occurs. There are two basic relaxation types: spin-spin relaxation and spin-lattice relaxation.

The emitted signal from the excited nuclide, known as free induction decay (FID), is detected as a time-dependent oscillating voltage due to the spin relaxation, and is applied with Fourier transformation to change the time domain data into frequency domain data so that meaningful sample information can be drawn (Claridge 2016, Simpson 2012).

The signals generated in 1-D NMR spectrum are generally using modified single-pulse sequence. A pulse sequence in 1-D NMR spectroscopy is consisted of three distinct time periods: relaxation delay; preparation time and the detection time. Ideally, sufficient S/N ratios will accumulate following repeated pulse cycles.

NMR has been widely used for DOM structural characterization with both qualitative identification and quantitative measurement of the functional groups. Different types of NMR are available, and among them solution-state and solid-state NMR are extensively utilized. Generally, solid-state NMR is performed on the solid samples like sediments and soils, while solution-state NMR is applied to liquid samples such as the extracted DOM, even possible for DOM samples at natural conditions without pretreatment. Solution-state NMR offers the advantage over solid-state NMR to allow multidimensional NMR spectroscopy for in-depth structural elucidation of relationships between groups of atomic nuclei (Hertkorn et al. 2014, Mopper et al. 2007, Simpson et al. 2012).

3.2.4.1 ^{1}H NMR

^{1}H NMR spectra enable the expedient identification and quantification of a broad range of DOM constituents such as aliphatics, CRAM, carbohydrates, olefins and aromatics (Hertkorn

et al., 2013). The most significant features of ^{1}H NMR spectra for DOM characterization reside in two aspects: firstly, non-discrimination compared to other techniques such as mass spectrometry or optical spectroscopy; secondly, desirable sensitivity compared to other NMR measurements. For this reason, ^{1}H NMR spectroscopy is advisable to be applied for screening DOM structures. The chemical shifts and the corresponding DOM structures are summarized in Table 3-7.

Table 3-7 Substructure properties of DOM at different ^{1}H chemical shifts.

δ (^{1}H) ppm	Key substructures	Properties
10-7.0	N-heterocycles in six-membered rings, polycyclic aromatics, (poly) carboxylic acids	Main contribution from oxidized aromatics (i.e. (poly) carboxylic acids); plausible products of DOM formation/oxidation from metabolites (the transition from common metabolic mixtures into DOM implies growth of carboxylic acid content)
7.3-7.0	Single aromatic rings with neutral substituents	Aromatics containing C and H substituents are less reactive than the other ones with COOH substitution ($\delta_H > 7.3$ ppm) or with OH, OR substitution ($\delta_H < 7$ ppm)
7.0-6.5	$C_{ar}\underline{H}$ with oxygenated substituents (OH, OR) in ortho and para positions; five membered heterocycles (O, N, S)	Phenols are likely candidates from terrestrial input; susceptible to photodegradation more expediently than other aromatic molecules; small proportions possibly produced as natural products from microorganisms
6.5-6.0	Conjugated double bonds, =C-C=C$\underline{H}$, five membered ring heterocycles (O, N, S)	Commonly polarized conjugated double bonds (especially in case of O=C-C=C units); their ^{1}H NMR resonances divided one in the olefinic section ($\delta H = 6.0\text{-}5.6$ ppm) and another one in the aromatic section ($\delta_H > 7$ ppm); commonly higher reactivity is observed for conjugated double bonds than isolated double bonds
6.0-5.3	Isolated double bonds, =C$\underline{H}$; $O_2C\underline{H}$	Isolated double bonds being characteristic of natural products; proton-carrying double bonds (the only ones visible in ^{1}H NMR spectra) surprisingly stable.
5.3-5.26	Isolated double bonds, =C$\underline{H}$; $O_2C\underline{H}$	Isolated double bonds are ofen being characteristic of natural products; anomeric protons from carbohydrates resonate in this section as well
4.9-3.1	OC$\underline{H}$ oxygenated aliphatics	Home to carbohydrates (mainly from δ_H: 3.4-4.3 ppm), alcohols (commonly $\delta_H < 3.4$ ppm) and esters (commonly $\delta_H > 4$ ppm); NMR resonance derived from methoxy groups (δ_H: 3.6-3.9 ppm); plausible products for reactive precursor molecules (which end up as methoxy derivatives) such as certain CHOS compounds in methanolic elution during SPE
3.1-2.1	OCC$\underline{H}$	Section typical of CRAM and other functionalized aliphatic molecules.
2.1-1.9	OCCC$\underline{H}$	Possible contribution from acetic acid (H_3CCOOH) and acetyl groups
1.9-1.35	OCCC$\underline{H}$, branched aliphatics, condensed alicyclic rings	Alicyclic rings, especially when fused
1.35-1.25	$(CH_2)_n$ polymethylene; certain branched aliphatics	Polymethylene commonly arises from lipid molecules
1.25-0.4	CCCC$\underline{H}$, C$\underline{H}_3$ groups	Section of "pure" aliphatics = steroids, hopanoids, peptide side chains (perhaps terrestrial markers)......

3.2.4.2 ^{13}C NMR

Supportive of ^{1}H NMR, ^{13}C NMR provides a wider range of chemical shifts with reduced spectral overlaps and allows for the observation of ketone and carboxylate functional groups and other quanternary carbon atoms which are not directly accessible by ^{1}H NMR spectroscopy (Claridge 2016, Simpson 2012). Analysis of different types of carbon nuclides in ^{13}C NMR spectra in DOM samples is listed below. Furthermore, DEPT (distortionless enhancement by polarization transfer) experiment by ^{13}C NMR spectroscopy enables to differentiate different carbon multiplicities (CH, CH$_2$ and CH$_3$). Key substructures at different ^{13}C chemical shifts can be found in Table 3-8. However, the biggest disadvantage of ^{13}C NMR spectra is the low sensitivity due to only 1.1% ^{13}C carbon nuclide at natural abundance and low gyromagnetic ratio of ^{13}C ($\sim$ 1/4 of ^{1}H). The comparison of ^{1}H and ^{13}C NMR spectra is shown in Table 3-9.

Table 3-8 Key substructures at different ^{13}C chemical shifts.

δ (^{13}C) ppm	Key substructures
220-187	**C**=O, ketone and aldehyde carbons
187-167	**C**OX, carboxyl, ester and aliphatic amide carbons
167-145	**C**$_{ar}$-O, oxygen-substituted aromatic carbons
145-108	**C**$_{ar}$-C, H, carbon-or proton-substituted aromatic carbons
108-90	O$_2$**C**H, carbohydrate carbons
90-47	O**C**H, methoxyl
47-0	C**C**H, paraffinc carbons

Table 3-9 Properties of ^{1}H and ^{13}C NMR spectra.

NMR measurement	General capability	Specific utility in DOM characterization	General characteristics
^{1}H NMR	Basic information about the proton chemical environment	Key strucutres (aliphatics, CRAM, carbohydrates, olefins, aromatics)	Sensitive, strong signal overlaps, good for screening
^{13}C NMR	Basic information about the carbon chemical environment	Supportive of ^{1}H NMR, but with recognition of ketone, carboxylate functional groups and other quanternary carbon atoms; differentiation of different types of carbon nuclei	Insensitive, reduced signal overlaps (compared to ^{1}H NMR spectra)

3.2.4.3 2-D NMR

A 2-D NMR spectrum is obtained with two Fourier transformations on a matrix of data, and cross peaks that correlate information on one axis with data on the other are generated in a 2-D spectrum. A 2-D NMR pulse sequence contains four distinct time periods: relaxation delay, evolution time, mixing time and detection period. Different from the preparation time in 1-D NMR pulse sequence, here two individual parts (evolution and mixing) are observed. Evolution time involves imparting the phase character to the spins in the sample, whereas the mixing time involves transmitting the phase-encoded spins with phase information to other spins (Claridge 2016, Simpson 2012). The widely applied 2-D NMR spectroscopy teniques are discussed below.

^{1}H, ^{1}H JRES (J-resolved spectroscopy) is a homonuclear NMR experiment with ^{1}H chemical shift along F2 axis and proton-proton coupling along the F1 axis. It separates chemical shifts from scalar couplings and allows for examination one parameter without complications arising from others. It is sensitive, and can reveal abundant molecular signatures (coupling constants and multiplicity) with reduced signal overlap (Claridge 2016, Simpson 2012).

^{1}H, ^{1}H TOSCY (total correlation spectroscopy) detects homonuclear correlations in the same spin system no matter whether they are directly connected to each other, which enables remote protons to be correlated within a continuous coupling system. In comparison with correlation spectroscopy (COSY) experiments, it avoids the problem of possible cancelation of antiphase cross peaks at higher linewidth (Claridge 2016, Simpson 2012). During TOCSY experiment, mixing time is of significance. The long mixing time generally allows for the observation of cross peaks from spins that are many bonds away. In the application on DOM, it is advisable for detection of minor signatures with absorptive line shape.

^{1}H, ^{1}H COSY (correlation spectroscopy) measures the homonuclear proton correlations of scalar couplings, an alternative to TOSCY. Compared with TOCSY, it is less sensitive and has the possibility to cancelation of antiphase cross peaks at higher linewidth. However, it allows for improved resolution of small couplings at high number of F1 increments with

attenuation from differential relaxation (Claridge 2016, Simpson 2012). For instance, COSY spectra presented more meaningful definition than TOSCY spectra for marine DOM at aliphatic section where superposition of abundant TOSCY cross peaks dominated the region (Hertkorn et al. 2013).

^{1}H, ^{13}C HSQC (heteronuclear single quantum coherence), as widely applied heteronuclear single bond correlation spectroscopy, correlates ^{1}H resonances with ^{13}C resonances across single H-C bonds with only single quantum magnetization (Claridge 2016, Simpson 2012). It is flexible for modification and extension of sequence. It provides absorptive line shape, and features good combination of sensitivity and large information content. In addition, the DEPT HSQC allows for informative NMR spectral editing according to carbon multiplicity. One classical example to exhibit the power of HSQC on DOM is the characterization of seven major groups in marine ultrafiltrated DOM (Hertkorn et al. 2006).

^{1}H, ^{13}C HMBC (heteronuclear multiple bond correlation) measures multiple bond correlations of ^{1}H resonances with ^{13}C resonances. It is less sensitive than HSQC and homonuclear NMR, but boasts the superconnectivity information and better resolution which allows for assembling of extended spin system across quaternary carbon and heteroatoms (Claridge 2016, Simpson 2012).

During 2-D NMR experiment, the measuring time shows the trend: TOSCY < JRES < COSY < HSQC << HMBC (HMBC requires more than 5 times than HSQC). A systematic summary of the 2-D NMR spectra can be found in Table 3-10.

Table 3-10 Characteristics of 2D NMR spectra.

NMR measurement	General capability	Specific utility in DOM characterization
^{1}H-^{1}H JRES (J-resolved spectroscopy)	Separating chemical shifts from scalar couplings, allowing examination one parameter without complications arising from others	Sensitive; revealing abundant molecular signatures (coupling constants and multiplicity); reduced signal overlaps
^{1}H-^{1}H TOCSY (total correlation spectroscopy)	Relayed proton J-couplings with a coupled spin system (remote protons could be correlated within a continuous coupling network)	Sensitive; detection of minor signatures with absorptive line shape; particularly important for the structure determination of high molecular weight substances with limited space spin systems
^{1}H-^{1}H COSY (correlation spectroscopy)	Homonuclear correlation based on scalar couplings (directly bonded ^{1}H)	Sensitive; improved resolution of small couplings at high number of F1 increments with attenuation from differential relaxation; possibility of cancelation of antiphase cross peaks at higher linewidth
^{1}H-^{13}C HSQC (heteronuclear single quantum coherence)	Atoms directly bonded to each, one-bond correlation	Absorptive line shape; good combination of sensitivity and large information content; informative NMR spectral editing according to carbon multicity feasible
^{1}H-^{13}C HMBC (heteronuclear multiple bond correlation)	Correlations across multiple bonds, long-range correlation	Discrimination in favor of abundant molecular signals; excellent peak dispersion; allowing assembly of extended spin systems across heteroatoms and quaternary carbon

3.2.5   Complementary analysis of DOM

The polydisperse and molecularly heterogeneous DOM samples are rich in compositional information, resulting in the requirement of the complementary instrumental analysis (Hertkorn et al. 2007). In theory, isolation techniques selectively collect structure-specific DOM fractions, which are subjected to different characterization approaches with distinct characteristics: optical spectroscopy relies on the presence and chemical environments of π- and n-electrons, and are therefore strongly structure-selective; FT-ICR MS shows rather ionization selectivity and only presents mass spectra of the ionized compounds; NMR provides the overall non-discriminative characterization and quantification of functional

groups in DOM samples. Three main analytical techinques, namely NMR spectroscopy, FT-ICR mass sepectrometry and separation jointly define a volumetric pixel space (Fig. 3-3) which describes the nominal capacity of these techniques to differentiate DOM characteristics (Hertkorn et al. 2007). The intrinsic nominal resolution of separation, NMR and FT-ICR MS were 10^{2-4}, 10^{2-5} and 10^{4-5} buckets, respectively. When two techniques were hyphenated, the expansion widened significantly, for instance, separation/NMR, separation/MS and NMR/MS could reach up to 10^{4-9}, 10^{6-9} and 10^{6-10} buckets respectively. It was estimated that the expansion of current available analytical techniques could reach 10^{8-14} buckets (Hertkorn et al. 2007). Thus, it's highly encouraging to combine different organic spectroscopy techniques for DOM characterization.

Up to date, remarkable distinctions of e.g. freshwater, marine, atmospheric and extraterrestrial DOM have been made with combination of FT-ICR MS and NMR spectroscopy (Hertkorn et al. 2013, Schmitt-Kopplin et al. 2010), and DOM molecular features have been merged with corresponding optical properties with structural spectroscopy (Kellerman et al. 2015, Hertkorn et al. 2016).
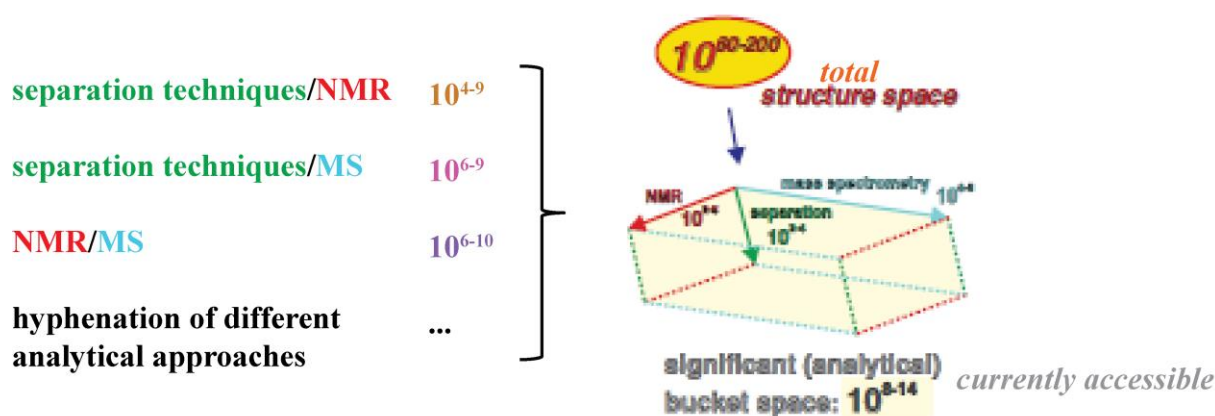
Fig. 3-3 Volumetric pixels in the form of analytical space for DOM characterization, adapted from Hertkorn et al. 2007.

In addition, complementary analysis of DOM samples with multi-level approaches generates large data sets, and their joint assessment enables in-depth elucidation or overall representation of DOM biogeochemical activities. DOM molecules have been successfully

associated with environmental parameters, optical characteristics, bacterial genes and backterioplankton communities (Lucas et al. 2016, Osterholtz et al. 2016, Traving et al. 2016), and link these correlated information to help us understand the DOM-related activities in a broader view. For example, cyanobacteria was found to be strongly correlated with protease activity; seasonal variation affected the function and community composition; community dynamics did not link to the pattern of substrate utilization capacity directly and the nitrogen-containing DOM was suggested to be of great significance to the bacteriaplankton (Traving et al. 2016).

3.3 References

Arakawa, N. and Aluwihare, L. (2015) Direct identification of diverse alicyclic terpenoids in Suwannee River Fulvic Acid. Environ Sci Technol 49(7), 4097-4105.

Ball, G. I. and Aluwihare L. (2014) CuO-oxidized dissolved organic matter (DOM) investigated with comprehensive two dimensional gas chromatography-time of flight-mass spectrometry (GC × GC-TOF-MS). Org Geochem75, 87–98.

Cao, D., Huang, H., Hu, M., Cui, L., Geng, F., Rao, Z., Niu, H., Cai, Y. and Kang, Y. (2015) Comprehensive characterization of natural organic matter by MALDI- and ESI-Fourier transform ion cyclotron resonance mass spectrometry. Anal Chim Acta 866, 48-58.

Chen, H., Stubbins, A., Perdue, E.M., Green, N.W., Helms, J.R., Mopper, K. and Hatcher, P.G. (2014) Ultrahigh resolution mass spectrometric differentiation of dissolved organic matter isolated by coupled reverse osmosis-electrodialysis from various major oceanic water masses. Mar Chem 164, 48-59.

Claridge, T.D.W. (2016) High-Resolution NMR Techniques in Organic Chemistry, 3rd Edition. Elsevier Science. ISBN: 9780080999869.

Cottrell, B.A., Cheng, W.R., Lam, B., Cooper, W. J., and Simpson, A. J. (2013) An enhanced capillary electrophoresis method for characterizing natural organic matter. Analyst, 138, 1174-1179.

Dittmar, T., Koch, B., Hertkorn, N. and Kattner, G. (2008) A simple and efficient method for the solid-phase extraction of dissolved organic matter (SPE-DOM) from seawater. Limnol Oceanogr-Meth 6(6), 230-235.

Driver, S.J. and Perdue, E.M. (2015) Acid-Base Chemistry of Natural Organic Matter, Hydrophobic Acids, and Transphilic Acids from the Suwannee River, Georgia, as Determined by Direct Potentiometric Titration. Environ Eng Sci 32(1), 66-70.

Fievre, A., Solouki, T., Marshall, A.G. and Cooper W.T. (1997). High-resolution Fourier transform ion cyclotron resonance mass spectrometry of humic and fulvic acids by laser desorption/ionization and electrospray ionization. Energ Feul 11, 554-560.

Gaspar, A., Harir, M., Hertkorn, N. and Schmitt-Kopplin, P. (2010) Preparative free-flow electrophoretic offline ESI-Fourier transform ion cyclotron resonance/MS analysis of Suwannee River fulvic acid. Electrophoresis 31(12), 2070-2079.

Green, N.W., Perdue, E.M., Aiken, G.R., Butler, K.D., Chen, H., Dittmar, T., Niggemann, J. and Stubbins, A. (2014) An intercomparison of three methods for the large-scale isolation of oceanic dissolved organic matter. Mar Chem 161, 14-19.

Gross, J.H. (2011) Mass spectrometry. Springer. ISBN: 978-3-642-42346-8.

Guo, L. and Sun M. (2009) Chapter 6: Isotope composition of organic matter in seawater. Practical guidelines for the analysis of seawater. CRC Press. DOI: 10.1201/9781420073072.ch6.

Hawkes, J.A., Dittmar, T., Patriarca, C., Tranvik, L. and Bergquist, J. (2016) Evaluation of the Orbitrap Mass Spectrometer for the Molecular Fingerprinting Analysis of Natural Dissolved Organic Matter. Anal Chem 88(15), 7698-7704.

He, W. and Hur, J. (2015) Conservative behavior of fluorescence EEM-PARAFAC components in resin fractionation processes and its applicability for characterizing dissolved organic matter. Water Res 83, 217-226.

He, Y., Harir, M., Chen, G., Gougeon, R.D., Zhang, L., Huang, X. and Schmitt-Kopplin, P. (2014) Capillary electrokinetic fractionation mass spectrometry (CEkF/MS): technology setup and application to metabolite fractionation from complex samples coupled at-line with ultrahigh-resolution mass spectrometry. Electrophoresis 35(14), 1965-1975.

Hertkorn, N., Benner, R., Frommberger, M., Schmitt-Kopplin, P., Witt, M., Kaiser, K., Kettrup, A. and Hedges, J.I. (2006) Characterization of a major refractory component of marine dissolved organic matter. Geochim Cosmochim Ac 70(12), 2990-3010.

Hertkorn, N., Ruecker, C., Meringer, M., Gugisch, R., Frommberger, M., Perdue, E.M., Witt, M. and Schmitt-Kopplin, P. (2007). High-precision frequency measurements: indispensable tools at the core of the molecular-level analysis of complex systems. Anal Bioanal Chem 389(5), 1311-1327.

Hertkorn, N., Frommberger, M., Witt, M., Koch, B.P., Schmitt-Kopplin, P. and Perdue, E.M., 2008. Natural organic matter and the event horizon of mass spectrometry. Anal Chem 80(23), 8908-8919.

Hertkorn, N., Harir, M., Koch, B.P., Michalke, B. and Schmitt-Kopplin, P. (2013) High-field NMR spectroscopy and FTICR mass spectrometry: powerful discovery tools for the molecular level characterization of marine dissolved organic matter. Biogeosciences 10(3), 1583-1624.

Hertkorn, N., Harir, M., Cawley, K.M., Schmitt-Kopplin, P. and Jaffé, R. (2016) Molecular characterization of dissolved organic matter from subtropical wetlands: a comparative study through the analysis of optical properties, NMR and FTICR/MS. Biogeosciences 13(8), 2257-2277.

Hoque, E., Wolf, M., Teichmann, G., Peller, E., Schimmack, W. and Buckau, G. (2003) Influence of ionic strength and organic modifier concentrations on characterization of aquatic fulvic and humic acids by high-performance size-exclusion chromatography. J Chromatogr A 1017(1-2), 97-105.

Imai, A., Fukushima, T., Matsushige, K. and Hwan Kim, Y. (2001) Fractionation and characterization of dissolved organic matter in a shallow eutrophic lake, its inflowing rivers, and other organic matter sources. Water Res 35(17), 4019-4028.

Kellerman, A.M., Dittmar, T., Kothawala, D.N. and Tranvik, L.J. (2014) Chemodiversity of dissolved organic matter in lakes driven by climate and hydrology. Nat Commun 5, 3804.

Kellerman, A.M., Kothawala, D.N., Dittmar, T. and Tranvik, L.J. (2015) Persistence of dissolved organic matter in lakes related to its molecular characteristics. Nat Geosci 8(6), 454-457.

Kido Soule, M.C., Longnecker, K., Giovannoni, S.J. and Kujawinski, E.B. (2010) Impact of instrument and experiment parameters on reproducibility of ultrahigh resolution ESI FT-ICR mass spectra of natural organic matter. Org Geochem 41(8), 725-733.

Kim, S., Kramer, R.W. and Hatcher, P.G. (2003) Graphical Method for Analysis of Ultrahigh-Resolution Broadband Mass Spectra of Natural Organic Matter, the Van Krevelen Diagram. Anal Chem 75(20), 5336-5344.

Kim, S., Simpson, A.J., Kujawinski, E.B., Freitas, M.A. and Hatcher, P.G. (2003) High resolution electrospray ionization mass spectrometry and 2D solution NMR for the analysis of DOM extracted by C18 solid phase disk. Org Geochem 34(9), 1325-1335.

Koch, B.P., Witt, M., Engbrodt, R., Dittmar, T. and Kattner, G. (2005) Molecular formulae of marine and terrigenous dissolved organic matter detected by electrospray ionization Fourier transform ion cyclotron resonance mass spectrometry. Geochim Cosmochim Ac 69(13), 3299-3308.

Koch, B.P., Dittmar, T., Witt, M. and Kattner, G. (2007) Fundamentals of molecular formula assignment to ultrahigh resolution mass data of natural organic matter. Anal Chem 79(4), 1758-1763.

Koch, B.P., Ludwichowski, K.-U., Kattner, G., Dittmar, T. and Witt, M. (2008) Advanced characterization of marine dissolved organic matter by combining reversed-phase liquid chromatography and FT-ICR-MS. Mar Chem 111(3-4), 233-241.

Koch, B.P., Kattner, G., Witt, M. and Passow, U. (2014) Molecular insights into the microbial formation of marine dissolved organic matter: recalcitrant or labile? Biogeosciences 11(15), 4173-4190.

Koprivnjak, J.F., Pfromm, P.H., Ingall, E., Vetter, T.A., Schmitt-Kopplin, P., Hertkorn, N., Frommberger, M., Knicker, H. and Perdue, E.M. (2009) Chemical and spectroscopic characterization of marine dissolved organic matter isolated using coupled reverse osmosis–electrodialysis. Geochim Cosmochim Ac 73(14), 4215-4231.

Kördel, W., Dassenakis, M., Lintelmann, J. and Padberg, S. (1997) The importance of natural organic material for environmental processes in waters and soils (Technical Report). Pure Appl Chem 69(7), 1571-1600.

Kruger, B.R., Dalzell, B.J. and Minor, E.C. (2011) Effect of organic matter source and salinity on dissolved organic matter isolation via ultrafiltration and solid phase extraction. Aquat Sci 73(3), 405-417.

Kujawinski, E.B. (2011) The impact of microbial metabolism on marine dissolved organic matter. Ann Rev Mar Sci 3, 567-599.

Lam, B. and Simpson, A.J. (2006) Passive sampler for dissolved organic matter in freshwater environments. Anal Chem 78(24), 8194-8199.

Li, H. and Minor, E.C. (2015) Dissolved organic matter in Lake Superior: insights into the effects of extraction methods on chemical composition. Environ Sci Process Impacts 17(10), 1829-1840.

Li, Y., Harir, M., Lucio, M., Kanawati, B., Smirnov, K., Flerus, R., Koch, B.P., Schmitt-Kopplin, P. and Hertkorn, N. (2016a) Proposed Guidelines for Solid Phase Extraction of Suwannee River Dissolved Organic Matter. Anal Chem 88(13), 6680-6688.

Li, Y., Harir, M., Lucio, M., Gonsior, M., Koch, B. P., Schmitt-Kopplin, P. and Hertkorn, N. (2016b) Comprehensive structure-selective characterization of dissolved organic matter by reducing molecular complexity and increasing analytical dimensions. Water Res 106, 477-487.

Lucus, J., Koester, I., Wichels, A., Niggemann, J., Dittmar, T., Callies, U., Wiltshire, K.H. and Gerdts G. (2016). Short-term dynamics of North Sea bacterioplankton – dissolved organic matter coherence on molecular level. Front Microbiol 7, 321.

Marshall, A.G., Hendrickson, C.L. and Jackson, G.S. (1998). Fouier transform ion cyclontron resonance mass spectrometry: a primer. Mass Spectrom Rev 17, 1-35.

Minor, E.C., Swenson, M.M., Mattson, B.M. and Oyler, A.R. (2014) Structural characterization of dissolved organic matter: a review of current techniques for isolation and analysis. Environ Sci Process Impacts 16(9), 2064-2079.

Mopper, K., Stubbins, A., Ritchie, J.D., Bialk, H.M. and Hatcher, P.G. (2007) Advanced instrumental approaches for characterization of marine dissolved organic matter: extraction techniques, mass spectrometry, and nuclear magnetic resonance spectroscopy. Chem Rev 107(2), 419-442.

Murphy, K.R., Stedmon, C.A., Graeber, D. and Bro, R. (2013) Fluorescence spectroscopy and multi-way techniques. PARAFAC. Anal Meth 5(23), 6557.

Nebbioso, A. and Piccolo, A. (2013) Molecular characterization of dissolved organic matter (DOM): a critical review. Anal Bioanal Chem 405(1), 109-124.

Nikolaev, E.N., Kostyukevich, Y.I. and Vladimirov, G.N. (2016) Fourier transform ion cyclotron resonance (FT ICR) mass spectrometry: Theory and simulations. Mass Spectrom Rev 35(2), 219-258.

Osterholz, H., Singer, G., Wemheuer, B., Daniel, R., Simon, M., Niggemann, J. and Dittmar, T. (2016) Deciphering associations between dissolved organic molecules and bacterial communities in a pelagic marine system. ISME J. 10(7), 1717-1730.

Perdue E.M. and Ritche J.D. Dissolved organic matter in fresh waters, Treatise on Geochemistry (eds, Holland H.D. and Turekian K.K.), Elsevier-Pergamon, Oxford, 2003, Vol. 5, 273-318.

Perminova, I.V., Konstantinov, A.I., Kunenkov, E.V., Gaspar, A., Schmitt-Kopplin, P., Hertkorn, N., Kulikova, N.A. and Hatfield, K. (2009) Separation technology as a powerful tool for unfolding molecular complexity of natural organic matter and humic substances. DOI: 10.1002/9780470494950. ch13.

Perminova, I.V., Dubinenkov, I.V., Kononikhin, A.S., Konstantinov, A.I., Zherebker, A.Y., Andzhushev, M.A., Lebedev, V.A., Bulygina, E., Holmes, R.M., Kostyukevich, Y.I., Popov, I.A. and Nikolaev, E.N. (2014) Molecular mapping of sorbent selectivities with respect to isolation of Arctic dissolved organic matter as measured by Fourier transform mass spectrometry. Environ Sci Technol 48(13), 7461-7468.

Raeke, J., Lechtenfeld, O.J., Wagner, M., Herzsprung, P. and Reemtsma, T. (2016) Selectivity of solid phase extraction of freshwater dissolved organic matter and its effect on ultrahigh resolution mass spectra. Environ Sci Process Impacts 18(7), 918-927.

Ratpukdi, T., Rice, J.A., Chilom, G., Bezbaruah, A. and Khan, E. (2009) Rapid Fractionation of Natural Organic Matter in Water Using a Novel Solid-Phase Extraction Technique. Water Environ Res 81(11), 2299-2308.

Reemtsma, T. (2009) Determination of molecular formulas of natural organic matter molecules by (ultra-) high-resolution mass spectrometry: status and needs. J Chromatogr A 1216(18), 3687-3701.

Remucal, C.K., Cory, R.M., Sander, M. and McNeill, K. (2012) Low molecular weight components in an aquatic humic substance as characterized by membrane dialysis and orbitrap mass spectrometry. Environ Sci Technol 46(17), 9350-9359.

Repeta, D.J. and Aluwihare, L.I. (2006) Radiocarbon analysis of neutral sugars in high-molecular-weight dissolved organic carbon: Implications for organic carbon cycling. Limnol Oceanogr 51(2), 1045-1053.

Ritchie, J.D. and Perdue, E.M. (2003) Proton-binding study of standard and reference fulvic acids, humic acids, and natural organic matter. Geochim Cosmochim Ac 67(1), 85-96.

Ruger, C.P., Sklorz, M., Schwemer, T. and Zimmermann, R. (2015) Characterisation of ship diesel primary particulate matter at the molecular level by means of ultra-high-resolution mass. Anal Bioanal Chem 407(20), 5923-5937

Sandron, S., Rojas, A., Wilson, R., Davies, N.W., Haddad, P.R., Shellie, R.A., Nesterenko, P.N., Kelleher, B.P. and Paull, B. (2015) Chromatographic methods for the isolation, separation and characterisation of dissolved organic matter. Environ Sci Process Impacts 17(9), 1531-1567.

Sandron, S., Wilson, R., Larragy, R., McCaul, M.V., Nesterenko, P.N., Kelleher, B. and Paull, B. (2014) Investigation into dissolved neutral sugars and their microbial conversion in natural and artificially produced dissolved organic matter using ion chromatography with pulsed amperometric detection and reversed-phase liquid chromatography-high resolution mass spectrometry. Anal. Methods 6(1), 107-114.

Schmitt-Kopplin, P. and Kettrup, A. (2003) Capillary electrophoresis--electrospray ionization--mass spectrometry for the characterization of natural organic matter: an evaluation

with free flow electrophoresis-off-line flow injection electrospray ionization-mass spectrometry. Electrophoresis 24(17), 3057-3066.

Schmitt-Kopplin, P., Gelencser, A., Dabek-Zlotorzynska, E., Kiss, G., Hertkorn, N., Harir, M., Hong, Y. and Gebefugi, I. (2010) Analysis of the unresolved organic fraction in atmospheric aerosols with ultrahigh-resolution mass spectrometry and nuclear magnetic resonance spectroscopy: organosulfates as photochemical smog constituents. Anal Chem 82(19), 8017-8026.

Schmitt-Kopplin, P., Liger-Belair, G., Koch, B.P., Flerus, R., Kattner, G., Harir, M., Kanawati, B., Lucio, M., Tziotis, D., Hertkorn, N. and Gebefügi, I. (2012) Dissolved organic matter in sea spray: a transfer study from marine surface water to aerosols. Biogeosciences 9(4), 1571-1582.

Simpson, A.J., Simpson, M.J. and Soong, R. (2012) Nuclear magnetic resonance spectroscopy and its key role in environmental research. Environ Sci Technol 46(21), 11488-11496.

Simpson, A.J., Tseng, L.H., Simpson, M.J., Spraul, M., Braumann, U., Kingery, W.L., Kelleherc, B. P. and Hayes, M.H.B (2004). The application of LC-NMR and LC-SPE-NMR to compositional studies of natural organic matter. Analyst, 129, 1216-1222.

Simpson, J. (2012) Organic Structure Determination Using 2-D NMR Spectroscopy, 2nd Edition. Academic Press. ISBN: 9780123849700.

Serkiz, S.M. and Perdue, E.M. (1990) Isolation of dissolved organic matter from the suwannee river using reverse osmosis. Water Res 24(7), 911-916.

Stedmon, C.A. and Bro, R. (2008) Characterizing dissolved organic matter fluorescence with parallel factor analysis: a tutorial. Limnol Oceanogr-Meth 6(11), 572-579.

Stenson, A.C. (2008) Reversed-Phase Chromatography Fractionation Tailored to Mass Spectral Characterization of Humic Substances. Environ Sci Technol 42(6), 2060-2065.

Swenson, M.M., Oyler, A.R. and Minor, E.C. (2014) Rapid solid phase extraction of dissolved organic matter. Limnol Oceanogr-Meth 12(10), 713-728.

Tfaily, M.M., Hodgkins, S., Podgorski, D.C., Chanton, J.P. and Cooper, W.T. (2012) Comparison of dialysis and solid-phase extraction for isolation and concentration of dissolved organic matter prior to Fourier transform ion cyclotron resonance mass spectrometry. Anal Bioanal Chem 404(2), 447-457.

Thurman, E. M. and Malcolm R. L. (1981) Preparative isolation of aquatic humic substances. Environ Sci Technol 15, 463-466.

Traving, S.J., Bentzon-Tilia, M., Knudsen-Leerbeck, H., Mantikci, M., Hansen, J.L.S., Stedmon, C.A., Sørensen, H., Markager, S. and Riemann, L. (2016) Coupling bacterioplankton populations and environment to community function in coastal temperate waters. Front Microbiol 7, 1533.

Tziotis, D., Hertkorn, N. and Schmitt-Kopplin, P. (2011) Kendrick-analogous network visualisation of ion cyclotron resonance Fourier transform mass spectra: Improved options for the assignment of elemental compositions and the classification of organic molecular complexity. Eur J Mass Spectrom 17(4), 415-421.

Wang, R. Druckenmüller, K., Elbers, G. Cuenther, K. and Croué, J.-P. (2014) Analysis of aquatic-phase natural organic matter by optimized LDI-MS method. J Mass Spectrom 49, 154-160.

Woods, G. C., Simpson, M. J., Kelleher, B. P., McCaul, M., Kingery, W. L. and Simpson A. J. (2010) Online high-performance size exclusion chromatography-nuclear magnetic resonance for the characterization of dissolved organic matter. Environ Sci Technol 44, 624-630.

Woods, G.C., Simpson, M.J., Koerner, P.J., Napoli, A. and Simpson, A.J. (2011) HILIC-NMR: toward the identification of individual molecular components in dissolved organic matter. Environ Sci Technol 45(9), 3880-3886.

Woods, G.C., Simpson, M.J. and Simpson, A.J. (2012) Oxidized sterols as a significant component of dissolved organic matter: evidence from 2D HPLC in combination with 2D and 3D NMR spectroscopy. Water Res 46(10), 3398-3408.

Zherebker, A.Y., Perminova, I.V., Konstantinov, A.I., Volikov, A.B., Kostyukevich, Y.I., Kononikhin, A.S. and Nikolaev, E.N. (2016) Extraction of humic substances from fresh waters on solid-phase cartridges and their study by Fourier transform ion cyclotron resonance mass spectrometry. J Anal Chem 71(4), 372-378.

Chapter 4

Proposed Guidelines for Solid Phase Extraction of Suwannee River Dissolved Organic Matter

4 Proposed Guidelines for Solid Phase Extraction of Suwannee River Dissolved Organic Matter

4.1 Summary

This work proposes improved guidelines for DOM isolation by means of SPE with PPL sorbent, which has become an established method for isolation of DOM from natural waters due to ease of application and appreciable carbon recovery. Suwannee River water was chosen to systematically study the effects of critical SPE variables such as loading mass, concentration, flow rate and up-scaling on the extraction selectivity of PPL sorbent. FT-ICR MS and ^{1}H NMR spectroscopy were employed to interpret the DOM chemical space of eluates as well as permeates and wash liquids with molecular resolution. Up to 89% DOC recovery was obtained with a DOC/PPL mass ratio of 1:800 at 20 mg/L DOC concentration. With larger loading volumes applied, less highly oxygenated compounds were retained on PPL sorbent. Effects of flow rate were marginal. Up-scaling had limited effects on the extraction selectivity with the exception of increased self-esterification with methanol solvent, resulting in methyl ester groups. Furthermore, SPE/PPL extract showed the highly representative characteristics by comparing with authentic water and reverse osmosis samples. These findings are useful to reproducibly isolate DOM with representative molecular compositions from various sources and concentrations as well as to minimize potential inconsistencies among interlaboratory comparative studies.

4.2 Author contributions

Yan Li, Mourad Harir, Philippe Schmitt-Kopplin and Norbert Hertkorn designed the experiment;

Yan Li conducted the experiment, measured on FT-ICR MS with the help of Basem Kanawati and measured on NMR with the help of Norbert Hertkorn;

Marianna Lucio and Kirill Smirnov helped to evaluate the data;

Ruth Flerus and Boris P. Koch measured DOC and gave great inputs on paper correction;

Yan Li wrote the paper together with Mourad Harir and Norbert Hertkorn with great contributions from Basem Kanawati and Philippe Schmitt-Kopplin.

Chapter 5

Comprehensive Structure Selective Characterization of Dissolved Organic Matter by Reducing Molecular Complexity and Increasing Analytical Dimensions

Published as: *Yan Li, Mourad Harir, Marianna Lucio, Michael Gonsior, Boris P. Koch, Philippe Schmitt-Kopplin, Norbert Hertkorn (2016). Comprehensive structure-selective characterization of dissolved organic matter by reducing molecular complexity and increasing analytical dimensions. Water Research. (106), 477-487.*© Copyright Elsevier.

5 Comprehensive Structure Selective Characterization of Dissolved Organic Matter by Reducing Molecular Complexity and Increasing Analytical Dimensions

5.1 Summary

Deciphering the molecular codes of dissolved organic matter (DOM) improves our understanding of its role in the global element cycles and its active involvement in ecosystem services. This study demonstrates comprehensive characterization of DOM by an initial polarity-based stepwise SPE with single methanol elution of the cartridges, but separate collection of equal aliquots of eluates. The reduction of molecular complexity in the individual DOM fractions attenuates intermolecular interactions and substantially increases the disposable resolution of any structure selective characterization. Suwannee River DOM (SR DOM) was used to collect five distinct SPE fractions with overall 91% DOC recovery. Optical spectroscopy (UV and fluorescence spectroscopy), FT-ICR MS and NMR spectroscopy showed analogous hierarchical clustering among the five eluates corroborating the robustness of this approach. Two abundant moderately hydrophobic fractions contained most of the SR DOM compounds, with substantial proportions of aliphatics, carboxylic-rich alicyclic molecules, carbohydrates and aromatics. A minor early eluting hydrophilic fraction was highly aliphatic and presented a large diversity of alicyclic carboxylic acids, whereas the two late eluting, minor hydrophobic fractions appeared as a largely defunctionalized mixture of aliphatic molecules. Comparative mass analysis showed that fractionation of SR DOM was governed by multiple molecular interactions depending on O/C ratio, molecular weight and aromaticity. The traditional optical indices $SUVA_{254}$ and fluorescence index (FI) indicated the relative aromaticity in agreement with FT-ICR mass and NMR spectra; the classical fluorescent peaks A and C were observed in all four latter eluates. This versatile approach can be easily expanded to preparative scale under field conditions, and transferred to different DOM sources and SPE conditions.

5.2 Author contributions

Yan Li, Mourad Harir, Philippe Schmitt-Kopplin and Norbert Hertkorn designed the experiment;

Yan Li conducted the experiment, measured on FT-ICR MS independently and measured on NMR with the help of Norbert Hertkorn;

Marianna Lucio created a new method for EEM analysis;

Michael Gonsior measured optical spectroscopy and corrected the manuscript;

Boris P. Koch measured DOC and gave great inputs on paper preparation and correction;

Yan Li wrote the paper together with Mourad Harir and Norbert Hertkorn with great contributions from Philippe Schmitt-Kopplin.

Chapter 6

How Representative Are Dissolved Organic Matter (DOM) Extracts? A Comprehensive Study of Sorbent Selectivity for DOM Isolation

6 How Representative Are Dissolved Organic Matter (DOM) Extracts? A Comprehensive Study of Sorbent Selectivity for DOM Isolation

6.1 Abstract

Solid phase extraction (SPE) has become a widespread method for isolating dissolved organic matter (DOM) of diverse origin such as fresh and marine waters. This study investigated the DOM extraction selectivity of 24 commercially available SPE sorbents under identical conditions (pH = 2, methanol elution) on the example of Suwannee River (SR) water and North Sea (NS) water by using DOC analysis and Fourier transform ion cyclotron resonance mass spectrometry (FT-ICR MS). Proton nuclear magnetic resonance (^{1}H NMR) spectroscopy was employed to assess leaching behavior, and HLB sorbent was found to leach substantially, among others. Scatter of average H/C and O/C elemental ratios and gross alignment in mass-edited H/C ratios according to five established coarse SPE characteristics was near identical for SR DOM and NS DOM. FTMS-based principal component analysis (PCA) provided essentially analogous alignment of SR DOM and NS DOM molecular compositions according to the five established groups of SPE classification, and corroborated the sorption-mechanism-based selectivity of DOM extraction in both cases. Evaluation of structural blanks and leaching of SPE cartridges requires NMR spectroscopy because FT-ICR mass spectrometry alone will not reveal inconspicuous displacements of continual bulk signatures caused by leaching of SPE resin constituents.

Keywords: DOM, SPE, NMR, FT-ICR MS, sorbent selectivity, leaching

6.2 Introduction

Dissolved organic matter (DOM) is a collection of organic compounds with ~50% carbon content and variable proportions of heteroatoms such as oxygen, nitrogen, sulphur and phosphorus (Perdue and Ritchie, 2003; Hertkorn et al., 2007). As one of the most abundant contributors to global carbon and other element cycles (Battin et al., 2009; Bianchi, 2011; Hertkorn et al., 2007; Ksionzek et al., 2016; Perdue and Ritchie, 2003), DOM is widely distributed in all terrestrial ecosystems and found in oceans, rivers, lakes, permafrost and soil, to name a few. DOM features ecosystem-dependent composition and structure and performs an array of relevant ecosystem services such as influencing microbial metabolism in waters, affecting greenhouse gas production and defining speciation of key nutrient and trace elements (Duarte and Duarte, 2015; Goldberg et al., 2015; Lucas et al., 2016; Mann et al., 2015;Osterholz et al., 2016). However, owing to its extensive molecular heterogeneity and polydispersity, a vast majority of DOM constituents remains unknown at the molecular level (Hertkorn et al., 2007; Minor et al., 2014; Sandron et al., 2015).

To this day, one of the most relevant challenges preceding DOM molecular characterization is efficient and reproducible collection of representative samples with appreciable recovery. DOM molecular structures reproduce ecosystems characteristics and vary significantly depending on origin (Hertkorn et al., 2016; Kruger et al., 2011). For instance, freshwater DOM shows high proportions of linear terpenoids (Lam et al., 2007) and carboxyl-rich alicyclic molecules (CRAM) (Arakawa and Aluwihare, 2015; Hertkorn et al., 2006). Marine DOM is composed of labile, semilabile and refractory components, encompassing compound classes as diverse as (labile) carbohydrates and (refractory) black carbon (Moran et al., 2016), thereby covering a wide range from polar to nonpolar compounds. While deep seawater DOM is enriched in CRAM (Hertkorn et al, 2006), surface seawater DOM contains up to 50% polysaccharides (Benner et al., 1992), particularly in nutrient-rich upwelling areas of high biological productivity.

DOM collection is a key as well as an error-prone step which directly influences the overall coverage and the consecutive instrumental analysis, and substantial efforts have been invested to improve the isolation methods of polydisperse and molecularly heterogeneous DOM (Minor et al., 2014; Nebbioso and Piccolo, 2013; Sandron et al., 2015). After more than two decades' endeavour, solid phase extraction (SPE) has become an established and widely used DOM isolation method combining ease of use and high extraction efficiency ($\geq 40\%$ DOC recovery) (Dittmar et al., 2008; Green et al., 2014; Kim et al., 2003; Tfaily et al., 2012). In particular, SPE with certain sorbents like PPL, C18 and HLB has enabled a broad coverage of DOM constituents in one single collection (Dittmar et al., 2008; Li and Minor, 2015; Perminova et al., 2014; Raeke et al., 2016; Ward et al., 2013).

With increasing focus on the molecular compositions of the obtained SPE extracts instead of merely evaluating DOC recovery, the DOM extraction selectivity of the SPE cartridges with respect to certain DOM compounds has drawn awareness, and DOM extracts obtained with different functionalized SPE sorbents have been com-pared (Minor et al., 2014; Sandron et al., 2015). While PPL was reported to retain higher proportions of nitrogen-containing compounds from both fresh- and marine waters (Dittmar et al., 2008; Perminova et al., 2014; Zherebker et al., 2016), C18 had shown affinity to more saturated molecules in arctic marine DOM and distinct DOM from oligotrophic Lake Superior (Li and Minor, 2015; Perminova et al., 2014); on the other hand, HLB could not completely elute freshwater DOM compounds with high molecular weight (Raeke et al., 2016). How-ever, the selectivity of relevant commercially available SPE sorbents of potential use for DOM isolation in fresh and marine water bodies has not yet been systematically investigated, and a structure-selective assessment of SPE leading behaviour is missing about entirely.

Our work firstly aimed to address the representativeness of SPE extracts in terms of DOC recovery and molecu-lar compositions by using 24 commercially available sorbents with different functionalities under identical con-ditions of extraction and elution (pH = 2; methanol elution). Suwannee River water (SR DOM) and North Sea water (NS DOM) were chosen to represent freshwater and oceanic DOM. Molecular elucidation of SPE selectiv-ity

was achieved mainly with Fourier transform ion cyclotron resonance mass spectrometry (FT-ICR MS).

In addition, structure-selective leaching behaviour of all these SPE sorbents was evaluated with proton nuclear magnetic resonance (^{1}H NMR) spectroscopy. High-field NMR spectroscopy provides the capability for quantita-tive and non-destructive de novo determination of chemical environments in polydisperse and molecularly heterogeneous environmental samples such as DOM (Hertkorn et al., 2007; Lam et al., 2007). Quantitative relationships between number of spins and area of NMR resonances operate in absence of differential NMR relaxation (Hertkorn 2015). This key feature implies the use of NMR spectroscopy as a quantitative reference for complementary structure-selective analytical methods, like mass spectrometry, which detects gas phase ions and is subject to ionization selectivity in case of complex mixtures (Hertkorn et al., 2008). NMR spectroscopy is particularly informative in the description of aliphatic chemical environments which are based on sp3-hybridized carbon.

6.3 Methods

6.3.1 Sample Preparation

Samples were taken in Suwannee River in May 2012 as described by Green et al. (Green et al., 2014), and in June 2014 in the Southern North Sea (54.1757 N / 7.8977 E; RV Heincke, Expedition HE 426 II). Water samples were immediately filtered after collection with 0.47 μm GF/F glass fiber (Whatman, precombusted at 450 ^{o}C) and adjusted to pH 2 (concentrated HCl, Merck). The acidified SR and NS water samples were stored at 4oC in the dark and consecutively subjected to SPE by using 24 commercially available cartridges (2OH, C1, C2, C8, C18, C18OH, CBA, CH, CN-E, CN-U, DPA-6S, ENV, HLB, MAX, MCX, NH2, PH, PPL, SAX, SCX, SI, Strata XC, WAX and WCX) as shown in Table S1. Blanks were performed using acidified Milli-Q water (pH 2). SPE procedures were performed in triplicates according to our standard protocols (Li et al, 2016). 1 mL SR water and 50 mL NS water were

loaded on the cartridges, respectively, and eluted with 1 mL methanol. After SPE, the extracts were kept at -25 °C in the dark prior to further analysis (Flerus et al., 2011).

6.3.2 DOC measurement

DOC was determined by high temperature catalytic oxidation and subsequent non-dispersive infrared spectros-copy and chemiluminescence detection (TOC-VCPN, Shimadzu). Final DOC concentrations are average values of triplicate measurements. If the standard variation or the coefficient of variation exceeded 0.1 μM or 1 %, respectively, up to two additional analyses were performed and outliers were eliminated. After each batch of five samples, one reference standard (DOC-DSR, Hansell Research Lab, University of Miami, USA), one ultrapure water blank and one potassium hydrogen phthalate standard were measured. The limit of detection (3σ of the blank) and quantitation (9σ of the blank) was 7 and 21 μmol C $L-1$, respectively. The accuracy was ±5 %. POC was determined by the difference between TOC and DOC measurements (Koch et al., 2014). Samples (100 μL of methanol eluates – equivalent to 1 mL SR water and 50 mL NS water) were evaporated and re-dissolved in 1 mL ultrapure water for analysis.

6.3.3 FT-ICR MS analysis

High field Fourier transform ion cyclotron resonance mass spectra were acquired by a 12 T Bruker Solarix mass spectrometer (Bruker Daltonics, Bremen, Germany) and an Apollo II electrospray ionization (ESI) source in negative ionization mode. Samples were diluted in methanol at a concentration of ~5 μg/mL, and injected into electrospray source at a flow rate of 120 μL/h with a nebulizer gas pressure of 138 kPa and a drying gas pressure of 103 kPa. Spectra were firstly calibrated externally on clusters of arginine in methanol (10 μg/mL), and then internally calibrated using extended CHO molecular series present in natural organic matter, reaching accuracy values lower than 500 ppb. The spectra were acquired with a time domain of 4 Mega words over a mass range of m/z 150-1000 amu, and 500 scans were accumulated for each spectrum. Elemental formulas were calculated for each peak in a batch mode by using in-house written software (Tziotis et al., 2011).

6.3.4 NMR analysis

All ^{1}H NMR spectra of SPE extracts (600 µL) were acquired with a Bruker Avance III 500 MHz spectrometer (B0 = 11.7 T) at 283 K from redissolved solids in CD_3OD (99.95% ^{2}H; Merck) with Bruker standard pulse se-quences using sealed 2.0 and 2.5 mm Bruker Match tubes. 1H NMR chemical shift reference of HD_2COD was 3.30 ppm. ^{1}H NMR spectra were recorded with solvent suppression by pre-saturation and 1 ms spin-lock (*noesypr1d*), 5 s acquisition time, 5 s relaxation delay (d1), typically 1024 scans, 1 Hz exponential line broadening. ^{1}H NMR spectra of SR DOM and NS DOM were acquired from ~2 mg of isolated solid with a Bruker Avance III 800 MHz spectrometer (B_0 = 18.7 T) in Bruker 3.0 mm Match tubes at otherwise identical conditions (Fig. S2).

6.3.5 Statistical analysis

Principal component analysis (PCA) was performed with SIMCA P-9.0. Because of the huge differences in mass peak amplitude between leachate and DOM molecules in certain SPE eluates, FT-ICR MS mass peak intensities were transposed into decadal logarithmic values prior to matrix generation; zeroes were substituted by ones (log 1 = 0). Only assigned mass peaks present in ≥3 extracts were chosen for PCA analysis in order to reduce the matrix complexity; consolidated (logarithmic values of) mass peak intensities were used. According to place-ment in PCA, two groups were defined: group A and group B, respectively (Figures 4 and 5). Mathematical comparison between group A and group B was performed by using Matrix Generator and, after filtering using mass peaks present in ≥3 extracts of each group A and B, led to the distinction of (a) assigned mass peaks pre-sent in group A (union, and not intersection counts), (b) assigned mass peaks present in group B (union, and not intersection counts), and (c) assigned mass peaks present in both groups A and B (intersection count). PCA-derived and other van Krevelen diagrams as well as mass-edited H/C ratios have been computed from averaged mass peak intensities. 1H NMR data section integrals were obtained by AMIX (Version 3.4.2, Bruker) at 0.01 ppm section integral bucket resolution with the exclusion of HDO and HD_2COD in the ^{1}H NMR chemical shift range from 0.5 – 9.5 ppm.

6.4   Results and discussion

6.4.1   Extraction efficiency

24 commercially available SPE sorbents with distinctive functionalities were chosen for isolation of SR DOM and NS DOM. All the cartridges were used under identical conditions (pH = 2; methanol elution) instead of under the manufacturers' instructions because comparison of DOC recovery and molecular structures under the same chemical environments of pH and solvent will attenuate certain selective adsorption and potential side reactions of DOM, like e.g. hydrolysis or pH-dependent dissociation. According to Fig. 1 and Fig. S1, DOC recoveries varied significantly not only among sorbents but also between the freshwater and marine sources. In general, DOC recoveries were comparatively higher in case of SR DOM with values ranging from 20-90%, and to this effect lower in case of NS DOM with values ranging from 10-50%. The nominal ratios of DOC recovery as expressed by SR DOC/NS DOC varied from ~ 3.5 in case of SCX and NH_2 down to ~ 1 in case of CBA, Strata XC and WCX (Fig. 6-1). Other studies had also observed a significant decrease in DOC recovery when dealing with marine DOM, and had attributed this phenomenon to the smaller molecular size and higher polarity in marine DOM (Dittmar et al., 2008; Osterholz et al., 2016). However, DOC recoveries of NS DOM were lowest when polar or ion exchange sorbents were employed (Fig. 1 and Fig. S1). This probably results from the fact that marine DOM is comprised of compounds with a wide range of polarities that cannot be extracted by one single sorbent with considerable recovery. In comparison, freshwater DOM, which contains large proportions of non-polar compounds (Lam et al., 2007; Ratpukdi et al., 2009) could be readily extracted by sorbents with non-polar functionalities, such as C8, C18, HLB and PPL (Dittmar et al., 2008; Perminova et al., 2014; Raeke et al., 2016; Li et al., 2016).

Common commercially available SPE sorbents comprise mainly silica-based and polymer-based materials (Fig. 6-1 and Fig. S1; Table S1). DOC recoveries were relatively high with polymer-based sorbents but more variable with silica-based sorbents (Fig. 1). For example, polymer-based sorbents such as DPA-6S, PPL, ENV and HLB exhibited higher DOC

97

recoveries, indicating high extraction efficiency, which may be affected by a variable degree of leaching from sorbents. Among the silica based cartridges, those with the mechanism of polar or ion exchange showed lower recoveries than those with non-polar mechanism. In addition, DOC recoveries in non-polar silica-based sorbents corresponded to their specified carbon loadings (Table S1), with higher carbon load-ing resulting in higher DOC recovery. For instance, in the series of C1, C2, C8 and C18 sorbents, a continual increase in DOC recovery was observed (Fig. 6-1 and Fig. S1; Table S1).
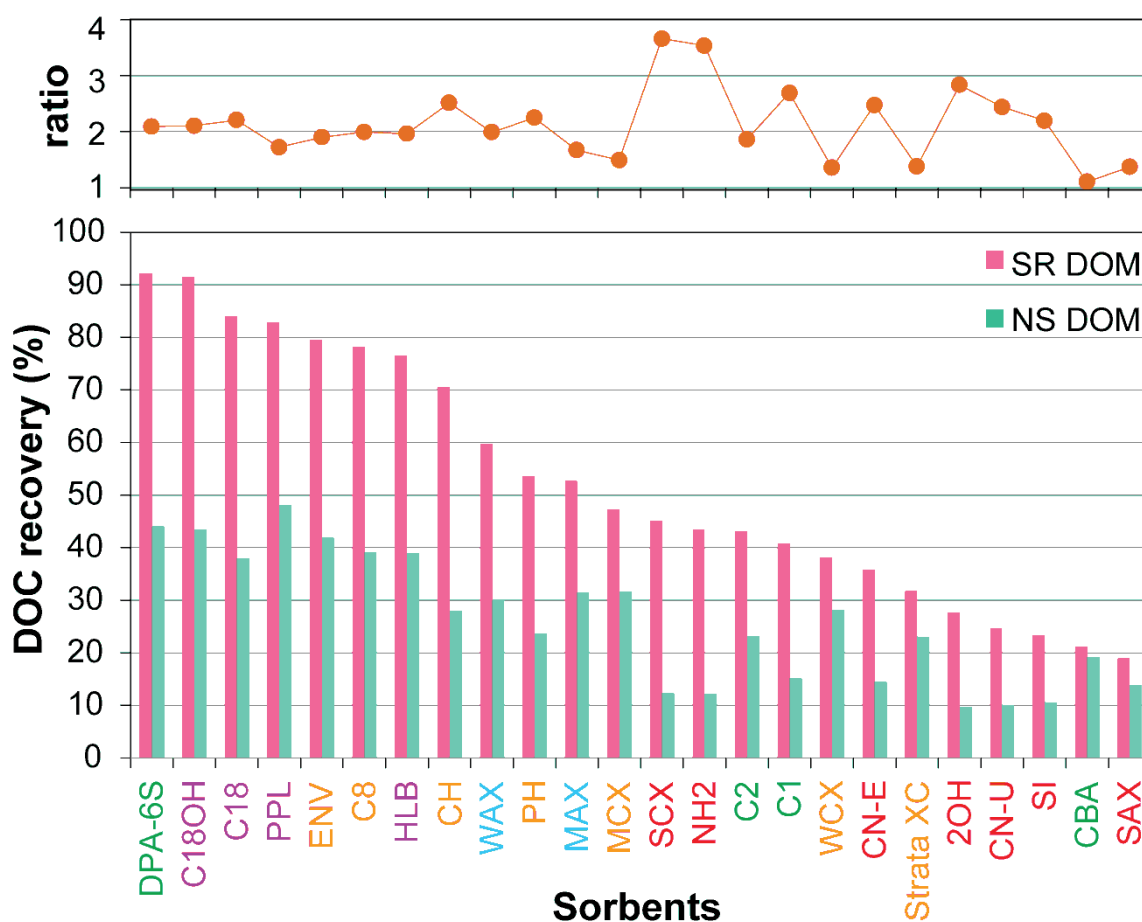
Fig. 6-1 DOC recoveries of DOM extracts obtained with 24 commercially available sorbents. The ratio was calculated with DOC recovery of SR DOM / DOC recovery of NS DOM. Purple: non-polar; blue: mixed mode with anion exchange; orange: moderately non-polar and mixed mode with cation exchange; green: weekly non-polar and mid-polar; red: polar and strong ion exchange.

6.4.2 FT-ICR mass spectrometry

Negative electrospray ionization (ESI) FT-ICR mass spectra of 24 SPE extracts allowed clear distinction of CHO, CHOS and CHNO molecular series and initially provided insights into its key chemical characteristics such as average elemental ratios, average molecular weight and relative unsaturation and oxygenation (Table S2 and S3). Van Krevelen diagrams and mass-edited H/C ratios showed larger scatter in case of NS SPE-DOM extracts when compared with SR SPE-DOM extracts (Fig. 6-2 and Fig. 6-3). The nominal variance of NS DOM and SR DOM ranged near Δ(H/C) ~ 0.55 vs. 0.40, and Δ(O/C) ~ 0.35 vs. 0.30. This was consistent with a more pronounced extraction selectivity in case of marine DOM as already indicated by the higher variations of NS DOC recovery described above (Fig. 6-1). Moreover, NS DOM extracts showed a higher H/C ratio and a lower O/C ratio than the SR DOM extracts. This was in agreement with ^{1}H NMR spectra that indicated higher aliphaticity of NS DOM compared with SR DOM (38% vs. 30% for purely aliphatic units CCCH; Fig. S2, Table S4), but lower content of unsaturated C_{sp2}H units than found in SR DOM (6% vs. 11%; Table S4).

In general, clustering according to decrease in average H/C and increase in average O/C ratio of SR DOM fol-lowed the order: polar or strong ion exchange < weakly non-polar or mid-polar < mid non-polar & mixed mode with cation exchange < mixed mode with anion exchange < non-polar (Fig. 6-2). With the exception of "polar and strong ion exchange" resins, the average molecular weights of the SR DOM extracts were largely confined to a rather narrow range of m/z ~380-400. For NS DOM extracts, "polar and strong ion exchange" SPE resins cov-ered a relatively large range of low average mass (m/z ~ 290 – 360), weakly non-polar and mid polar resins produced NSDOM ranging from m/z ~ 360 – 390, whereas all other DOM extracts covered a narrow mass range of m/z ~ 370 – 390 (Fig. 6-3; Table S3). In case of SR DOM, the polar and strong ion exchange extracts NH_2, 2OH and SCX were most oxygen-depleted (O/C ratio < 0.3), of lowest average mass (m/z < 360; Fig. 6-2, Fig. 6-3), and their mass spectra were strongly depleted of organic matter signatures, suggesting dominant contributions by molecules leaching from the SPE cartridges (Fig. S4, Fig. S5) in agreement with ^{1}H NMR spectra (Fig. S3). Analogous, but attenuated behavior was demonstrated for the

other members of this series, i.e. SI, SAX, CN-U and CN-E resins, all of which showed weaker oxygen-depletion (O/C ratio ~ 0.30-0.36) and a low average mass (m/z ~ 360-390). All these samples showed visible proportions of common DOM signatures in its mass spectra (Fig. S4, Fig. S5). Overall, these results clearly demonstrated that polar sorbents exhibited stronger affinity to less oxygenated compounds under the selected experimental conditions whereas non-polar sorbents were enriched in rather oxygenated and more unsaturated compounds, which also had produced pronounced signatures of organic matter in their MS-derived van Krevelen diagrams (Figs. S4-S7).

A notable example is the SPE series C1, C2, C8 and C18, in which the DOC yield had increased continually with carbon loading as expected (cf. above; Fig. 6-1 and Table S1); however, the relative aliphaticity of the respective SPE extracts was not increased as seemed likely. In both SR DOM and NS DOM extracts, average H/C ratios decreased while retaining a similar average mass range when SPE sorbents changed from C1 through C18 (Fig. 6-2, Fig. 6-3; Table S2, Table S3). Probably, aliphatic interactions were not decisive in this DOM isolation process but relative unsaturation also played a role. A gradual increase in average DBE and DBE/C in the DOM extracts was observed when C1 increased to C18, still validating the polarity-based separation that non-polar sorbents preferentially extract non-polar compounds. However, a continual increase in average O/C ratios was found as well, implying a decisive role of oxygen-containing functional groups in DOM retention. As nominal unsatura-tion of DOM molecules may refer to aromatic, olefinic, and carbonyl double bonds as well as alicyclic rings, a certain importance of carboxylic groups in this DOC retention series might apply.

The SPE sorbents most widely used for DOM isolation are PPL, C18 and HLB, and belong to the group of non-polar sorbents. Both respective SR DOM and NS DOM extracts project on a limited average mass range (SR / NS DOM: m/z ~ 390 / 380; Tab. S2, Fig. 3) and a rather confined area of average H/C and O/C ratios (Fig. 6-2 and Fig. 6-3). Compared to PPL, C18 extracted SR DOM and NS DOM compounds with slightly higher saturation (higher H/C ratios and lower O/C ratios; Table S2 and Table S3), in accordance with previous findings

when isolating arctic DOM, oligotrophic Lake Superior DOM and other freshwater DOM (Li and Minor, 2015; Perminova et al., 2014; Raeke et al., 2016). HLB extracts showed higher average O/C ratios than C18 extracts, in analogy to the finding that HLB extracts of freshwater contained a comparatively higher proportion of oxygen-rich compounds (Raeke et al., 2016).

FTMS-derived principal component analysis (PCA) of the SR SPE-DOM extracts produced a well separated clustering according to proposed SPE sorption mechanisms, with a continual evolution from "non-polar" to "polar and strong ion exchange" SPE resins (Fig. 4A) while the count of assigned molecular compositions fol-lowed these trends as well: non-polar > mixed mode with anion exchange > mid-polar and mixed mode with cation exchange > weakly non-polar and mid-polar > polar and strong ion exchange (Fig. 6-4; Table S2). This finding implies that non-polar interactions caused optimum retention for Suwannee River DOM. The acidic characteristics of SR DOM facilitated anion exchange-based retention as well, explaining the improved DOM retention characteristics compared with those of cation exchange-based SPE resins.
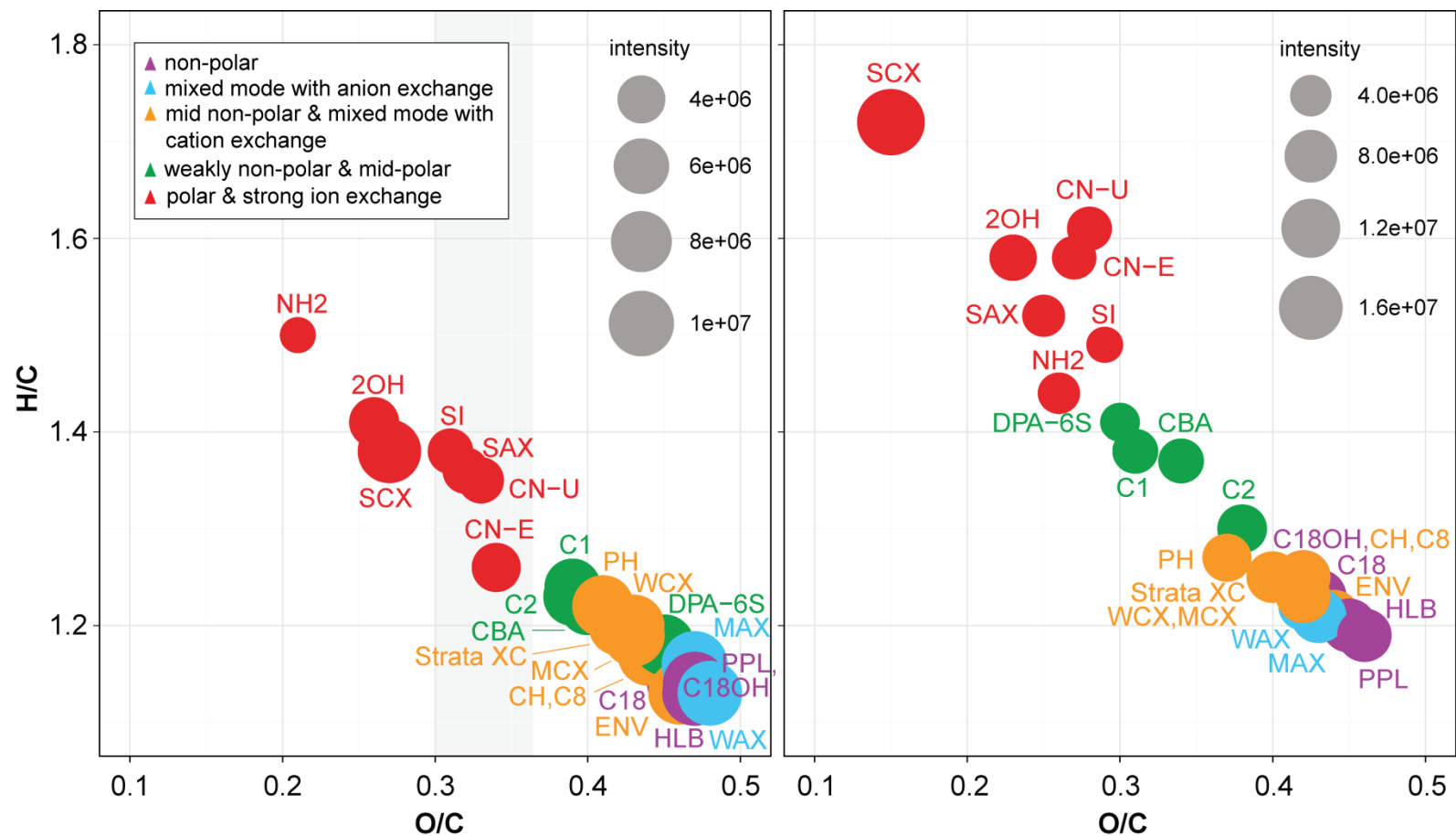
Fig. 6-2 Average H/C and O/C elemental ratios of (left panel): SR DOM extracts, and (right panel): NS DOM extracts derived from negative ESI FT-ICR mass spectra. Bubble size indicated the average intensity obtained by FT-ICR mass spectra. The shaded section indicates two groups of polar and strong ion exchange SPE resins, differing in relative oxygen-deficiency (cf. text)
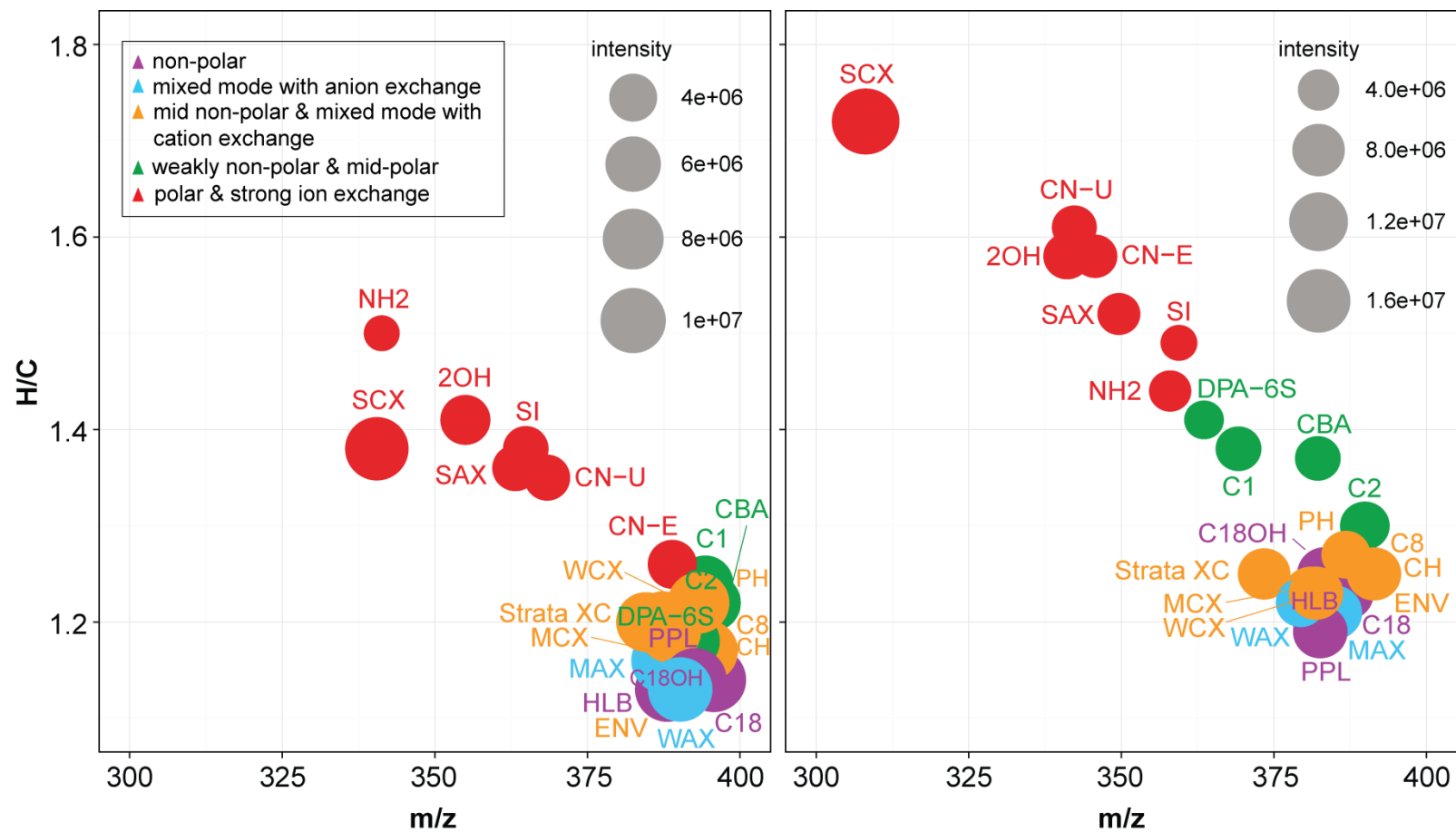
Fig. 6-3 Average mass-edited H/C ratios of (left panel): SR DOM extracts, and (right panel): NS DOM extracts derived from negative ESI FT-ICR mass spectra. Bubble size indicated the average intensity obtained by FT-ICR mass spectra

Two major groups of molecular compositions, group A and group B, contributed to the distinction of SR DOM in the FT-ICR MS-derived PCA analysis (Fig. 4A). According to van Krevelen diagrams and mass-edited H/C ratios, molecular compositions common in both groups A and B reflected an overall ~50% of total molecular compositions, and were largely comprised of a contiguous assembly of low mass (m/z < 500) CHO compounds of average H/C and O/C ratio, with an admixture of <10% of assigned numbers of CHNO and CHOS com-pounds. The latter were primarily saturated (H/C ratio > 2) and unsaturated (H/C ratio ~ 1.65) sulfolipids (Hertkorn et al., 2016). Molecular compositions unique to group A were more numerous than the common ones, whereas those specific to group B comprised a very few scattered CHO, CHNO, CHOS and CHNOS compounds of no conceivable structural relevance (Fig. 4B, Fig. 4C). The molecular compositions unique to group A (i. e. those present in mid- to non-polar SPE-DOM) were comprised of ~50% CHO, ~35% CHNO and ~15% CHOS compounds (Fig. 6-4B, Fig. 6-4C). While the CHO compounds encircled those common to groups A in the van Krevelen diagram, while reaching out to remarkable oxygenation (O/C ratio up to 0.9), the unique CHNO com-pounds were clustered at a H/C ratio of 1.1 ± 0.2 and a O/C ratio of 0.5 ± 0.1 and a mass range of m/z $\sim 350 \pm 100$, indicative of common DOM molecules with a restricted overall chemical diversity (Fig. 6-4B and Fig. 6-4C). CHOS compounds represented a set of rather low mass (m/z $\sim$ 350-450) unsaturated sulfolipids at a H/C ratio of 1.40 ± 0.15, with O/C ratios of 0.2 ± 0.1 and a peculiar set of aromatic black sulfur CHOS compounds (Hertkorn et al., 2013, 2016) with an aromaticity index above 0.5 (Koch and Dittmar, 2006), showing a H/C ratio of 0.8 ± 0.2, and a O/C ratio of 0.23 ± 0.15. Overall, the molecular compositions present in group A (common to group A and group B plus unique to group A) comprised the entire inventory of Suwannee River organic molecules whereas those present in group B (common to group A and group B plus unique to group B) represented a subset of limited chemical diversity as demonstrated by the smaller area covered in van Krevelen diagrams and mass-edited H/C ratios, which showed fewer CHNO and CHOS compounds.

In comparison with SR DOM, PCA assessment of NS DOM showed a related but clearly distinct pattern, again corroborating relevant differences in chemical diversity. At first, clustering according to groups of SPE resins was, although of the same order, less distinct than in case of SR DOM (Fig. 6-4A, Fig. 6-5A). While similar counts of shared molecular compositions, common to groups A and group B, were observed for SR DOM and NS DOM, the latter comprised ~20% of CHNO compounds which were nearly absent in shared SR DOM molecular com-positions. Overall, CHO compounds of NS DOM were displaced to higher saturation (H/C ratio > 0.8) at lesser oxygenation (O/C ratio < 0.65), while saturated sulfolipids seemed common to both SR DOM and NS DOM. The CHOS compounds unique to group A in NS DOM were distinct from those found in SR DOM, more numerous and reached to higher mass (up to m/z ~ 480) (Fig. 6-4, Fig. 6-5). However, CHNO compounds unique to group A contributed ~50% of the total number of molecular formulas. They were highly diverse as shown by its substantial mass range (m/z ~ 220 – 550) and coverage of a large area in van Krevelen diagrams, considerably exceeding the respective range observed for unique SR DOM CHNO molecular series, and even extending into the aromatic region (O/C ratio 0.38 ± 0.15; H/C ratio: 0.5 ± 0.2; m/z ~ 390 ± 30). CHO compounds unique to group A in NS DOM again reached to greater oxygenation as well as broader bandwidth of unsaturation than those common to groups A and B, in analogy to SR DOM (cf. above).
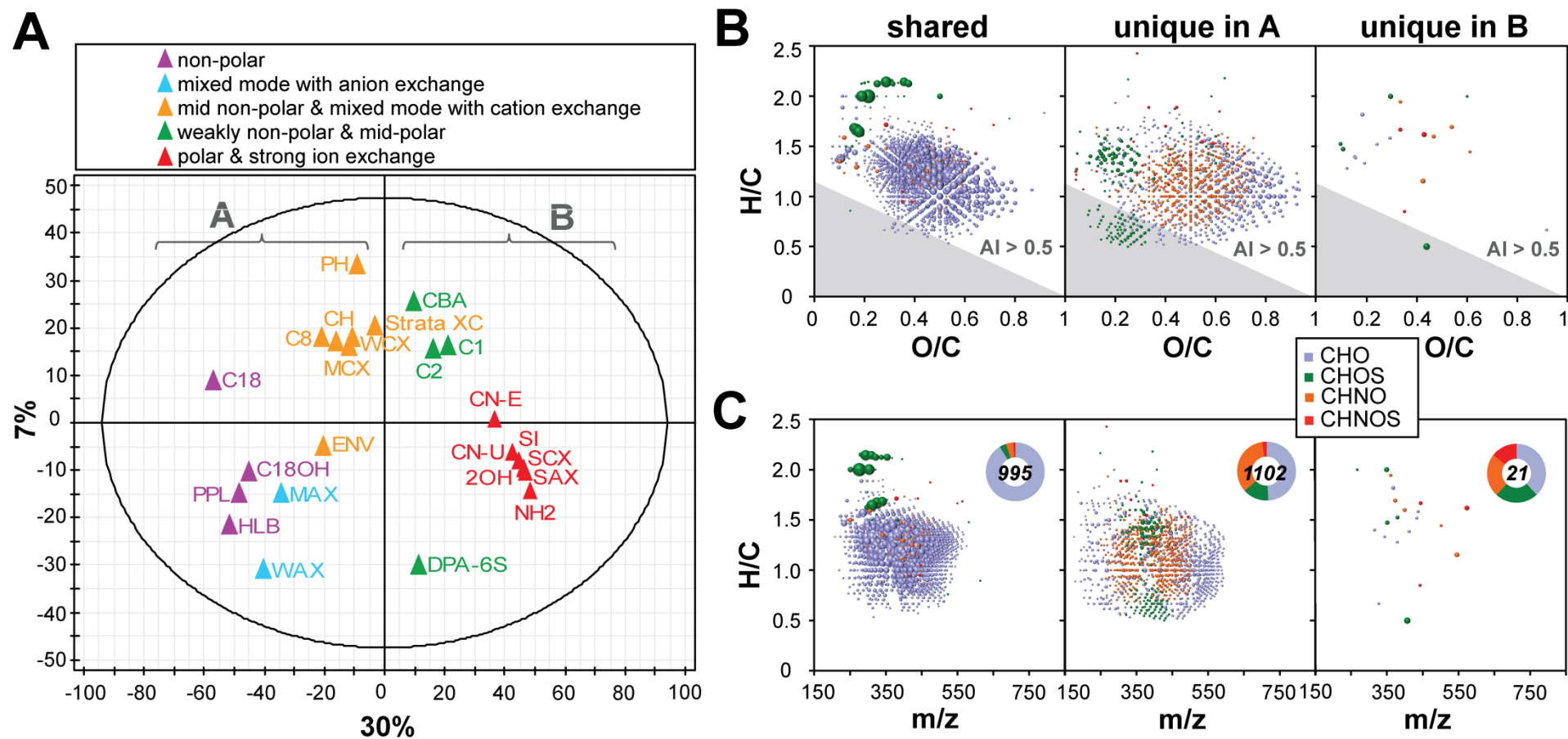
Fig. 6-4 (A) PCA of SR SPE-DOM extracts derived from negative ESI FT-ICR mass spectra; (B) van Krevelen diagrams of the masses detected in common, unique in group A and unique in group B; (C) mass-edited H/C ratios of the masses detected in common, unique in group A and unique in group B.
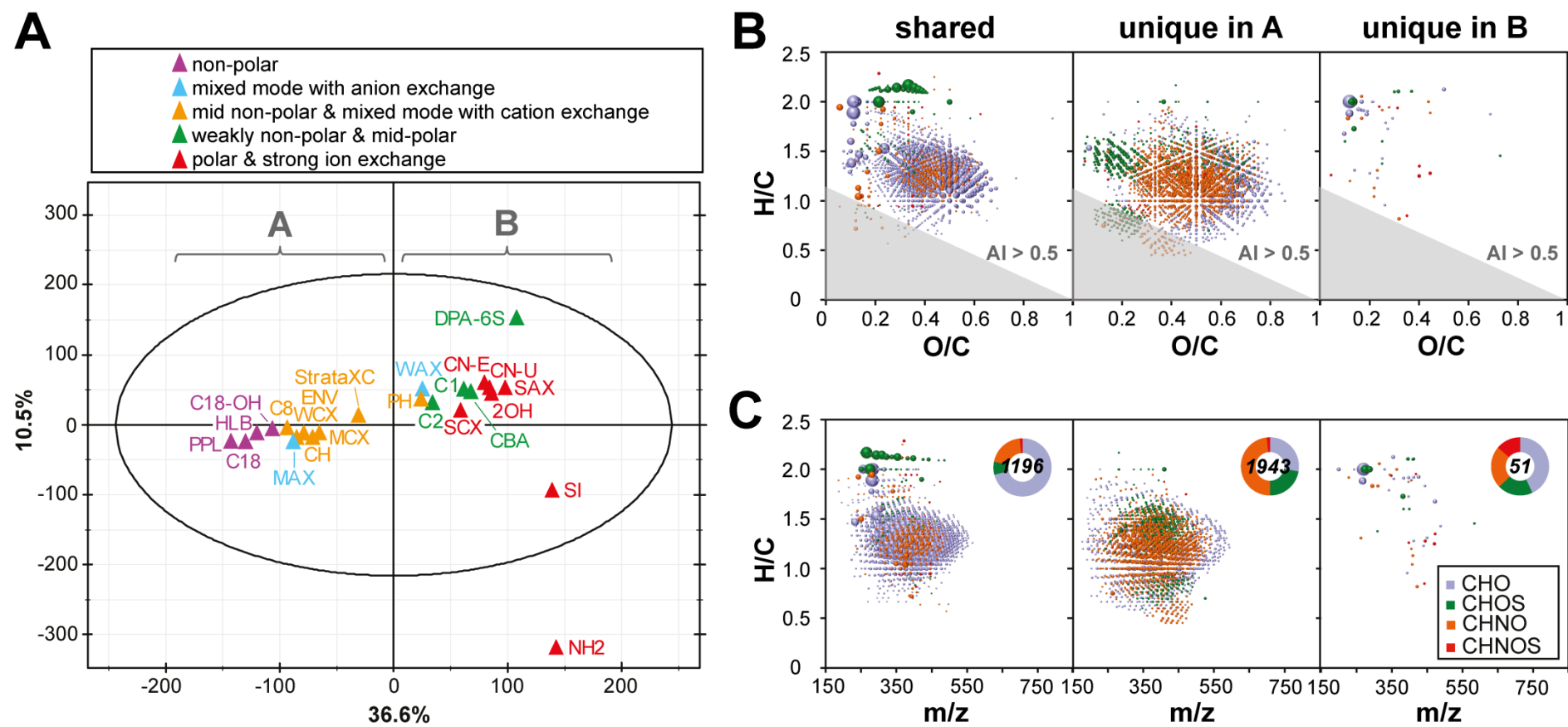
Fig. 6-5 (A) PCA of NS SPE-DOM extracts derived from negative ESI FT-ICR mass spectra; (B) van Krevelen diagrams of the masses detected in common, unique in group A and unique in group B; (C) mass-edited H/C ratios of the masses detected in common, unique in group A and unique in group B.

6.4.3 ^{1}H NMR spectroscopic assessment of leaching behavior

Sensitive ^{1}H NMR spectroscopy was employed to assess leaching behavior of the 24 SPE cartridges at low load-ing of Suwannee River water to emphasize the presence of leachate molecules originating from the SPE car-tridges itself. Leaching of SPE cartridges will result in increased apparent DOC recovery, while enhanced pro-portions of leachate may produce certain fragments in FT-ICR mass spectra of DOM eluates. A more extensive leaching of hydrocarbon-rich molecules will result in a displacement of average elemental ratios, with larger average H/C and lower O/C elemental ratios than produced from DOM alone.

^{1}H NMR spectra of SPE sorbents such as 2OH, C18-OH, DPA-6S, HLB, SCX, Strata XC and WAX indicated extensive leaching of molecules under the selected operational conditions which were in accordance with the proposed functionalization of the respective resins (Fig. S3). High proportions of leachate as found e.g. in DPA-6S and C18OH were very probably responsible for the high apparent DOC recovery observed (Fig. 6-1 and Fig. S1). The observed leaching of aliphatic compounds in case of HLB sorbent which has been widely applied for DOM isolation (Raeke et al., 2016; Ward et al. 2013; Waska et al., 2015) deserves special mention.

According to PCA analysis (Fig. 6-6), SR DOM SPE extracts clustered different in 1H NMR and FT-ICR mass spectra. In particular, NMR-derived PCA analysis showed substantial overlap for the "mid non-polar & mixed mode with cation exchange" and the "weakly non-polar & mid-polar" DOM extracts, whereas those were grouped apart in FTMS-derived PCA analysis (Fig. 6-4).
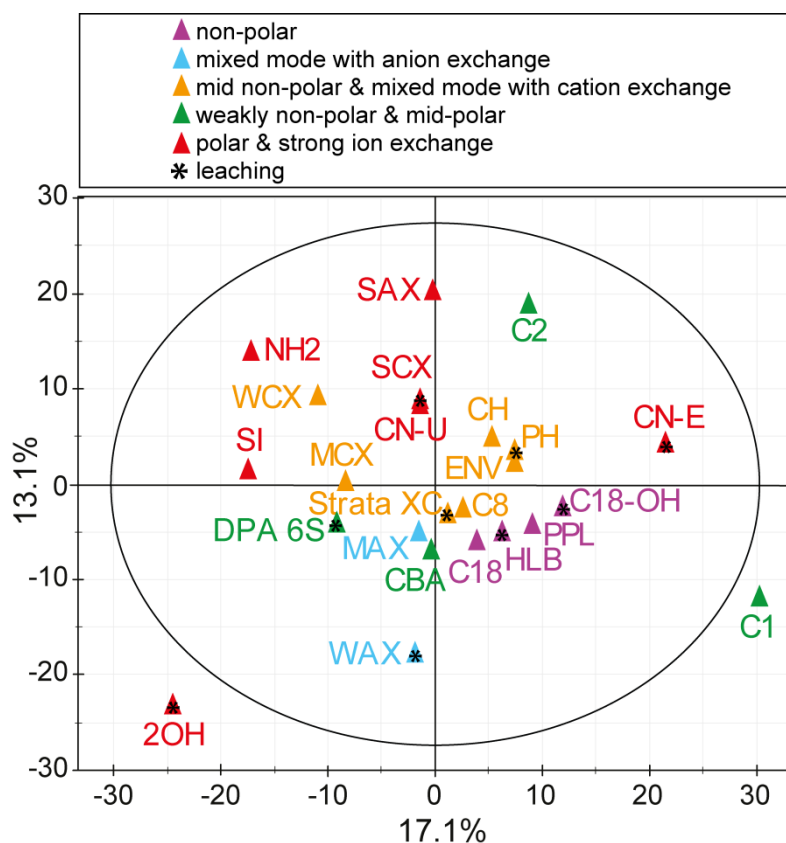
Fig. 6-6 PCA of original SR SPE-DOM extracts derived from ^1H NMR section integrals (0.01 ppm resolution).

In the course of this and other studies (e.g. Li et al., 2016; unpublished data) we have repeatedly observed that the individual combinations of SPE and DOM produced a very complex evolution of DOM and cartridge-specific, structure selective blank and leaching behavior in NMR spectra, which depend on many conditions, in particular the loading mass ratio of DOM / SPE (Li et al., 2016). In this study, we simply wanted to assess the extent and selectivity of leaching of SPE cartridges under realistic conditions of DOM extraction by NMR spectroscopy. It is clear that at higher DOM / SPE mass ratios, higher proportions of DOM will be retained, but in-creased shares of DOM may be transferred to permeates and wash liquids as well (Li et al., 2016). In case of larger cartridge size and higher loading of DOC, FT-ICR mass spectra with common DOM characteristics such as smooth, skewed near Gaussian-type mass peak distributions dominated by $\Delta m(CH_2)$ and $\Delta m(H_2)$ which appear inconspicuous on sight and mathematical analysis may hid substantial leaching of aliphatic compounds which are clearly visible and perhaps even dominant in 1H NMR spectra, relevant examples include CN-E and certain C8 cartridges (data not shown). Owing to chemical diversity and polydispersity of all DOM, these mutual dependencies, which are governed by

an array of diverse intermolecular interactions between DOM and SPE resin molecules are very complex and depend on individual conditions. A further complication is an often undisclosed alteration of proprietary conditions in the manufacture of commercial SPE resins which is even more elaborate because various SPE cartridge sizes even by the same manufacturer may behave differently. This important cautionary note wants to draw awareness to the complexity of DOM/SPE interactions, and to the necessity to perform credible studies of structural blanks especially in case of using SPE for isolation of polydisperse and molecularly heterogeneous DOM.

6.5 Conclusions

In a set of 24 different SPE resins, which were classified into five established groups of sorption mechanisms, analogous molecular interactions operated for both Suwannee river water and North Sea water at pH = 2 and methanol elution. While leaching of some resins caused inflation of bulk DOC recovery and displacement of averaged mass spectral properties, carefully performed NMR spectroscopy on adapted series of samples will allow a reliable assessment of structural blanks. With the exception of strongly polar and ion exchanging resins, the distinction of freshwater and marine DOM by SPE appears driven by intrinsic molecular properties of DOM rather than by peculiar specific interactions. Coupling of distinctive sorbents under the same operational conditions may achieve a more comprehensive extraction of DOM from various sources.

6.6 Acknowledgements

6.7 References

Arakawa, N. and Aluwihare, L. (2015) Direct identification of diverse alicyclic terpenoids in Suwannee River fluvic acid. Environ Sci Technol 49, 4097-4105.

Battin, T.J., Luyssaert, S., Kaplan, L.A., Aufdenkampe, A.K., Richter, A. and Tranvik, L.J. (2009) The boundless carbon cycle. Nat Geosci 2(9), 598-600.

Benner, R., Pakulski, J.D., McCarthy, M., Hedges, J.I. and Hatcher, P.G. (1992) Bulk chemical characteristics of dissolved organic matter in the ocean. Science 255, 1561–1564.

Bianchi, T.S. (2011) The role of terrestrially derived organic carbon in the coastal ocean: a changing paradigm and the priming effect. Proc Natl Acad Sci U S A 108(49), 19473-19481.

Chen, M. and Hur, J. (2015) Pre-treatments, characteristics, and biogeochemical dynamics of dissolved organic matter in sediments: A review. Water Res 79, 10-25.

Croué, J.-P. (2004) Isolation of Humic and Non-Humic NOM Fractions: Structural Characterization. Environ-mental Monitoring and Assessment 92(1-3), 193-207.

Dittmar, T., Koch, B., Hertkorn, N. and Kattner, G. (2008) A simple and efficient method for the solid-phase extraction of dissolved organic matter (SPE-DOM) from seawater. Limnol Oceanogr-Meth 6(6), 230-235.

Duarte, R.M. and Duarte, A.C. (2015) Unraveling the structural features of organic aerosols by NMR spectros-copy: a review. Magn Reson Chem 53(9), 658-666.

Flerus, R., Koch, B.P., Schmitt-Kopplin, P., Witt, M. and Kattner, G. (2011) Molecular level investigation of reactions between dissolved organic matter and extraction solvents using FT-ICR MS. Mar Chem 124(1-4), 100-107.

Goldberg, S.J., Ball, G.I., Allen, B.C., Schladow, S.G., Simpson, A.J., Masoom, H., Soong, R., Graven, H.D. and Aluwihare, L.I. (2015) Refractory dissolved organic nitrogen accumulation in high-elevation lakes. Nat Commun 6, 6347.

Green, N.W.; Mclnnis, D., Hertkorn, N.; Maurice, P.A. and Perdue E.M. (2014) Suwannee River natural organic matter: isolation of the 2R101N reference sample by reverse osmosis. Environ Eng Sci 32, 1-7.

Green, N.W., Perdue, E.M., Aiken, G.R., Butler, K.D., Chen, H., Dittmar, T., Niggemann, J. and Stubbins, A. (2014) An intercomparison of three methods for the large-scale isolation of oceanic dissolved organic matter. Mar Chem 161, 14-19.

He, W. and Hur, J. (2015) Conservative behavior of fluorescence EEM-PARAFAC components in resin fraction-ation processes and its applicability for characterizing dissolved organic matter. Water Res 83, 217-226.

Hertkorn, N., Ruecker, C., Meringer, M., Gugisch, R., Frommberger, M., Perdue, E.M., Witt, M. and Schmitt-Kopplin, P. (2007) High-precision frequency measurements: indispensable tools at the core of the molecu-lar-level analysis of complex systems. Anal Bioanal Chem 389(5), 1311-1327.

Hertkorn, N., Frommberger, M., Witt, M., Koch, B.P., Schmitt-Kopplin, P. and Perdue, E.M. (2008) Natural organic matter and the event horizon of mass spectrometry. Anal Chem 80(23), 8908-8919.

Hertkorn, N., Harir, M. and Schmitt-Kopplin, P. (2015) Nontarget analysis of Murchison soluble organic matter by high-field NMR spectroscopy and FTICR mass spectrometry. Magn Reson Chem 53(9), 754-768.

Hertkorn, N., Harir, M., Cawley, K.M., Schmitt-Kopplin, P. and Jaffé, R. (2016) Molecular characterization of dissolved organic matter from subtropical wetlands: a comparative study through the analysis of optical properties, NMR and FTICR/MS. Biogeosciences 13(8), 2257-2277.

Kellerman, A.M., Kothawala, D.N., Dittmar, T. and Tranvik, L.J. (2015) Persistence of dissolved organic matter in lakes related to its molecular characteristics. Nat Geosci 8(6), 454-457.

Kim, S., Simpson, A.J., Kujawinski, E.B., Freitas, M.A. and Hatcher, P.G. (2003) High resolution electrospray ionization mass spectrometry and 2D solution NMR for the analysis of DOM extracted by C18 solid phase disk. Org Geochem 34(9), 1325-1335.

Koch, B.P. and Dittmar, T. (2006) From mass to structure: an aromaticity index for high-resolution mass data of natural organic matter. Rapid Commun Mass Sp 20(5), 926-932.

Koch B.P., Kattner G., Witt M., Passow U. (2014). Molecular insights into the microbial formation of marine dissolved organic matter: Recalcitrant or labile? Biogeosciences, 11, 4173-4190.

Koprivnjak, J.F., Pfromm, P.H., Ingall, E., Vetter, T.A., Schmitt-Kopplin, P., Hertkorn, N., Frommberger, M., Knicker, H. and Perdue, E.M. (2009) Chemical and spectroscopic characterization of marine dissolved or-ganic matter isolated using coupled reverse osmosis–electrodialysis. Geochim Cosmochim Ac 73(14), 4215-4231.

Ksionzek K.B., Lechtenfeld O.J., McCallister S.L., Schmitt-Kopplin P., Geuer J.K., Geibert W., Koch B.P. (2016). Dissolved organic sulfur in the ocean: Biogeochemistry of a petagram inventory. Science, 354, 456-459.

Kruger, B.R., Dalzell, B.J. and Minor, E.C. (2011) Effect of organic matter source and salinity on dissolved or-ganic matter isolation via ultrafiltration and solid phase extraction. Aquat Sci 73(3), 405-417.

Kujawinski, E.B. (2011) The impact of microbial metabolism on marine dissolved organic matter. Ann Rev Mar Sci 3, 567-599.

Lam, B. and Simpson, A.J. (2006) Passive sampler for dissolved organic matter in freshwater environments. Anal Chem 78(24), 8194-8199.

Lam, B., Baer, A., Alaee, M., Lefebvre, B., Moser, A., Williams, A. and Simpson, A.J. (2007) Major Structural Components in Freshwater Dissolved Organic Matter. Environ Sci Technol 41(24), 8240-8247.

Lara, R.J. and Thomas, D.N. (1994) Isolation of Marine Dissolved Organic Matter: Evaluation of Sequential Combinations of XAD Resins 2, 4, and 7. Anal Chem 66(14), 2417-2419.

Leenheer, J.A., Wershaw, R., Reddy, M.M., (1995) Strong-acid, carboxyl-group structures in fulvic acid from the Suwannee River, Georgia.2. Major structures. Environ Sci Technol 29(2), 399-405.

Li, H. and Minor, E.C. (2015) Dissolved organic matter in Lake Superior: insights into the effects of extraction methods on chemical composition. Environ Sci Process Impacts 17(10), 1829-1840.

Li, Y., Harir, M., Lucio, M., Kanawati, B., Smirnov, K., Flerus, R., Koch, B.P., Schmitt-Kopplin, P. and Hertkorn, N. (2016) Proposed Guidelines for Solid Phase Extraction of Suwannee River Dissolved Organic Matter. Anal Chem 88(13), 6680-6688.

Lucas, J., Koester, I., Wichels, A., Niggemann, J., Dittmar, T., Callies, U., Wiltshire, K.H. and Gerdts, G. (2016) Short-Term Dynamics of North Sea Bacterioplankton-Dissolved Organic Matter Coherence on Molecular Level. Front Microbiol 7, 321.

Mann, P.J., Eglinton, T. I., McIntyre C. P., Zimov, N., Davydova, A., Vonk, J. E., Holmes, R. M. and Spencer, R. G. M. (2016) Utilization of ancient permafrost carbon in headwaters of Arctic fluvial networks. Nat. Commun. 6, 7856.

Minor, E.C., Swenson, M.M., Mattson, B.M. and Oyler, A.R. (2014) Structural characterization of dissolved organic matter: a review of current techniques for isolation and analysis. Environ Sci Process Impacts 16(9), 2064-2079.

Moran, M. A.; Kujawinski, E. B.; Stubbins, A.; Fatand, R.; Aluwihare, A.; Buchan, A.; Crump, B. C.; Dorrestein, P. C.; Dyhrman, S. T.; Hess, N. J.; Howe, B.; Longnecker, K.; Medeiros, P. M.;Niggemann, J.; Obernosterer., I.; Repeta, D. J. and Waldbauer, J. R. (2016) Deciphering ocean carbon in a changing world. Proc Natl Acad Sci U S A 113(12), 3143-3151.

Nebbioso, A. and Piccolo, A. (2013) Molecular characterization of dissolved organic matter (DOM): a critical review. Anal Bioanal Chem 405(1), 109-124.

Nkambule, T.I., Krause, R.W.M., Haarhoff, J. and Mamba, B.B. (2011) Treatability and characterization of Natural Organic Matter (Kashiyama et al.) in South African waters using newly developed methods. Physics and Chemistry of the Earth, Parts A/B/C 36(14-15), 1159-1166.

Osterholz, H., Singer, G., Wemheuer, B., Daniel, R., Simon, M., Niggemann, J. and Dittmar, T. (2016) Deciphering associations between dissolved organic molecules and bacterial communities in a pelagic marine system. ISME J. 10(7), 1717-1730.

Perdue E. M. and Ritche J. D. (2003). Dissolved organic matter in fresh waters, Treatise on Geochemistry (eds, Holland H. D. and Turekian K. K.), Elsevier-Pergamon, Oxford, Vol. 5, 273-318.

Perminova, I.V., Dubinenkov, I.V., Kononikhin, A.S., Konstantinov, A.I., Zherebker, A.Y., Andzhushev, M.A., Lebedev, V.A., Bulygina, E., Holmes, R.M., Kostyukevich, Y.I., Popov, I.A. and Nikolaev, E.N. (2014) Mo-lecular mapping of sorbent selectivities with respect to isolation of Arctic dissolved organic matter as measured by Fourier transform mass spectrometry. Environ Sci Technol 48(13), 7461-7468.

Raeke, J., Lechtenfeld, O.J., Wagner, M., Herzsprung, P. and Reemtsma, T. (2016) Selectivity of solid phase extraction of freshwater dissolved organic matter and its effect on ultrahigh resolution mass spectra. Environ Sci Process Impacts 18, 918-927.

Ratpukdi, T., Rice, J.A., Chilom, G., Bezbaruah, A. and Khan, E. (2009) Rapid Fractionation of Natural Organic Matter in Water Using a Novel Solid-Phase Extraction Technique. Water Environ Res 81(11), 2299-2308.

Sandron, S., Rojas, A., Wilson, R., Davies, N.W., Haddad, P.R., Shellie, R.A., Nesterenko, P.N., Kelleher, B.P. and Paull, B. (2015) Chromatographic methods for the isolation, separation and characterisation of dissolved organic matter. Environ Sci Process Impacts 17(9), 1531-1567.

Swenson, M.M., Oyler, A.R. and Minor, E.C. (2014) Rapid solid phase extraction of dissolved organic matter. Limnol Oceanogr-Meth 12(10), 713-728.

Thurman, E.M. and Malcolm, R.L. (1981) Preparative isolation of aquatic humic substances. Environ Sci Tech-nol 15(4), 463-466.

Tfaily, M.M., Hodgkins, S., Podgorski, D.C., Chanton, J.P. and Cooper, W.T. (2012) Comparison of dialysis and solid-phase extraction for isolation and concentration of dissolved organic matter prior to Fourier transform ion cyclotron resonance mass spectrometry. Anal Bioanal Chem 404(2), 447-457.

Tziotis, D., Hertkorn, N. and Schmitt-Kopplin, P. (2011) Kendrick-analogous network visualisation of ion cyclo-tron resonance Fourier transform mass spectra: improved options for the assignment of elemental compositions and the classification of organic molecular complexity. Eur J Mass Spectrom (Chichester, Eng) 17(4), 415-421.

Ward, N.D., Keil, R.G., Medeiros, P.M., Brito, D.C., Cunha, A.C., Dittmar, T., Yager, P.L., Krusche, A.V. and Richey, J.E. (2013) Degradation of terrestrially derived macromolecules in the Amazon River. Nat Geosci 6(7), 530-533.

Waska, H.; Koschinsky, A.; Chancho, M.J.R. and Dittmar, T. (2015) Investigating the potential of solid-phase extraction and Fourier-transform ion cyclotron resonance mass spectrometry (FT-ICR-MS) for the isolation and identification of dissolved metal-organic complexes from natural waters. Mar Chem 173, 78-92.

Zhang, F., Harir, M., Moritz, F., Zhang, J., Witting, M., Wu, Y., Schmitt-Kopplin, P., Fekete, A., Gaspar, A. and Hertkorn, N. (2014) Molecular and structural characterization of dissolved organic matter during and post cyanobacterial bloom in Taihu by combination of NMR spectroscopy and FTICR mass spectrometry. Water Res 57, 280-294.

Zherebker, A.Y., Perminova, I.V., Konstantionov, A.I., Volikov, A.B., Kostyukevich, Y.I., Kononikhin, A.S., Nikolaev, E.N., (2016) Extraction of humic substances from fresh waters on solid-phase cartridges and their study by Fourier transform ion cyclotron resonance mass spectrometry. J Anal Chem 71(4), 372-378.

Chapter 7

Insights into Dissolved Organic Matter Compositions and Structures by Phase-optimized Solid Phase Extraction (POP SPE)

7 Insights into Dissolved Organic Matter Compositions and Structures by Phase-optimized Solid Phase Extraction (POP SPE)

7.1 Abstract

This proof of concept study proposes a novel and effective fractionation of Suwannee River dissolved organic matter (SR DOM) by phase-optimized solid phase extraction (POP SPE), coupling three sorbents with different selectivity in sequence and separate collection of fractions by isocratic elution of methanol. POP SPE had advantages over the traditional SPE with individual sorbents in terms of desirable DOC recovery, overall more representative compounds and selectively fractionated functional groups. High-field Fourier transform ion cyclotron (FT-ICR) mass spectra showed the wide coverage of compositional groups and mass ranges in POP SPE fractions. ^{1}H nuclear magnetic resonance (NMR) displayed the variations of aromatics, olefins, carbohydrates in POP SPE extracts, and ^{13}C NMR spectra presented selectivity of carbonyl carbons, functionalized aromatics, methyl, methylene and methine groups. Blue shift in fluorescence spectra was observed in the first two eluting POP SPE fractions, indicative of smaller molecular weights and less extent of aromatic condensation. This method possesses enhanced isolation expectancies, improved isolation power and selective separation resulting in reduced intermolecular interactions, and has the potential as a more standardized approach for isolation of variable and heterogeneous DOM samples which are not possible to be well extracted by single sorbent.

7.2 Introduction

Dissolved organic matter (DOM) is the largest reservoir of organic carbon on Earth and it is widely distributed in all terrestrial ecosystems (Bianchi 2011). DOM is an extremely complex (super)mixture of organic compounds with ~50% of carbon content and variable proportions of heteroatoms such as oxygen, nitrogen, sulfur and phosphorus which cannot be resolved into individual compounds at present (Hertkorn et al. 2007). Hence, DOM molecular diversity which reflects key ecosystem processes and services such as speciation of nutrient and trace metals, binding and mobility of organic molecules and pollutants, biodiversity and food web composition, to name a few (Fasching et al. 2014, Kujawinski 2011, Lucas et al. 2016, Moran et al. 2016, Osterholz et al. 2016), is poorly constrained and understood at present (Hertkorn et al. 2007, Ksionzek et al. 2016). The concentration, composition and structure of DOM results from the integration cross interdependent physical, chemical and biological processes with different spatial and temporal resolution. Remarkable variance in the molecular compositions may be observed in individual DOM samples even if average bulk DOM properties are often confined to rather narrow, ecosystem-specific ranges (Kruger et al. 2011, Perdue and Ritchie 2003).

While carbohydrates, peptides and lipids are present in soil, aquatic and marine DOM, and can be retrieved by degradative analysis (Shen et al. 2014), the linkages of these key structural units remain largely unknown even today (Bianchi 2011). Other prominent DOM constituents like combustion-derived black carbon (Schmidt et al., 2009), black nitrogen (Knicker 2010), black sulfur (Hertkorn et al. 2013, 2016), lignin-oxidation (DiDonato et al. 2016, Waggoner et al. 2015) and photodegradation products (Gonsior et al. 2014, Schmitt-Kopplin et al. 1998) result primarily from abiotic reactions and hence cover a larger compositional and structural diversity than biologically derived molecules. One of the most relevant prerequisites of DOM molecular characterization is a reproducible collection of representative samples with appreciable recovery.

The last two decades brought significant improvements of DOM isolation techniques, and solid phase extraction (SPE), preferentially with functionalized styrene-divinylbenzene polymer (PPL sorbent) (Minor et al. 2014, Nebbioso and Piccolo 2013, Sandron et al. 2015, Thurman and Malcolm 1981), has emerged as a widespread method due to its satisfactory DOC recovery (~50%) and ease of use, in particular for demanding field work. The observed range of DOM recovery when using PPL sorbent, for instance, was 43% for marine DOM, 65%

for salt marsh DOM, and >80% for Suwannee River DOM (Dittmar et al. 2008, Li et al. 2016a, Raeke et al. 2016), indicating a substantial compositional and structural variance of these DOM. Alternative SPE sorbents frequently applied for DOM isolation were C18, which preferentially retains colored dissolved organic matter (CDOM) rich in C_{sp2}-units (Kim et al. 2003), and HLB and XAD (Perminova et al. 2009). While it will remain impossible to extract the entire complement of organic molecules from polydisperse DOM with one single SPE sorbent, PPL resin appears to recover the largest bandwidth of aliphatic molecules with a sizable range of polarities.

Non-target molecular characterization of DOM attempts to describe the entire pool of carbon and its chemical environments by means of information-rich structure-selective methods such as fluorescence spectroscopy (determines chromophoric dissolved organic matter, CDOM), ultrahigh-resolution FT-ICR mass spectrometry (determines thousands of molecular compositions directly out of mixtures) and NMR spectroscopy (detects atomic environments of primarily hydrogen and carbon). However, even these advanced methods often suffer from extensive selectivity and loss of information, when applied to the characterization of polydisperse DOM. Optical spectroscopy primarily detects C_{sp2}-based structures with limited structural resolution (Hertkorn et al., 2016), while standard FT-ICR mass spectrometry inevitably detects only ions and furthermore projects all different isomers onto single molecular compositions (Hertkorn et al. 2007, 2008). NMR spectra offer unparalleled, quantitative insights into structural detail, but suffer from a comparatively low sensitivity and massive projection of a huge number of atomic environments on limited ranges of chemical shift. Furthermore, the NMR linewidth is affected by (differential) transverse NMR relaxation which might interfere with the quantitative relationships between area of NMR resonances and number of accountable nuclear spins.

The intractability of DOM molecular diversity does not only arise from the huge number of different chemical environments present in the samples but also on the interactions between molecules, which operate on different time scales and are often pH- and concentration dependent. Fractionation of DOM, e.g. by liquid chromatography (Koch et al. 2008, Stenson et al. 2008, Woods et al. 2011, 2012), parallel and sequential elution by multiple SPE cartridges (Ratpukdi et al. 2009, Swenson et al. 2014), and 2-dimensional gas chromatography (Arakawa and Aluwihare 2015, Ball and Aluwihare 2014) efficiently reduces DOM molecular complexity. This attenuates the extent of projection of data in any analytical

methods as well as decreases the operating molecular interactions. Cleaner and more informative spectra are obtained, when consolidated information from multiple DOM fractions is confronted with the respective data from bulk DOM (Gaspar et al. 2009, Li et al. 2016b).

Stationary Phase Optimized Selectivity Liquid Chromatography (SOS-LC) (Deconinck et al. 2015, 2016, Delahaye and Lynen 2014, Nyiredy et al. 2006, 2007), or in brief, phase-optimized (POP) separation, is a method in which the stationary phase becomes a tunable parameter (Deconinck, 2016; Delahaye and Lynen 2014), and dedicated kits of columns and algorithms are available for mixture fractionation to produce short overall analysis time at optimal resolution of individual compounds which may often differ widely in polarity (Deconinck et al. 2015, 2016, Delahaye and Lynen 2014, Nyiredy et al. 2006, 2007). This study transfers the POP-concept to a SPE-based fractionation of Suwannee River DOM using a sequence of three distinctive and complementary, non-leaching SPE sorbents with appreciable DOM retention selected from a previous study of 24 SPE sorbents (Li et al., 2016c).

The selection of SPE sorbents for sequential adsorption of Suwannee River water was aimed at a desirable maximum overall diversity of retained DOM molecules by POP SPE, with meaningful distinction in the individual eluates. For optimum differentiation of DOM constituents, a decreasing order of selectivity was used as follows: C8 (1st) → MAX (2nd) → PPL (3rd) with three POP SPE fractions to be collected separately. Characterization of these sequential POP SPE extracts alongside with the traditional SPE extracts resulting from single sorbents was performed by fluorescence and nuclear magnetic resonance (NMR) spectroscopy as well as high-field Fourier transform ion cyclotron mass spectrometry (FT-ICR MS).

7.3 Experimental section

7.3.1 Sample preparation

Suwannee River water DOM (SR DOM, 80 mg/L) was collected and filtered immediately after sampling as described by Green et al. in May 2012 (Green et al. 2015). Filtered sample was adjusted to pH 2 with 10 N HCl (31%, Merck, Germany) of analytical grade, and followed by SPE and POP SPE. SPE with individual sorbents (100 mg C8 (Agilent), 120 mg MAX (Waters) and 100 mg PPL (Agilent, Bond Elut)) and blanks were performed according

to our method (Li et al. 2016a). In POP SPE scheme, C8, MAX and PPL cartridges were coupled in sequence by Luer adaptors. Blanks were used with acidified Milli-Q water (HCl, pH 2). All the experiments were performed in triplicates, and a volume of 18.75 mL SR DOM was loaded on each so that overload was avoided (Li el al. 2016a). After loading the sample, the POP SPE cartridges were rinsed with 3 mL of pH 2 Milli-Q water, and then dispersed from the POP scheme. They were dried separately with nitrogen gas for 10 min, and eluted with 1 mL methanol respectively. The final eluates collected from POP SPE were named as POP SPE-1C8, -2MAX and -3PPL. POP SPE was conducted over 60 replicates in order to get enough samples for ^{13}C NMR. All of these eluates were kept at $-20^{\circ}C$ in the dark prior to further analysis.

7.3.2 DOC measurement

DOC concentrations were measured by high temperature catalytic oxidation with a Shimadzu TOC-VCPN analyzer. 100 μL aliquots of the eluates were evaporated and re-dissolved in 1 mL ultra-pure water for DOC analysis (Flerus et al. 2012).

7.3.3 High-field FT-ICR MS analysis

High-field FT-ICR mass spectra were acquired by a 12 T Bruker Solarix mass spectrometer (Bruker Daltonics, Bremen, Germany) and an Apollo II electrospray ionization (ESI) source in negative ionization mode. Samples were diluted in methanol to ~5 μg/mL DOC, and then injected into the electrospray source at a flow rate of 120 μL/h with a nebulizer gas pressure of 138 kPa and a dry gas pressure of 103 kPa. Spectra were first externally calibrated based on clusters of arginine in methanol (5 μg/mL), and internal calibration was systematically performed using specific DOM reference mass list, reaching accuracy values lower than 500 ppb. The spectra were acquired with a time domain of 4 Mega words over a mass range of m/z 150-1000 amu, and 500 scans were accumulated for each mass spectrum. Elemental formulae were computed for each peak in a batch mode by using custom-built software (Tziotis et al. 2011). Final elemental formulae were generated and categorized into groups containing CHO, CHNO, CHOS or CHNOS molecular series which were used to reconstruct the group-selective mass spectra.

7.3.4 NMR analysis

^1H NMR detected spectra of eluates were acquired with a 800 MHz Bruker Avance III spectrometer (B_0 = 18.7 T) and ^{13}C NMR spectra were with 500 MHz spectrometer (B_0=11.7

T) at 283 K with ~0.3-30 mg of solid (~0.1-1 mg for ^{1}H NMR and 17-30 mg for ^{13}C NMR) obtained by evaporation of original methanol-h_4 solution, dissolved in approx. 200 µL CD$_3$OD (Merck. 99.95% ^{2}H) solution with a 3 mm z-gradient QCO ^{13}C (^{15}N, ^{31}P) / ^{1}H cryogenic probe (90° excitation pulses: ^{13}C ~ 5.3 and ^{1}H ~ 17 µs) with Bruker standard pulse sequences in sealed 3 mm Bruker MATCH tubes. Detailed parameters of NMR have been described by Hertkorn et al. (Hertkorn et al. 2013, 2016). ^{1}H NMR chemical shift reference of CD$_3$OD was 3.3 ppm and ^{13}C NMR chemical shift reference of CD$_3$OD was 49.00 ppm. ^{1}H NMR spectra were recorded with solvent suppression with pre-saturation and 1 ms spin-lock (*noesypr1d)*, 5 s acquisition time, 5 s relaxation delay (d1), typically 2048 scans. ^{13}C DEPT NMR spectra (distortionless enhanced polarization transfer) were acquired with aq = 1 s and d1 = 2 s. The NMR section integrals were obtained by using Bruker AMIX software (version 3.9.4) with a bucket resolution of 0.01 ppm chemical shifts for ^{1}H NMR and 1 ppm chemical shift for ^{13}C NMR, and with exclusion of methanol and water.

7.3.5   Optical spectroscopy

1 mL of the eluates were dried and re-dissolved in Milli-Q water at the original concentrations and then diluted to achieve raw absorbance of less than 0.4 at 300 nm. The dilution factor was used to calculate initial fluorescence intensity. The dilution was necessary to be able to correct for inner filtering effects and to not exceed the linear range of fluorescence response. Absorbance and EEM spectra were recorded simultaneously using a Horiba Aqualog fluorometer at excitation wavelengths from 240 to 500 nm (3 nm increments) and an emission range between 230 to 600 nm (~3 nm increments). The fluorescence was then corrected for Raleigh scattering and inner filter effects. The raw fluorescence intensity was then normalized to a 1 ppm Starna quinine sulfate reference cell (Gonsior et al. 2013).

7.4   Results and discussions

7.4.1   DOC recovery

Based on a previous study of 24 commercially available SPE sorbents eluted, three SPE sorbents were selected for a sequential POP-based DOM elution from Suwannee River water: the moderately non-polar SPE resin C8 (1st), the non-polar mixed mode with moderate anion exchange polymer MAX (2nd), and the modified non-polar PPL (3rd). These three SPE cartridges all had retained complex, but somewhat complementary mixtures of DOM molecules at appreciable recovery, with limited (C8) to absent leaching (MAX and PPL). The

DOC recoveries of the three individual SPE extracts from Suwannee River water produced in this study with methanolic elution at pH = 2 for cartridges C8 (48±2%), MAX (25±1%) and PPL (70±4%) were consistent with our previous findings (Li et al. 2016c).

The DOC recovery of the three POP SPE extracts was 47±1% (POP SPE-1C8), 6±0.5% (POP SPE-2MAX), and 5±0.3% (POP SPE-3PPL), respectively. This demonstrated a fair congruence for the two initial C8 eluates but very extensive fractionation and extraction selectivity among the consecutive pairs of eluates MAX / POP SPE-2MAX and PPL / POP SPE-3PPL. Surprisingly, the overall DOC extraction yield of the POP SPE sequential elution (~58%) was lower than that of PPL alone (~70%) testifying to a rather complex and dynamic behavior of molecular interactions effecting the retention of polydisperse DOM by SPE. The lower DOC recovery in POP SPE was mainly due to the operating conditions for MAX which was recommended by the manufactures. In our study, a homogenous condition was applied for three cartridges with different functionaries in order to minimize the side reactions as well as easy operation.

7.4.2   NMR spectra

All ^{1}H NMR spectra of the three individual DOM extracts showed the typical characteristics of complex organic matter, with broad, smooth bulk envelopes across the entire range of chemical shift, resulting from superposition of a huge number ($> 10^6$) number of individual NMR resonances, each denoting an individual atomic environment of DOM. From higher to lower field (from right to left), aliphatics, carboxylic-rich alicyclic molecules (CRAM) (Hertkorn et al. 2006), carbohydrates-like and methoxy, olefins and aromatics were observed in variable proportions (Table 7-1): aromatics and olefic protons declined in the order eluates C8 < PPL << MAX; OC**H**-units increased according to eluates MAX < C8 < PPL, while functionalized aliphatics (XCC**H** units, like CRAM: X = HOOC) increased slightly from eluates C8 < PPL ~ MAX; Finally, pure aliphatic chemical environments (CCC**H** units) increased in the order PPL < C8 < MAX. Overall, eluate MAX was particularly rich in aliphatics but depleted in unsaturated carbon and oxygenated aliphatics; eluate C8 showed abundant unsaturated aromatic and olefinic protons while being depleted in functionalized aliphatics. Eluate PPL showed substantial unsaturation, high content of oxygenated aliphatics and was depleted in extended aliphatic systems.
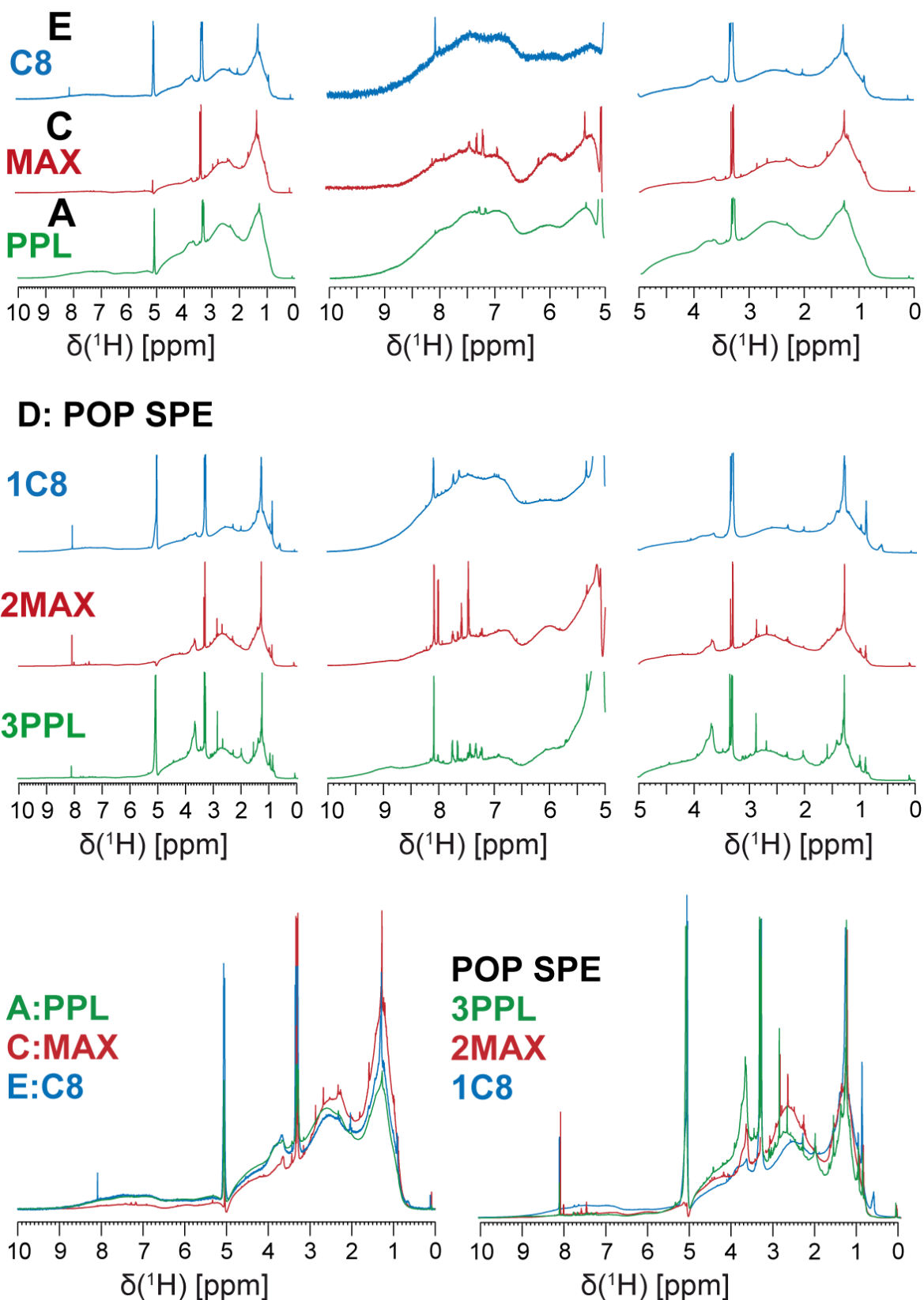
Fig. 7-1 ^1H NMR spectra (800 MHz, CD$_3$OD) of individual (upper panel) and (middle panel) POP SPE Suwannee River eluates. Bottom panel: Area-normalized superposition of (left) individual and (right) POP SPE-eluates; color code: C8 (blue), MAX (red), PPL (green).

125

Table 7-1 ^{1}H NMR section integral (800 MHz, CD$_3$OD) for key substructures of eluates (manual integration)

δ(^{1}H) [ppm]	key substructures	C8	MAX	PPL	POP SPE C8	POP SPE MAX	POP SPE PPL	Δ C8	Δ MAX	Δ PPL
10.0 - 7.0 ppm	=C$_{ar}$**H**	6.5	1.7	5.5	6.9	2.3	1.4	0.4	0.7	-4.1
7.0 - 5.0 ppm	=C**H**, O$_2$C**H**	5.9	2.7	5.8	5.7	4.3	3.3	-0.2	1.6	-2.5
5.0 - 3.1 ppm	OC**H**	23.2	19.9	26.2	22.9	28.2	39.7	-0.3	8.3	13.5
3.1 - 1.9 ppm	XCC**H**	29.1	32.5	32.2	27.8	35.7	30.3	-1.3	3.2	-1.9
1.9 - 0.5 ppm	CCC**H**	35.5	43.4	30.5	36.7	29.5	25.3	1.2	-13.9	-5.2

At closer inspection, manual superposition revealed near identical curvature of ^{1}H NMR resonances in eluates C8 and MAX, ranging from δ$_H$ ~ 2.75 – 1.75, implying remarkable superficial resemblance of functionalized aliphatic units in these two eluates. When comparing POP SPE eluates, remarkable congruence was found for POP SPE eluates -2MAX and -3PPL from δ$_H$ ~ 3.0 – 2.3, implying superficial resemblance of functionalized aliphatic units with higher oxygen content (smaller average distance).

Comparison of POP SPE and individual SPE

In case of eluate C8, the difference ^{1}H NMR spectrum"POP SPE minus individual eluate" provided strictly aliphatic NMR resonances at δ$_H$ of 0.6, 0.9 and 1.38 ppm which likely indicated selective leaching in eluate POP SPE-1C8, driving all other aliphatic NMR resonances to higher apparent abundance in individual eluate C8. The difference ^{1}H NMR spectrum POP SPE-2MAX minus MAX already denoted substantial disparity, with the ratio of "total difference ^{1}H NMR integral / average ^{1}H NMR integral of the two eluates" reaching 33%. Here, functionalized and oxygenated aliphatics (δ$_H$: 2.1 - 4.4 ppm) were enriched in eluate POP SPE-2MAX, and purely aliphatic units (CCC**H**; δ$_H$: < 2.0 ppm) were enriched in individual eluate MAX. With +1/3 of total average NMR integral, the difference ^{1}H NMR spectrum of eluates POP SPE-3PPL minus PPL again denoted substantial distinction between these two eluates. Here, unsaturated protons (δ$_H$ > 5.5 ppm) as well as functionalized and normal aliphatics (δ$_H$ < 2.5 ppm) were depleted in eluate PPLwhereas OCH-units were enriched in eluate POP SPE-3PPL. The large resonance at (δ$_H$: 3.65 ± 0.15 ppm) corresponded to aliphatic methyl esters and likely originated from transesterification of labile DOM molecules during elution from a large cartridge (cf. Fig. 7-2; Schmitt-Kopplin et al., 2010).

Frequently, the amplitude of this NMR resonance depends on rather subtle variations of sample conditions (Fig. 7-2). In general, larger cartridges with increased residence time of methanol during methanol elution tends to increase this overall NMR amplitude, but other DOM invariably shows this NMR resonance. Even when the variability of this NMR resonance may appear as a nuisance, it nevertheless makes other NMR-invisible labile protons amenable for NMR characterization.

However, even non-recognition of this extra NMR resonance would not modify the essential distinction between these eluates. The dominant positive aliphatic NMR resonances found in difference NMR spectrum POP SPE-1C8 minus C8 were also found in the difference NMR spectrum POP SPE-3PPL minus PPL, although at much smaller amplitude; NMR resonances originating from acetate and acetyl groups (δ_H: 2.0 ± 0.15 ppm) were rather prominent in eluate POP SPE-3PPL.

Three POP SPE fractions showed different ^{13}C NMR resonance envelopes: 1C8 typical of terrestrial DOM whereas 2MAX and 3PPL similar to marine DOM (Figure 5, Hertkorn et al. 2013, 2016). Carbonyl carbon, oxygenated aromatics and C-aromatics were dominant in 1C8 fraction, in line with ^{1}H NMR results that 1C8 was enriched of aromatics. Carbohydrate related NMR resonances (i.e. H$\underline{C}$O and H$\underline{C}$O$_2$ groups) were abundant in 3PPL fraction, corroborating the above ^{1}H spectra.
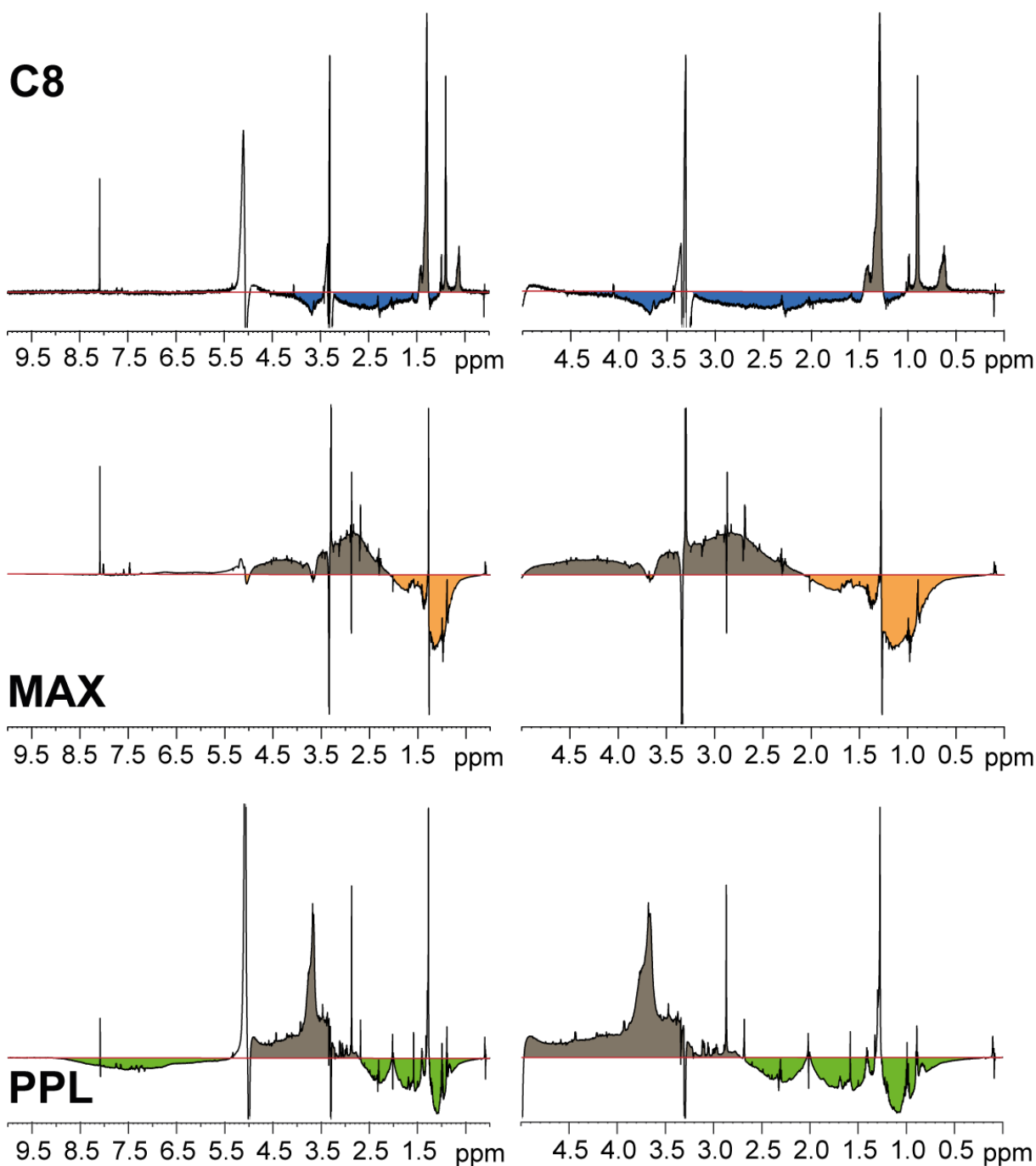
Fig. 7-2 ^{1}H NMR difference spectra (800 MHz, CD$_3$OD) of Suwannee River DOM: POP SPE minus individual SPE cartridges: intensity > 0 is more abundant in POP SPE cartridges; intensity < 0 is less abundant in POP SPE cartridges.Numbers provided denotes ratio of difference / total integral; from top to bottom: C8 (blue, 1st), MAX (red, 2nd), PPL (green, 3rd). Superposition of area-normalized ^{1}H NMR spectra for both individual and POP SPE eluates (Fig. 7-1) confirmed the abundance order of the key substructures in accordance with the substructure integral values (Table 7-1): unsaturated C$_{sp2}$H units eluates individual versus POP SPE: C8 > PPL >> MAX versus 1_C8 > 3_PPL > 2_MAX; OCH$_n$ units: PPL > MAX > C8 versus POP SPE-3PPL > -2MAX > -1C8; XCCH: MAX > PPL > C8 versus POP SPE-2MAX > -3PPL > -1C8, and CCCH: C8 > MAX > PPL versus POP SPE-1C8 >POP SPE-2MAX > POP SPE-3PPL.

The individual ^{13}C DEPT-45, -90 and -135 NMR spectra were measured and further computed to present the meaningful methine (CH), methylene (CH$_2$) and methyl (CH$_3$), shown in Fig. 7-3. H$\underline{\textbf{C}}_{\textbf{ar}}$-C group was selectively enriched in 1C8 extract whereas O-H$\underline{\textbf{C}}$-O and H$\underline{\textbf{C}}$-O groups were characterized in 3PPL extract, in agreement with the ^{13}C NMR spectra above. 2MAX was abundant in H$\underline{\textbf{C}}$-O and oxygenated methylene (H$_2$$\underline{\textbf{C}}$-O) groups. Overall, POP SPE had the separation power enhanced with combination of optimized phases, and extracted DOM with different carbon characteristics.

Table 7-2 ^{13}C NMR section integral (125 MHz, ^{12}CD$_3$OD; percent of total carbon) and key substructures of eluates. Middle: substructures used for NMR-derived reverse mixing model with nominal H/C and O/C ratios provided. Bottom: Percentage of methine, methylene and methyl carbon related to total protonated ^{13}C NMR integrals as derived from ^{13}C DEPT NMR spectra of eluates according to carbon multiplicity (left 3 colums) and relative proportions of the CH$_n$ units binding to oxygen versus carbon chemical environments (cf. Fig. 7-3).

δ (^{13}C) ppm	220-187	187-167	167-145	145-108	108-90	90-47	47-0	H/C ratio	O/C ratio
Key substructures	$\underline{\textbf{C}}$=O	$\underline{\textbf{C}}$OX	$\underline{\textbf{C}}_{ar}$-O	$\underline{\textbf{C}}^{ar}$-C,H	O$_2$$\underline{\textbf{C}}$H	O$\underline{\textbf{C}}$H	C$\underline{\textbf{C}}$H		
POP SPE-1C8	4.4	18.4	9.6	20.6	4.4	15.4	27.2	1.132	0.750
POP SPE-2MAX	1.9	14.2	3.0	8.2	5.4	32.1	35.2	1.303	0.762
POP SPE-3PPL	3.0	13.3	1.1	7.4	7.4	39.9	28.0	1.240	0.854
C8	2.8	14.0	6.2	14.3	3.1	39.1	20.5	1.115	0.823
MAX	1.3	13.2	1.3	6.6	3.6	32.6	41.3	1.386	0.688
PPL	4.9	18.3	5.0	15.1	3.0	19.5	34.3	1.245	0.720
NMR mixing model	$\underline{\textbf{C}}$=O	$\underline{\textbf{C}}$OOH	$\underline{\textbf{C}}_{ar}$-O	$\underline{\textbf{C}}_{ar}$-H	O$_2$$\underline{\textbf{C}}$H	O$\underline{\textbf{C}}$H	$\underline{\textbf{C}}$H$_2$		
H/C ratio	0	1	0	1	1	1	2		
O/C ratio	1	2	1	0	2	1	0		

Fig. 7-3 ^{13}C NMR spectra of SR DOM extracts obtained by POP SPE-1C8, -2MAX and -3PPL respectively. Superimposed protonated carbon NMR resonances $CH+CH_2+CH_3$ (the first column); DEPT-45 ^{13}C NMR spectra (the second column) and multiplicity-edited ^{13}C NMR spectra of CH (the third column), CH_2 (the fourth column) and CH_3 (the fifth column).

7.4.3   FT-ICR mass spectra

MS-derived bulk parameters of individual SPE eluates

All three individual SPE eluates showed abundant mass peaks with a mass peak distribution of common, polydisperse DOM such as a skewed, near Gaussian distribution of a few thousands of mass peaks with dominant mass spacings of methylene ($\Delta m = 14.654$ Da) and H_2 ($\Delta m = 2.1234$ Da) (Fig.7-4). The counts of assigned molecular formulas grew from eluate MAX (ne = 3172) < C8 (ne = 3466) < PPL (ne = 3899), and the proportions of CHO continually increased from PPL < MAX < C8, while MAX showed the smallest proportion of CHOS compounds (~2%) and the highest proportion of CHNO compounds (~36%). The computed average H/C ratios declined in the order MAX > C8 > PPL, corresponding to a concomitant increase in average DBE/C, equivalent to a mounting average unsaturation of retained DOM molecules. On the other hand, the average O/C ratios evolved according to MAX ~ C8 < PPL, while the average masses followed the order MAX < PPL < C8 (Table 7-3).

The absence of universal trends in the evolution of eluates C8 → MAX → PPL testified for the individuality of the operating molecular interactions of DOM retention in the three selected SPE cartridges. However, relevant characteristics of eluates emerged already at this bulk resolution: The C8 extract (ne = 3466) was a CHO-rich, less oxygenated (O/C ratio < 0.8) high mass complement of DOM molecules with nevertheless notable contributions of both CHNO and CHOS molecules at intermediate to elevated nominal unsaturation which could arise from C=C and C=O double bonds as well as from alicyclic rings. The MAX extract (ne = 3172) contained ~2/3 highly oxygenated CHO molecules up to an O/C ratio of 0.9 and ~1/3 of slightly less oxygenated CHNO molecules. It was further depleted in CHOS compounds and in higher mass molecules and showed a rather low aromaticity. The PPL extract showed the highest count of assigned molecular compositions (ne = 3899) with a sizable share of rather saturated CHOS molecules of variable oxygenation (O/C ratio: 0.3-0.8), and contained aromatic as well as highly oxygenated CHO molecules.
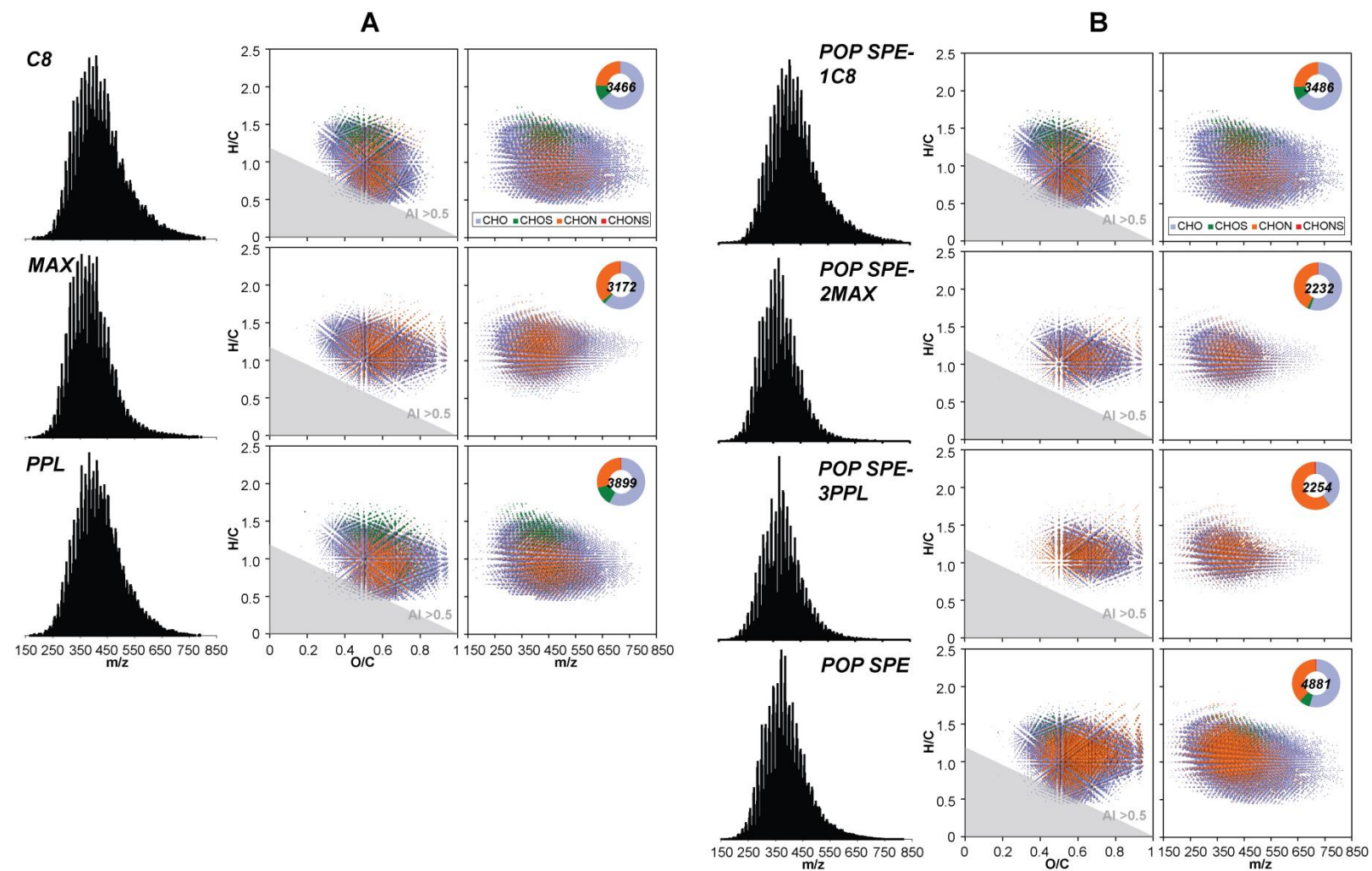
Fig. 7-4 Negative electrospray 12T FT-ICR mass spectra of (Panel A) individual SPE eluates and (panel B) POP SPE eluates; (left columns) mass spectra; (center columns): van Krevelen diagrams and (right columns): mass-edited H/C ratios. The bottom row denotes the consolidated molecular compositions of all three respective POP SPE eluates; bubble areas correspond to the mass peak intensities.

132

Table 7-3 Counts of mass peaks as computed from negative ESI FT-ICR mass spectra for singly charged ions with nitrogen rule check and 500 ppb tolerance. Left panels: individual SPE-eluates; center panel, shaded: consolidated POP SPE eluates; right panels: individual POP SPE-eluates.

members of molecular series	C8	MAX	PPL	POP SPE	POP-1C8	POP-2MAX	POP-3PPL
CHO-compounds	2244 (64.8%)	1950 (61.5%)	2270 (58.2%)	2664 (54.6%)	2260 (64.8%)	1241 (55.6%)	900 (39.9%)
CHOS-compounds	351 (10.1%)	66 (2.1%)	498 (12.8%)	353 (7.2%)	356 (10.2%)	42 (1.9%)	6 (0.3%)
CHNO-compounds	870 (25.1%)	1152 (36.3%)	1118 (28.7%)	1850 (37.9%)	870 (25.0%)	947 (42.4%)	1336 (59.3%)
CHNOS-compounds	1 (0%)	4 (0.1%)	13 (0.3%)	14 (0.3%)	0 (0%)	2 (0.1%)	12 (0.5%)
total number of assigned mass peaks	3465	3172	3899	4881	3486	2232	2254
average H [%]	4.48	5.08	4.14	4.51	4.44	4.53	4.35
average C [%]	54.56	54.47	52.63	52.08	54.57	51.70	49.63
average O [%]	40.41	39.90	42.49	41.87	40.42	43.08	44.50
average N [%]	0.31	0.52	0.39	0.71	0.31	0.67	1.51
average S [%]	0.23	0.02	0.35	0.11	0.25	0.02	0.01
computed average H/C ratio	0.99	1.12	0.94	1.03	0.99	1.05	1.05
computed average O/C ratio	0.56	0.55	0.61	0.59	0.56	0.62	0.67
computed average C/N ratio	205	122	157	86	205	90	38
computed average C/S ratio	633	7263	401	1263	582	6893	13235
double bond equivalent (DBE) average	11.1	8.8	10.7	9.6	11.1	8.6	8.4
DBE/C average	0.53	0.48	0.56	0.52	0.53	0.51	0.52
mass weighted average	455.8	414.0	438.6	420.1	455.8	390.4	393.5

MS-derived bulk properties of POP SPE eluates

All three singular POP SPE eluates again showed a mass peak distribution typical of a polydisperse DOM as described above for the individual SPE eluates. However, the counts of assigned molecular formulae declined from eluate POP SPE-1C8 (ne = 3486) to eluates POP SPE-2MAX and POP SPE-3PPL (ne = 2232 and 2254). Also, the proportions of CHO molecules continually decreased in the order eluate POP SPE-1C8 (~70%) > POP SPE-2MAX (~60%) > POP SPE-3PPL (< 40%), while the remainder were mainly CHNO

molecules, with the exception of POP SPE-1C8 in which ~10% CHOS compounds were observed (by count).

The computed average H/C ratios followed the order eluate POP SPE-1C8 < POP SPE-2MAX ~ POP SPE-3PPL, corresponding to a concomitant decrease in average DBE/C. On the other hand, the average O/C ratios evolved according to eluate POP SPE-1C8 < POP SPE-2MAX ~ C8 < POP SPE-3PPL, while the average mass followed the order eluate POP SPE-1C8 > POP SPE-3PPL ~ POP SPE-2MAX. Therefore, considerable variances between the pairs of eluates MAX / POP SPE-2MAX and PPL / POP SPE-3PPL became already obvious at bulk resolution.

Noteworthily, the FT-ICR MS-derived elemental ratios had the lower values than NMR-derived results, -0.2 units in O/C ratios and ~ -0.1 units in H/C ratios. It was more evident in 3PPL extract where carbohydrates accounted for ~ 50% in NMR spectra that ~ -Δ0.15 units in H/C ratios were observed. The lower displacement of elemental ratios in FT-ICR MS-derived data might be attributed to limited ionization efficiencies of oxygenated and hydrogen-saturated compounds such as carbohydrates (Hertkorn et al. 2008).

Comparison of the pairs of individual and POP SPE eluates at bulk resolution

Comparative mass analysis between three corresponding pairs of individual and POP SPE eluates provided further insights into the molecular selectivity of the SPE-based sequential DOM retention and elution process. Both extracts C8 and POP SPE-1C8 showed near perfectly identical mass spectra, confirming the reproducibility of C8-based DOM retention (Table 7-3). Those of the pairs MAX / POP SPE-2MAX and PPL / POP SPE-3PPL differed remarkably in molecular compositions (Table 7-3).

In comparison with individual eluate MAX, eluate POP SPE-2MAX showed smaller proportion of CHO (55.6% vs. 61.5%) and higher proportion of CHNO (42.4% vs. 36.3%) compounds at nearly unchanged, limited shares of CHOS and CHNOS compounds (Table 7-3). The overall counts of assigned molecular compositions had declined from 3172 to 2232, suggesting that the removal of DOM molecules from Suwannee River water by the preceding eluate POP SPE-1C8 had a stronger influence on the mass spectrum than a potential attenuation of ion suppression in an already complexity-reduced material (Gaspar et al. 2009, Hertkorn et al. 2008). At bulk resolution, eluate POP SPE-2MAX showed higher average unsaturation (H/C ratio: 1.05 vs. 1.12; DBE/C: 0.51 vs. 0.48) and average oxygenation (O/C

ratio: 0.62 vs. 0.55) than eluate MAX and in particular, showed smaller average mass (390.4 vs. 414.0 Da) (Table 7-3). In Fig. 7-5, the eluates MAX and POP SPE-2MAX shared an abundant (ne = 1904), contiguous assembly of diverse CHO (~60% of total ions) and CHNO (~40% of total ions) compounds with a sound coverage of the CHO and CHNO compositional space at elevated saturation (H/C ratio: 0.8 – 1.6) and oxygenation (O/C ratio: 0.4 – 0.9); CHOS compounds played a minor (< 2%) role. Unique to eluate MAX was a numerous (ne = 1267) set of ~70% less oxygenated (O/C ratio: 0.4±0.1), moderately saturated (H/C ratio: 1.3±0.2), high mass CHO molecules (up to m/z ~ 750), and a scattered set of ~30% more oxidized, lower mass (m/z < 550) CHNO compounds, with an admixture of <3% CHOS compounds. Unique to eluate POP SPE-2MAX was a limited (ne = 328) set of ~35% oxygenated (O/C ratio > 0.4) CHO compounds of diverse mass (m/z ~150-750), supplemented by ~60% of chemically diverse CHNO molecules, together with ~4% CHOS compounds.

Fig. 7-5 Negative electrospray 12T FT-ICR mass spectra: comparative analysis of individual SPE extract MAX and extract POP SPE-2MAX. Top panel: molecular compositions common in both extracts MAX and POP SPE 2_MAX; center panel: molecular compositions unique to individual extract MAX; bottom panel: molecular compositions unique to extract POP SPE-2MAX. Left panels: van Krevelen diagrams of SR DOM extracts; right panels: mass edited H/C ratios of SR DOM extracts.

The eluates PPL and POP SPE-3PPL shared an abundant set (ne = 1428) of ~55% of rather oxygenated CHO (O/C ratio: 0.4 – 0.95) and ~45% CHNO (O/C ratio: 0.4 – 0.8) compounds; common CHOS and CHNOS compounds were nearly absent. Unique to PPL (ne = 2470) were CHO (~65%), CHOS (~25%) and CHNO (~20%) compounds, which clearly differed in average saturation. CHOS compounds were comparatively saturated of average oxygenation, and ranged of m/z ~ 250-550, with a narrower bandwidth at higher unsaturation. CHNO compounds were preferentially unsaturated (H/C ratio < 1), of considerable oxygenation (O/C ratio: 0.4 – 0.8) and mass range (m/z ~ 400-650). CHO compounds covered all H/C, O/C ratios and mass range of CHOS and CHNO compounds, and reached out to lower oxygenation (O/C ratio > 0.25) and to higher mass (m/z < 750) than both CHOS and CHNO compounds. Unique to eluate POP SPE-3PPL (ne = 826) was an extended set (~80%) of oxidized CHNO (O/C ratio 0.35 – 0.9) compounds with H/C ratios ranging from 0.85 – 1.75, accompanied by ~20% of more saturated CHO with a broad mass range (m/z ~ 180-750). The compositional differences between eluates PPL and POP SPE-3PPL were rather pronounced (Fig. 7-6). Here, the overall counts of assigned molecular compositions had declined from 3899 to 2254 while shifts in relative proportions of CHO (58.2% vs. 39.9%), CHNO (28.7% vs. 59.3%) and CHOS (12.8% vs. 0.3%) were particularly distinctive. Apparently, POP SPE-1C8 had already removed the vast majority of ionizable CHOS compounds from Suwannee River water. Compared with the single PPL eluate, the eluate POP SPE-3PPL appeared more saturated (H/C ratio: 1.05 vs. 0.94; DBE/C: 0.52 vs. 0.56) and more oxygenated (O/C ratio: 0.67 vs. 0.61), and showed significantly smaller average mass (393.5 vs. 438.6 Da). Overall, eluate POP SPE-3PPL showed higher counts (1336 vs. 1118) and molecular diversity of CHNO compounds than the single eluate PPL, confirming the presence of ion suppression in all three individual Suwannee River DOM isolates.
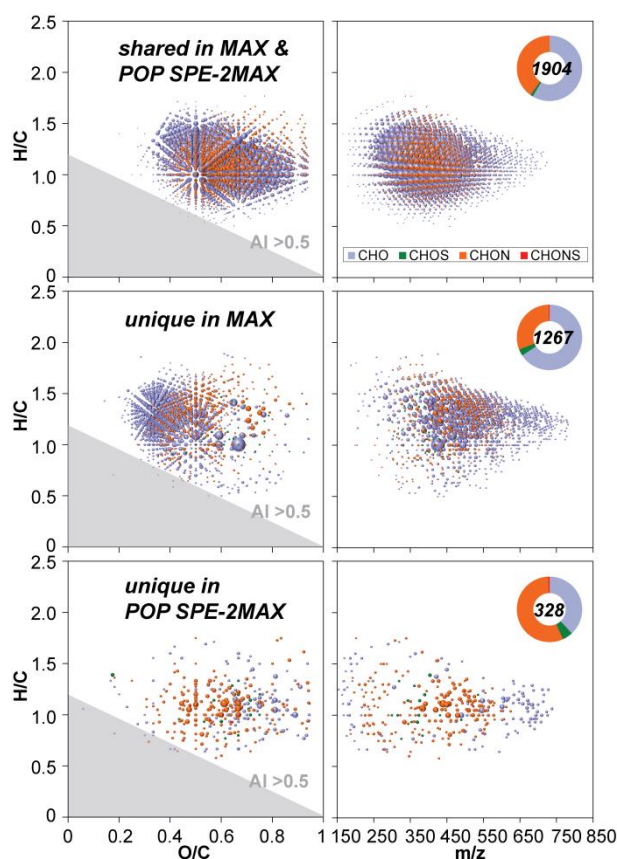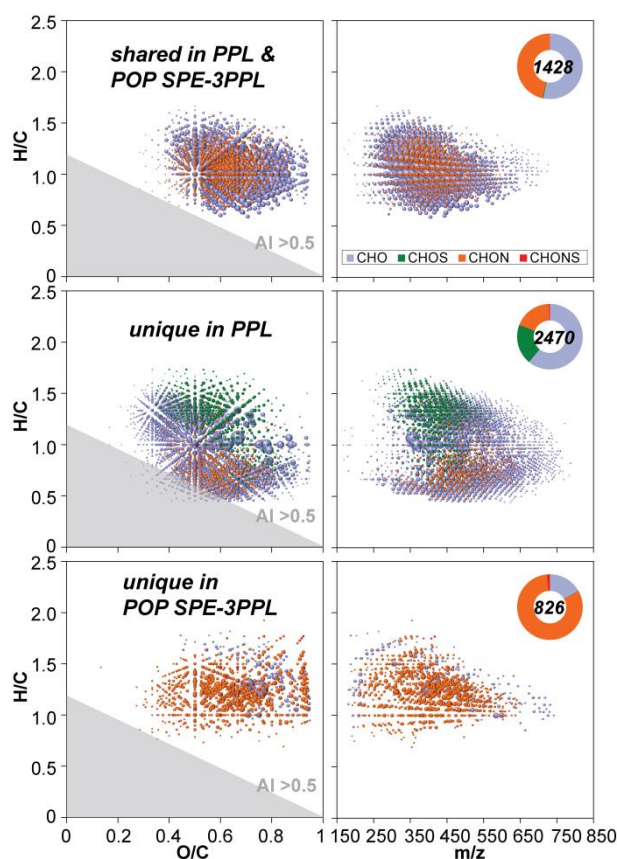
Fig. 7-6 Negative electrospray 12T FT-ICR mass spectra: comparative analysis of individual SPE extract PPL and extract POP SPE-3PPL. Top panel: molecular compositions common to both extracts PPL and POP SPE 3_PPL; center panel: molecular compositions unique to individual extract PPL; bottom panel: molecular compositions unique to extract POP SPE-3PPL. Left panels: van Krevelen diagrams of SR DOM extracts; right panel: mass edited H/C ratios of SR DOM extracts.

Comparison of consolidated individual and POP SPE extracts

Comparison of consolidated individual (ne = 5263) and consolidated POP SPE extracts (ne = 4881) provided 4259 common molecular compositions, distributed among CHO (~60%), CHNO (~30%) and CHOS (~10%) molecular series. Overall, CHO compounds covered a similar but slightly larger area in van Krevelen diagrams than CHNO compounds, i.e. were chemically more diverse. In comparison, CHOS compounds appeared on average more saturated, less oxygenated and of lower mass (Fig. 7-7). Compounds unique to POP SPE extracts (ne = 621) were mainly CHNO (~80%) compounds which were well oxygenated (maximum at a O/C ratio: 0.62±0.12) and reached to m/z ~ 550. About ~20% CHO compounds were even more oxygenated (O/C ratio > 0.6), and reached to higher mass, up to m/z ~ 750. Respective unique CHOS and CHNOS compounds were very few. In contrast, CHO (~40%), CHNO (~40%) and CHOS (~30%) compounds unique to consolidated individual SPE extracts (ne = 1003) occupied distinct sections in van Krevelen diagrams and

137

in mass-edited H/C ratios, confirming fundamentally different chemical structures. CHOS compounds were fairly oxygenated (O/C ratio: 0.5-0.9) and covered a wide range of relative (un)saturation (H/C ratio: 0.5-1.6) at rather low masses (m/z < 550). Respective CHNO compounds appeared to represent two distinct groups: one fairly saturated (H/C ratio: 1.1-1.6) and passively oxygenated (O/C ratio: 0.3-0.7) set and another unsaturated (H/C ratio < 1) but oxygenated (O/C ratio: 0.4-0.9) set of molecules. Unique CHO molecules were primarily strongly oxidized (O/C ratio: 0.6-0.95), and of high mass, up to m/z ~ 800.
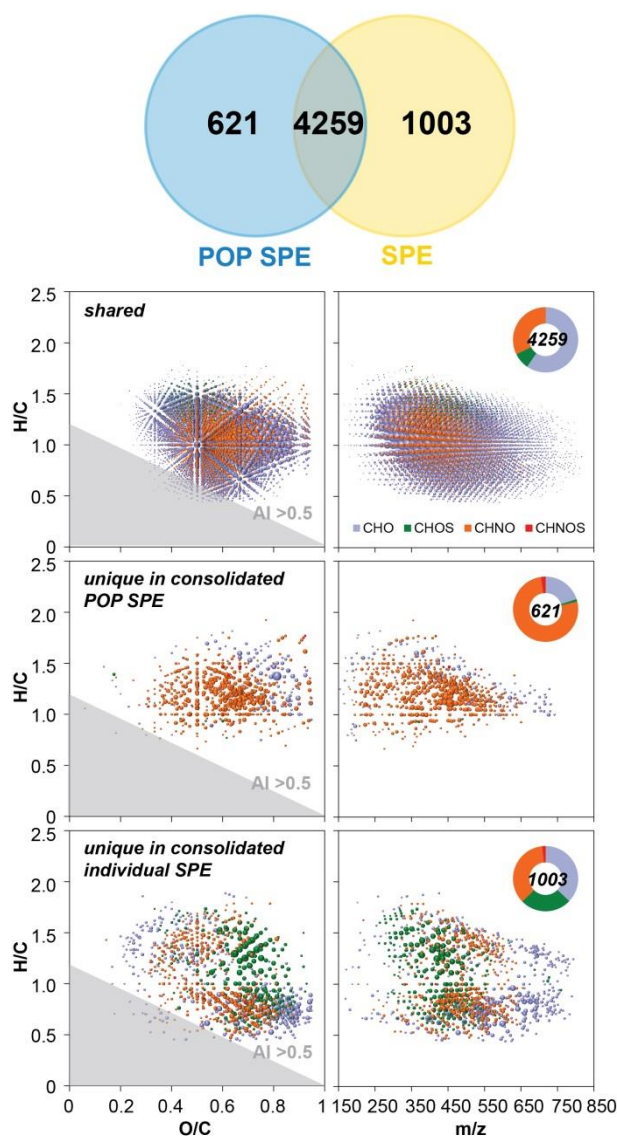
Fig. 7-7 Comparison of consolidated individual SPE extracts and consolidated POP SPE extracts: Venn diagrams of the assigned molecular compositions: Venn diagram showing counts of POP SPE extracts (blue) and individual extracts (yellow) in individual SPE extracts; van Krevelen diagrams and mass edited H/C ratios of the molecular compositions, from top to bottom: common to consolidated individual and POP SPE extracts; center: unique in consolidated POP SPE extracts; bottom: unique to consolidated individual SPE extracts.

Comparison of individual selectivity within individual and POP SPE eluates

The two groups of individual and POP SPE eluates were divided by definition into three single sections, three paired sections and a single common section for each system. Comparing the FT-ICR mass spectra of these seven combinations better reveal the effects of projection and ion suppression, which made common high quality FT-ICR mass spectra of DOM seemingly look alike (Hertkorn et al. 2008), and the distinction of the individual eluates became much more apparent (Fig. 7-8 and 7-9). Already, the total counts of consolidated molecular compositions in individual eluates (ne = 5263) exceeds that of consolidated POP SPE eluates (ne = 4881); this effects largely arises from the depletion of molecules in eluates POP SPE-2MAX and POP SPE-3PPL compared with the respective individual eluates MAX (ne = 2232 vs. 3172) and PPL (ne = 2254 vs. 3899). This had two major consequences: the count of molecular compositions common to all three eluates was much smaller in POP SPE (ne = 930) than in the individual eluates (ne = 1875); otherwise, the proportion of C8-derived unique (ne = 1952 vs. 513) and common molecular compositions were enhanced in POP SPE eluates. The overall coverage of the compositional space by molecular compositions common to all three eluates was substantially larger in the consolidated individual than the consolidated POP SPE eluates; this meant that the individual disparity between the POP SPE eluates was considerably larger than that of the individual eluates. The molecular compositions unique to eluates C8 in both systems followed the order CHO > CHNO > CHOS, with a relatively higher proportion of CHO molecules in the eluate POP SPE 1-C8 (~65% vs. ~55%). They were also much more numerous (ne = 1952 vs. 513), but interestingly, covered analogous spaces in both van Krevelen diagrams as well as mass-edited H/C ratios. While CHOS compounds were of intermediate unsaturation (H/C ratio: 1.3 ± 0.3), oxygenation (O/C ratio: 0.5 ± 0.15) at rather low masses (m/z < 550), CHNO compounds were, at only slightly higher oxygenation, considerably more unsaturated (H/C ratio > 0.5) and reached to aromatic compounds with AI > 0.5 (Koch and Dittmar 2006).
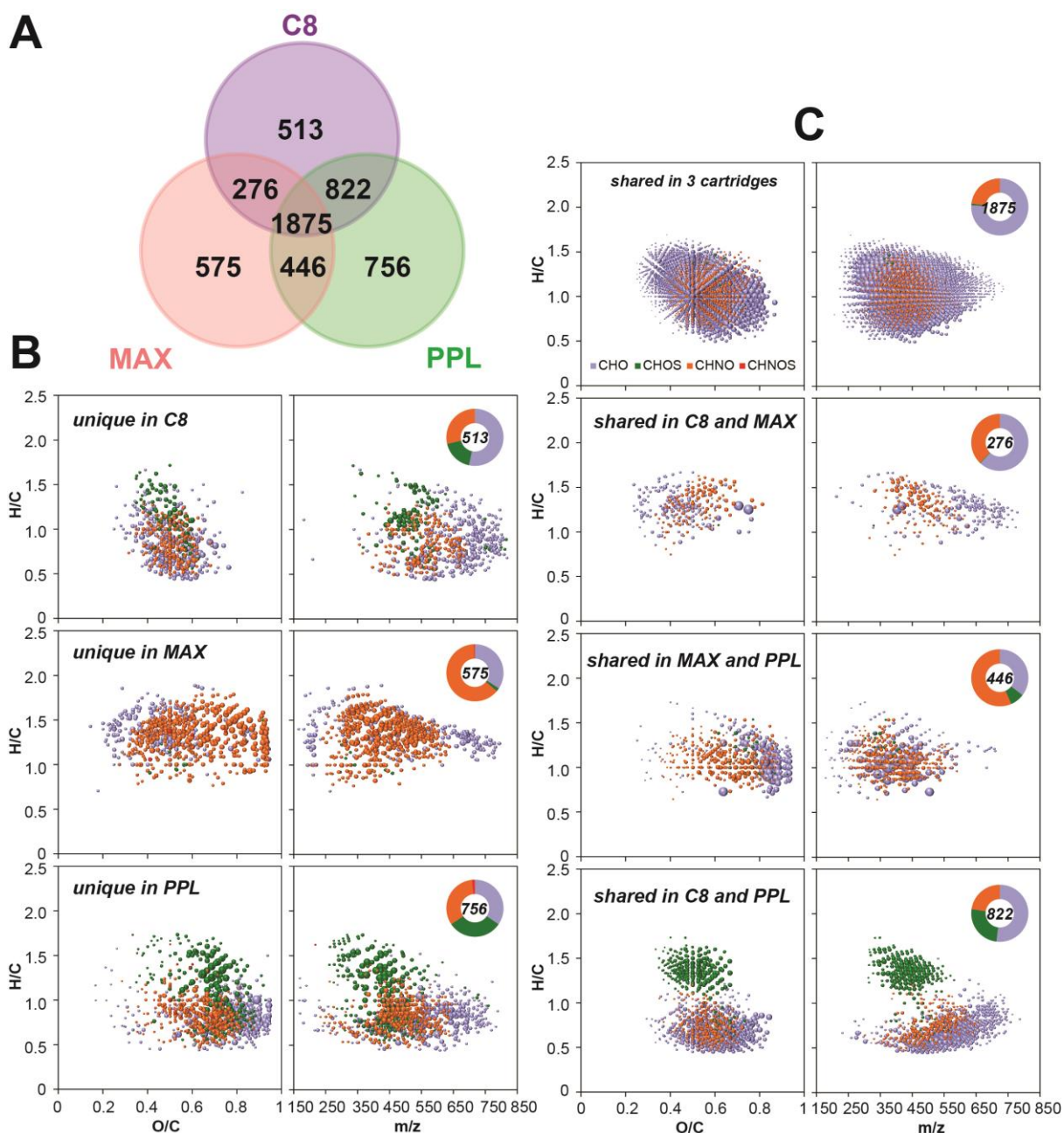
Fig. 7-8 Comparison of the three individual SPE extracts, with (panel A) Venn diagrams, showing the counts of the assigned molecular compositions; respective (left panels) van Krevelen diagrams and (right panels) mass-edited H/C ratios of the respective (panel B) unique and (panel C) shared compositions in (top row) all three SPE cartridges and respective pairs of eluates as depicted in the figure.
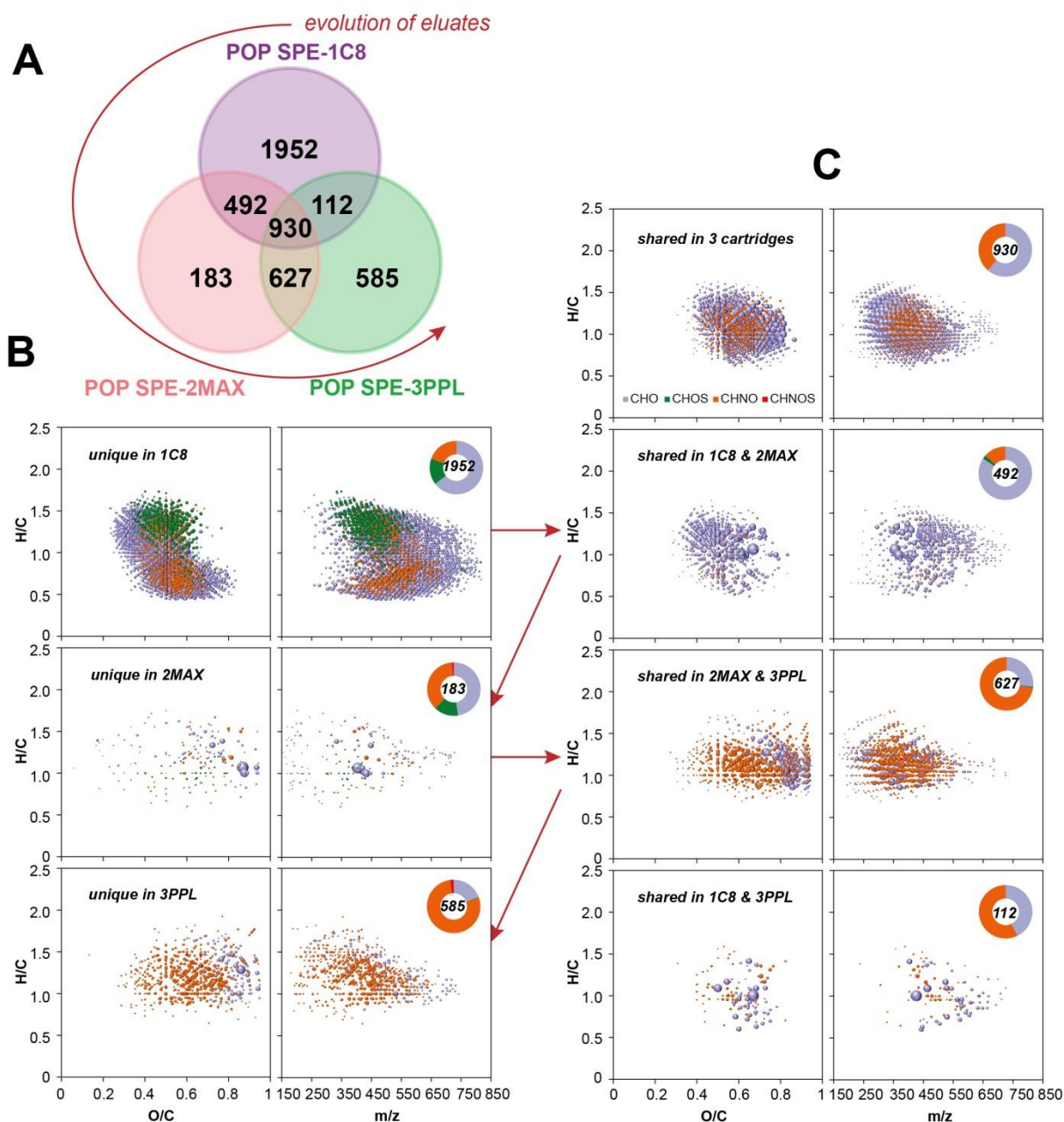
Fig. 7-9 Comparison and evolution of the three POP SPE extracts, with (panel A) Venn diagrams, showing the counts of the assigned molecular compositions; respective (left panels) van Krevelen diagrams and (right panels) mass-edited H/C ratios of the respective (left column) unique, denoting manifest eluates, and (right column) computed shared molecular compositions

7.4.4 Fluorescence spectra

In contrast to FT-ICR mass spectra and NMR spectra described above, the excitation emission matrix (EEM) fluorescence spectra of the three pairs of SPE eluates were largely similar. EEM analysis was performed by means of traditional peak picking instead of parallel factor analysis (PARAFAC) which is inappropriate in the case of limited number of samples, especially when intra- and inter-molecular interactions are involved (Stedmon and Bro 2008).

Classical fluorescent peaks A (Ex/Em of 240/430 nm; humic-like DOM) and C (Ex/Em of 335/440 nm; humic-like, terrestrial DOM) were prominent in the three individual and in the three POP SPE eluates (Fig. 7-10; http://or.water.usgs.gov/proj/carbon/EEMS.html). The EEM spectra of the C8-derived extracts were nearly identical as expected, while the two pairs of MAX- and PPL-derived extracts showed relative blue shifts (shorter excitation and emission wavelengths) indicative of lower molecular weights and smaller proportions of aromatic compounds and aromatic condensation (Rodriguez et al. 2014) in agreement with FT-ICR mass and NMR spectra (Fig. 4; Table 1, Table 3). Very small blue shifts in the order of 2 nm were observed between the pairs of eluates MAX / POP SPE-2MAX and PPL / POP SPE-3PPL, suggesting further decrease in molecular weight from individual to POP SPE eluates as observed again in FT-ICR mass spectra.

Fluorescence spectroscopy selectively detects the excitation and emission wavelength of π- and n-electrons, and is selectively influenced by long and short intra- and/or inter molecular interactions (Lacowics 2006). While the reduced molecular complexity in POP SPE eluates appeared to have no perceptible effect on the EEM spectra, a conceivable attenuation of intermolecular interactions in POP SPE eluates, which was expected to increase fluorescence, was also too small to be recognized (Rodriguez et al. 2014).
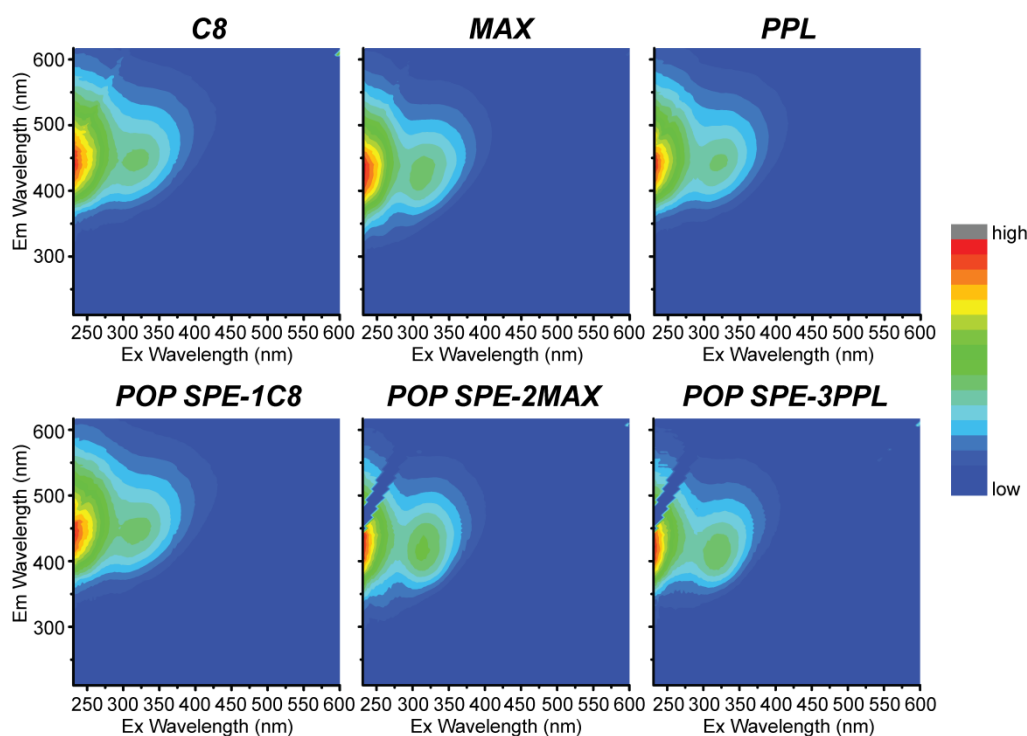
Fig. 7-10 Excitation and emission matrix (EEM) fluorescence spectra of the (top row) individual and (bottom row) POP SPE eluates.

7.4.5 Complementary analysis

During solid phase extraction of polydisperse DOM, the composition of the complex organic mixture was continually altered because the molecules which were most strongly binded to the solid phase were progressively depleted from the solution phase. Hence, from top to bottom (in a standard elution set-up) a continuous reorganization of the DOM assembly took place. This was a dynamic process which encompassed organic molecules of considerable chemical diversity as well as divergent time scales of weakening and strengthening intermolecular interactions. We have recently demonstrated chemoselective sequential elution of Suwannee River organic matter from PPL cartridges, and chemically diverse DOM compositions were observed in the five fractions (Li et al., 2016b).

The C8 cartridge effectively removed almost half of DOM molecules from Suwannee River water, leaving a depleted organic matter for consecutive POP SPE-2MAX and -3PPL. In general, the C8 cartridges caused depletion of aromatic and purely aliphatic molecules while oxygen-rich molecules were less effectively retained. This left DOM molecules rich in oxygen-containing functional groups available for consecutive elution.

Due to constant elution condition (methanol, pH = 2), the MAX cartridge did not operate with maximum retention and recovery capacity under the conditions recommended by the manufacture that washing with 5% NH_4OH and eluting with acid-containing organic solvent. We have observed color on MAX cartridges following elution; rinsing with acidified methanol (2% HCOOH) provided minor lipid-rich effluents and color was still retained on the cartridges, implying substantial shares of non-elution DOM molecules. The commonly rather efficient PPL cartridge then obviously could draw from only a minor abundance and diversity of DOM molecules.

In short, this version of POP SPE did not serve to increase the overall yield of DOM extraction from Suwannee River water, because PPL alone showed larger yield (~70%) than the consolidated POP SPE eluates (~60%). However, the production of three pairs of eluates which behaved remarkably similar in NMR, FT-ICR MS and fluorescence spectra had provided better understanding of intrinsic molecules diversity of Suwannee River water which is normally hidden by projection of many molecular or atomic properties on limited ranges of data. Comparative mathematical analysis revealed appreciable molecular differences between

these fractions which could serve in further work for targeted enrichment of certain classes of compounds.

Furthermore, the molecular and structural diversity of DOM varies significantly among different sources. It is well known that PPL cartridges have good performances on freshwater DOM but have drimination against carbohydrates and lipids with around 50% recovery for marine DOM (Dittmar et al. 2008, Raeke et al. 2016). The setup of POP SPE shows the potential to extract a more representative DOM fraction on molecular level across a wide range of DOM samples.

7.5 Conclusions

Phase-optimized solid phase extraction (POP SPE) of DOM produced novel fractionation different from individual SPE eluates. Compositional and structural properties of DOM molecules will drive DOM fractionation while reorganization of complex mixtures during the SPE-based fractionation will expose new binding sites for DOM-sorbent interaction during elution. This kind of complexity reduction operates semi-orthogonal to known DOM fractionation procedures and offers substantial potential in investigating fundamental molecular differences between e.g. soil, freshwater and marine derived DOM, which share many common molecular compositions but may behave different in POP SPE based experiments.

7.6 Acknowledgements

7.7 References

Arakawa, N. and Aluwihare, L. (2015) Direct identification of diverse alicyclic terpenoids in Suwannee River Fulvic Acid. Environ Sci Technol 49(7), 4097-4105.

Ball, G. I. and Aluwihare L. (2014) CuO-oxidized dissolved organic matter (DOM) investigated with comprehensive two dimensional gas chromatography-time of flight-mass spectrometry (GC × GC-TOF-MS). Org Geochem 75, 87–98.

Bianchi, T.S. (2011) The role of terrestrially derived organic carbon in the coastal ocean: a changing paradigm and the priming effect. Proc Natl Acad Sci U S A 108(49), 19473-19481.

Deconinck, E., Kamugisha, A., Van Campenhout, P., Courselle, P. and De Beer, J.O. (2015) Development of a Stationary Phase Optimised Selectivity Liquid Chromatography based screening method for adulterations of food supplements for the treatment of pain. Talanta 138, 240-246.

Deconinck, E., Ghijs, L., Kamugisha, A. and Courselle, P. (2016) Comparison of three development approaches for Stationary Phase Optimised Selectivity Liquid Chromatography based screening methods Part II: A group of structural analogues (PDE-5 inhibitors in food supplements). Talanta 148, 346-355.

Delahaye, S. and Lynen, F. (2014) Implementing stationary-phase optimized selectivity in supercritical fluid chromatography. Anal Chem 86(24), 12220-12228.

DiDonato, N., Chen, H., Waggoner, D. and Hatcher P.G. (2016) Potential origin and formation for molecular components of humic acids in soils. Geochim Cosmochim Ac 178, 210-222.

Fasching, C., Behounek, B., Singer, G.A. and Battin, T.J. (2014) Microbial degradation of terrigenous dissolved organic matter and potential consequences for carbon cycling in brown-water streams. Sci Rep 4, 4981.

Flerus, R., Lechtenfeld, O.J., Koch, B.P., McCallister, S.L., Schmitt-Kopplin, P., Benner, R., Kaiser, K. and Kattner, G. (2012) A molecular perspective on the ageing of marine dissolved organic matter. Biogeosciences 9(6), 1935-1955.

Gaspar, A., Harir, M., Hertkorn, N. and Schmitt-Kopplin, P. (2010) Preparative free-flow electrophoretic offline ESI-Fourier transform ion cyclotron resonance/MS analysis of Suwannee River fulvic acid. Electrophoresis 31(12), 2070-2079.

Gonsior, M., Schmitt-Kopplin, P. and Bastviken, D. (2013). Depth-dependent molecular composition and photo-reactivity of dissolved organic matter in a boreal lake under winter and summer conditions. Biogeosciences 10 (11), 6945-6956.

Gonsior, M., Hertkorn, N., Conte, M.H., Cooper, W.J., Bastviken, D., Druffel, E. and Schmitt-Kopplin, P. (2014) Photochemical production of polyols arising from significant photo-

transformation of dissolved organic matter in the oligotrophic surface ocean. Mar Chem 163, 10-18.

Green, N.W., McInnis, D., Hertkorn, N., Maurice, P.A. and Perdue, E.M. (2015) Suwannee River Natural Organic Matter: Isolation of the 2R101N Reference Sample by Reverse Osmosis. Environ Eng Sci 32(1), 38-44.

Hertkorn, N., Benner, R., Frommberger, M., Schmitt-Kopplin, P., Witt, M., Kaiser, K., Kettrup, A. and Hedges, J.I. (2006) Characterization of a major refractory component of marine dissolved organic matter. Geochim Cosmochim Ac 70(12), 2990-3010.

Hertkorn, N., Ruecker, C., Meringer, M., Gugisch, R., Frommberger, M., Perdue, E.M., Witt, M. and Schmitt-Kopplin, P. (2007) High-precision frequency measurements: indispensable tools at the core of the molecular-level analysis of complex systems. Anal Bioanal Chem 389(5), 1311-1327.

Hertkorn, N., Frommberger, M., Witt, M., Koch, B.P., Schmitt-Kopplin, P. and Perdue, E.M. (2008) Natural organic matter and the event horizon of mass spectrometry. Anal Chem 80(23), 8908-8919.

Hertkorn, N., Harir, M., Koch, B.P., Michalke, B. and Schmitt-Kopplin, P. (2013) High-field NMR spectroscopy and FTICR mass spectrometry: powerful discovery tools for the molecular level characterization of marine dissolved organic matter. Biogeosciences 10(3), 1583-1624.

Hertkorn, N., Harir, M., Cawley, K.M., Schmitt-Kopplin, P. and Jaffé, R. (2016) Molecular characterization of dissolved organic matter from subtropical wetlands: a comparative study through the analysis of optical properties, NMR and FTICR/MS. Biogeosciences 13(8), 2257-2277.

Kim, S., Simpson, A.J., Kujawinski, E.B., Freitas, M.A. and Hatcher, P.G. (2003) High resolution electrospray ionization mass spectrometry and 2D solution NMR for the analysis of DOM extracted by C18 solid phase disk. Org Geochem 34(9), 1325-1335.

Knicker, H. (2010) "Black nitrogen" – an important fraction in determining the recalcitrance of charcoal. Org Geochem 41, 947-950.

Koch, B.P. and Dittmar, T. (2006) From mass to structure: an aromaticity index for high-resolution mass data of natural organic matter. Rapid Commun Mass Sp 20(5), 926-932.

Koch, B.P., Ludwichowski, K.-U., Kattner, G., Dittmar, T. and Witt, M. (2008) Advanced characterization of marine dissolved organic matter by combining reversed-phase liquid chromatography and FT-ICR-MS. Mar Chem 111(3-4), 233-241.

Ksionzek, K.B., Lechtenfeld, O.J., McCallister, S.L., Schmitt-Kopplin, P., Geuer, J.K., Geibert, W. and Koch, B.P. (2016) Dissolved organic sulfur in the ocean: Biogeochemistry of a petagram inventory. Science 354(6311), 456-459.

Kruger, B.R., Dalzell, B.J. and Minor, E.C. (2011) Effect of organic matter source and salinity on dissolved organic matter isolation via ultrafiltration and solid phase extraction. Aquat Sci 73(3), 405-417.

Kujawinski, E.B. (2011) The impact of microbial metabolism on marine dissolved organic matter. Ann Rev Mar Sci 3, 567-599.

Lacowics, J. R. (2006) Principle of fluorescence spectroscopy. Springer.

Li, Y., Harir, M., Lucio, M., Kanawati, B., Smirnov, K., Flerus, R., Koch, B.P., Schmitt-Kopplin, P. and Hertkorn, N. (2016a) Proposed Guidelines for Solid Phase Extraction of Suwannee River Dissolved Organic Matter. Anal Chem 88(13), 6680-6688.

Li, Y. Harir, M., Lucio, M., Gonsior, M., Koch, B. P., Schmitt-Kopplin, P., Hertkorn, N. (2016b) Comprehensive structure-selective characterization of dissolved organic matter by reducing molecular complexity and increasing analytical dimensions. Water Res 106, 477-487.

Li, Y., Harir, M., Uhl, J., Kanawati, B., Lucio, M., Smirnov, K., Koch, B. P., Schmitt-Kopplin, P. and Hertkorn N. (2016c) How Representative Are Dissolved Organic Matter (DOM) Extracts? A Comprehensive Study of Sorbent Selectivity for DOM Isolation. Water Res, under revision.

Lucas, J., Koester, I., Wichels, A., Niggemann, J., Dittmar, T., Callies, U., Wiltshire, K.H. and Gerdts, G. (2016) Short-Term Dynamics of North Sea Bacterioplankton-Dissolved Organic Matter Coherence on Molecular Level. Front Microbiol 7, 321.

Minor, E.C., Swenson, M.M., Mattson, B.M. and Oyler, A.R. (2014) Structural characterization of dissolved organic matter: a review of current techniques for isolation and analysis. Environ Sci Process Impacts 16(9), 2064-2079.

Moran, M.A., Kujawinski, E.B., Stubbins, A., Fatland, R., Aluwihare, L.I., Buchan, A., Crump, B.C., Dorrestein, P.C., Dyhrman, S.T., Hess, N.J., Howe, B., Longnecker, K., Medeiros, P.M., Niggemann, J., Obernosterer, I., Repeta, D.J. and Waldbauer, J.R. (2016) Deciphering ocean carbon in a changing world. Proc Natl Acad Sci U S A 113(12), 3143-3151.

Nebbioso, A. and Piccolo, A. (2013) Molecular characterization of dissolved organic matter (DOM): a critical review. Anal Bioanal Chem 405(1), 109-124.

Nyiredy, S., Szűcs, Z. and Szepesy, L. (2006) Stationary-Phase Optimized Selectivity LC (SOS-LC): Separation Examples and Practical Aspects. Chromatographia 63(S13), S3-S9.

Nyiredy, S., Szucs, Z. and Szepesy, L. (2007) Stationary phase optimized selectivity liquid chromatography: Basic possibilities of serially connected columns using the "PRISMA" principle. J Chromatogr A 1157(1-2), 122-130.

Osterholz, H., Dittmar, T. and Niggemann, J. (2014) Molecular evidence for rapid dissolved organic matter turnover in Arctic fjords. Mar Chem 160, 1-10.

Perdue E. M. and Ritche J. D.Dissolved organic matter in fresh waters, Treatise on Geochemistry (eds, Holland H. D. and Turekian K. K.), Elsevier-Pergamon, Oxford, 2003, Vol. 5, 273-318.

Perminova, I.V., Dubinenkov, I.V., Kononikhin, A.S., Konstantinov, A.I., Zherebker, A.Y., Andzhushev, M.A., Lebedev, V.A., Bulygina, E., Holmes, R.M., Kostyukevich, Y.I., Popov, I.A. and Nikolaev, E.N. (2014) Molecular mapping of sorbent selectivities with respect to isolation of Arctic dissolved organic matter as measured by Fourier transform mass spectrometry. Environ Sci Technol 48(13), 7461-7468.

Raeke, J., Lechtenfeld, O.J., Wagner, M., Herzsprung, P. and Reemtsma, T. (2016) Selectivity of solid phase extraction of freshwater dissolved organic matter and its effect on ultrahigh resolution mass spectra. Environ Sci Process Impacts 18(7), 918-927.

Ratpukdi, T., Rice, J.A., Chilom, G., Bezbaruah, A. and Khan, E. (2009) Rapid Fractionation of Natural Organic Matter in Water Using a Novel Solid-Phase Extraction Technique. Water Environ Res 81(11), 2299-2308.

Rodriguez, F.J., Schlenger, P. and Garcia-Valverde, M. (2014) A comprehensive structural evaluation of humic substances using several fluorescence techniques before and after ozonation. Part I: structural characterization of humic substances. Sci Total Environ 476-477, 718-730.

Sandron, S., Rojas, A., Wilson, R., Davies, N.W., Haddad, P.R., Shellie, R.A., Nesterenko, P.N., Kelleher, B.P. and Paull, B. (2015) Chromatographic methods for the isolation, separation and characterisation of dissolved organic matter. Environ Sci Process Impacts 17(9), 1531-1567.

Schmidt, F., Elvert, M., Koch, B.P., Witt, M. and Hinrichs, K.-U. (2009) Molecular characterization of dissolved organic matter in pore water of continental shelf sediments. Geochim Cosmochim Ac 73(11), 3337-3358.

Schmitt-Kopplin, P, Hertkorn, N., Schulten, H.-R., Kettrup, A. (1998) Structural changes in a dissolved soil humic acid during photochemical degradation processes under O_2 and N_2 atmosphere. Environ. Sci. Technol. 32, 2531-2541.

Schmitt-Kopplin, P., Gelencser, A., Dabek-Zlotorzynska, E., Kiss, G., Hertkorn, N., Harir, M., Hong, Y. and Gebefugi, I. (2010) Analysis of the unresolved organic fraction in atmospheric aerosols with ultrahigh-resolution mass spectrometry and nuclear magnetic resonance spectroscopy: organosulfates as photochemical smog constituents. Anal Chem 82(19), 8017-8026.

Shen, Y., Chapelle, F.H., Strom, E.W. and Benner, R. (2014) Origins and bioavailability of dissolved organic matter in groundwater. Biogeochemistry 122(1), 61-78.

Stedmon, C.A. and Bro, R. (2008) Characterizing dissolved organic matter fluorescence with parallel factor analysis: a tutorial. Limnol Oceanogr-Meth 6(11), 572-579.

Stenson, A.C. (2008) Reversed-Phase Chromatography Fractionation Tailored to Mass Spectral Characterization of Humic Substances. Environ. Sci. Technol. 42(6), 2060-2065.

Swenson, M.M., Oyler, A.R. and Minor, E.C. (2014) Rapid solid phase extraction of dissolved organic matter. Limnol Oceanogr-Meth 12(10), 713-728.

Thurman, E.M. and Malcolm, R.L. (1981) Preparative isolation of aquatic humic substances. Environ Sci Technol 15(4), 463-466.

Tziotis, D., Hertkorn, N. and Schmitt-Kopplin, P. (2011) Kendrick-analogous network visualisation of ion cyclotron resonance Fourier transform mass spectra: improved options for the assignment of elemental compositions and the classification of organic molecular complexity. Eur J Mass Spectrom (Chichester) 17(4), 415-421.

Waggoner, D. C., Chen, H., Willoughby, A. S. and Hatcher P. G. (2015) Formation of black carbon-like and alicyclic aliphatic compounds by hydroxyl radical initiated degradation of lignin. Org Geochem 82, 69-76.

Woods, G.C., Simpson, M.J., Koerner, P.J., Napoli, A. and Simpson, A.J. (2011) HILIC-NMR: toward the identification of individual molecular components in dissolved organic matter. Environ Sci Technol 45(9), 3880-3886.

Woods, G.C., Simpson, M.J. and Simpson, A.J. (2012) Oxidized sterols as a significant component of dissolved organic matter: evidence from 2D HPLC in combination with 2D and 3D NMR spectroscopy. Water Res 46(10), 3398-3408.

Chapter 8

Conclusions and Future Directions

8 Conclusions and Future Directions

8.1 Optimization of SPE procedure during eluting step

The SPE method of DOM isolation has been evaluated in detail with respect to the influence of all critical parameters such as loading mass, concentration, flow rate and up-scaling on the example of Suwannee River water (Li et al., 2016a). Owing to the molecular heterogeneity and polydispersity of DOM in general and the substantial variance of individual molecules present in any individual DOM, these parameters have to be adapted in principle for every individual combination of SPE resin and DOM sample. However, DOM can be grouped according to origin, like freshwater, estuarine, marine, soil and atmospheric DOM. These materials will share more common bulk characteristics and proportions of certain leading molecules. The definition of optimum SPE conditions in terms of loading mass, concentration, flow rate and up-scaling would contribute to obtain reproducible DOM fractions from different natural environments. An observance of good experimental practice would also minimize the potential inconsistencies among different labs, allowing for a reasonable comparison of different DOM samples.

One critical question is the origin of the methoxy NMR resonance in ^{1}H and ^{13}C NMR spectra of SPE eluates which can be differentiated by heteronuclear ^{1}H, ^{13}C HSQC NMR spectroscopy into aliphatic and aromatic methyl ethers and aliphatic and aromatic methyl ethers (Zhang et al. 2014). In accordance with others, previous studies (Flerus et al. 2011, McIntyre and McRae 2005), we have also observed potential transesterification reactions happening during methanolic elution at pH = 2. The extent of this reaction does not only depend on DOM alone but also on the SPE cartridge manufacturers and even batch type and size of SPE cartridge delivered from the same manufacturer. It appears that manufactures regularly change their SPE cartridge production process without disclosing this proprietary information to the scientific community. The pH value of two is sufficiently low to induce transesterification reactions of methanol with reactive DOM precursor molecules. In the case of CHOS compounds, this side reaction is not entirely destructive because it makes otherwise NMR-invisible compounds in complex mixtures such as sulfate esters amenable to NMR analysis. Otherwise, formation of methyl esters which can be solely detected by NMR spectroscopy inflates the apparent carbon recovery of the isolation process and causes displacement towards higher mass molecules in FT-ICR mass spectra.

Flerus et al. (Flerus et al. 2011) clearly demonstrated that esterification of marine DOM occurred in methanol extract at 20 ^{o}C for 4 weeks in the dark. In our study, the change in DOC recovery remained within 5% when esterification occurred under the experimental conditions. Systematic studies using various labelled forms of methanol, e.g. CD_3OD, $^{13}CD_3OD$, $^{13}CH_3OH$ in conjunction with NMR and mass spectrometry could advance the mechanistic understanding of this side reaction and its dependence of DOM properties.

Further method development of avoiding/attenuating esterification could focus on practical aspects of the SPE process such as careful drying preceding methanol elution, a wash step with small amounts of pure water following the wash step with acidic water, while collecting this initial fraction separately. Using mixed solvents like gradients of water / methanol mixtures during the eluting step, instead of applying pure methanol, would be also helpful to mitigate esterification (McIntyre and McRae 2005). Certain criteria such as the overall DOC recovery, molecular compositions and structures should be addressed.

Methanol is an versatile and benign SPE elution solvent in many respects: it appears to dissolve the broadest bandwidth of different DOM molecules and is particularly beneficial for NMR spectroscopy: its ^{1}H NMR (δ_H = 3.30 ppm) and ^{13}C NMR resonances (δ_C = 49 ppm) do not overly interfere with NMR resonances originating from DOM itself. Acetonitrile which is an attractive alternative solvent, interferes in ^{1}H NMR spectra (δ_H = 1.93 ppm) with critical aliphatic DOM molecules and in ^{13}C NMR spectra with critical aromatic DOM molecules (δ_C = 117.3 ppm; its aliphatic NMR resonance (δ_H = 1.25 ppm) resides at the upfield section of aliphatic DOM molecules). Nevertheless, acetonitrile shows different extraction selectivity with commonly smaller extraction yield in the SPE process of DOM (Flerus et al., 2011) and may be used in sequence and in parallel with methanolic elution to further gain valuable insight into the molecular characteristics of DOM.

8.2 Further adaption of stepwise SPE of DOM and its applications

Selective fractionation of SR DOM by means of stepwise SPE elution which collects limited quantities of eluate separately has been proposed by us as a very facile method to obtain distinct, complexity reduced DOM fractions (Li et al., 2016b). Spectral resolution in FT-MS, NMR and optical spectra is greatly improved in comparison with those of bulk DOM, and these three complementary structure-selective correlated data have shown analogous hierarchical clustering according to the fractions. SPE of DOM follows primarily a polarity-

based mechanism, different from LC-based fractionation of DOM. For instance, sequential elution of Elbe Rive DOM provided continual decrease of carboxylic content but continual increase of aromatics (Fig. 8-1). Within the elution sequence the aliphatic groups increased whereas the CRAMs decreased as well as the carbohydrates and methoxl groups (Fig. 8-2).

sequential elution of Elbe River water SPE extracts (5 g PPL): ^{13}C NMR spectra in ^{12}CD$_3$OD
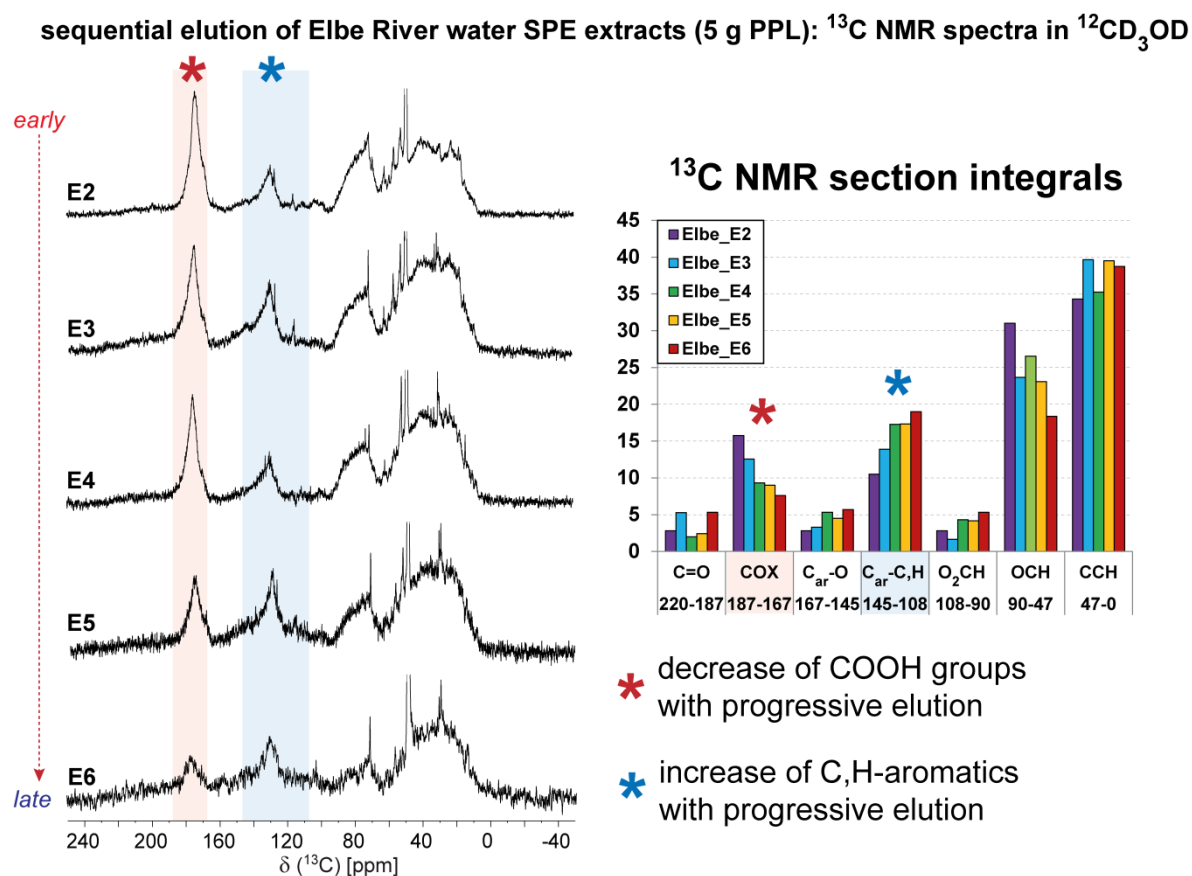
Fig. 8-1 ^{13}C NMR spectra (^{12}CD$_3$OD; 125 MHz) and ^{13}C NMR section integrals of River Elbe DOM obtained by sequential elution of SPE/PPL with equal aliquots of methanol, showing a continual decrease of carboxylic content and continual increase of aromatic carbon during stepwise fractionation.

Further work can be done based on the preliminary findings. First of all, this method can be applied to different DOM materials, for instance, soil, riverine, marine and atmospheric DOM. Fractions can be compared by in-depth spectroscopic analysis to reveal insights into their molecular and structural information. Stable ($^{12/13}$C, $^{1/2}$H and $^{14/15}$N) as well as radiocarbon (^{14}C) isotope studies will add valuable insights about DOM temporal evolution. This will contribute to a better comprehension to the participation of DOM compounds in various ecosystem processes. An attractive example would be a comparison of the DOM fractions from land to sea, i.e. from riverine though estuarine to marine origin.

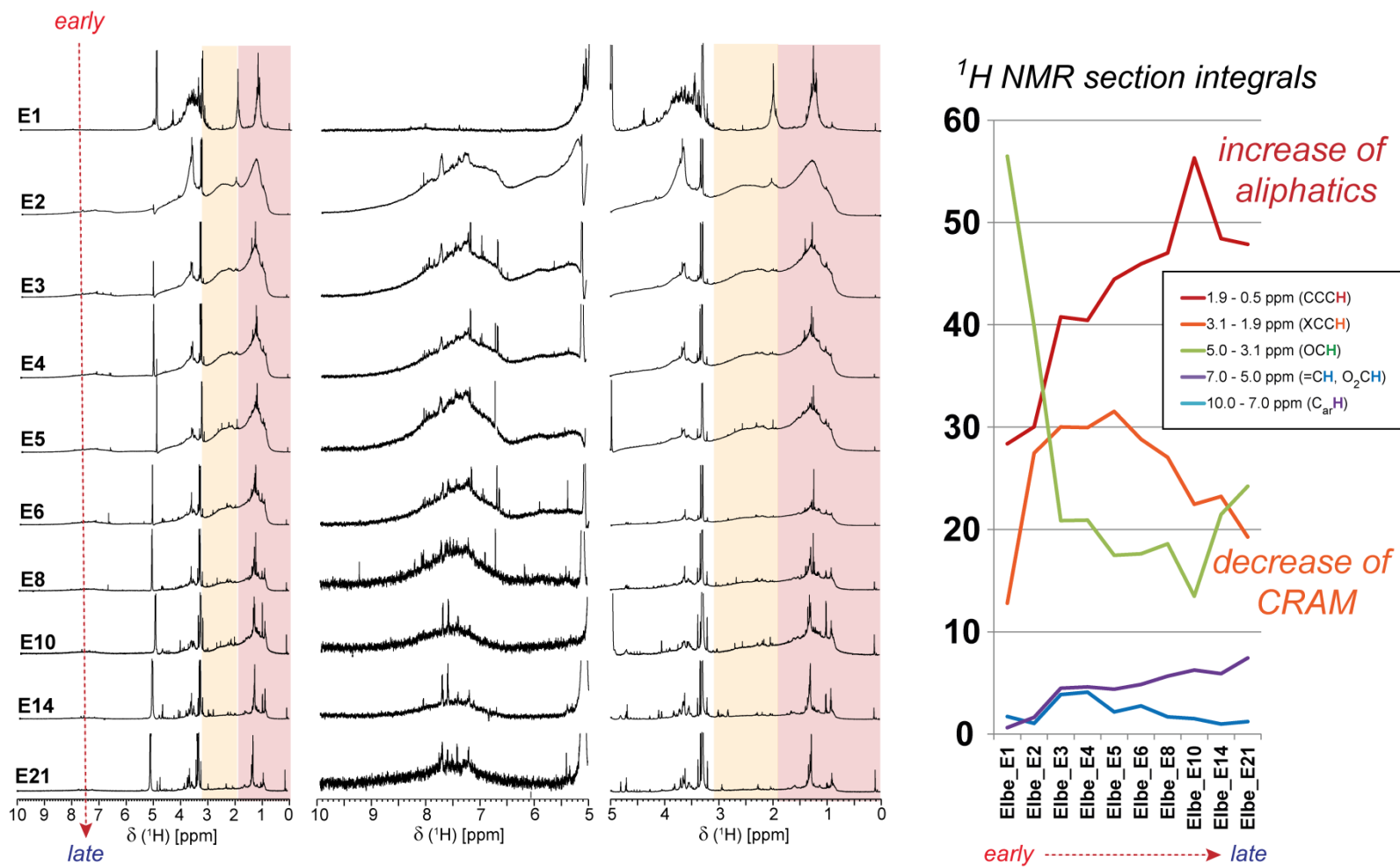*Fig. 8-2 ^{1}H NMR spectra (^{12}CD$_3$OD, 800 MHz) and 1H NMR section integrals of Elbe River DOM obtained by sequential elution of SPE/PPL with equal aliquots of methanol, showing a distinct presence of carbohydrates in the initial fraction, followed by a continual decrease of CRAM and a continual increase of aliphatic protons during stepwise fractionation.*

8.3 POP SPE of DOM

The behavior of 24 commercially available SPE sorbents has been investigated under SPE conditions of pH = 2 and methanolic elution for Suwannee River and North Sea DOM (cf. chapter 6 of this thesis). Pronounced selectivity and leaching behavior towards different SPE resins and DOM composition has been observed. The selectivity was based on sorption mechanisms, and has shown distinct behaviors towards CHNO, CHOS compounds, unsaturated compounds, and lipids. While the widely used HLB cartridge was found to leach under these conditions, SPE resins C8, MAX and PPL have shown rather high recovery for DOM isolation at limited leaching. These extracts have shown rather distinct and complementary information.

The subsequently developed phase-optimized SPE (POP SPE) which combines several cartridges with different sorbent phases for the isolation of polydisperse and molecularly heterogeneous DOM can be further improved:

1. The sequence of the SPE sorbents on DOM isolation can be further varied. In combination with sequential elution by pure and mixed solvents in-depth fine fractionation of DOM can be carried out. Application of careful bulk, isotope and spectroscopic characterization in combination with comprehensive integrated data analysis will reveal highly improved understanding of DOM structures, evolution and functions in the environment.

2. These optimized separation and characterization protocols POP SPE should be adapted to different DOM materials like soil, freshwater, estuarine, marine and atmospheric DOM.

8.4 Advanced structure-related complementary analysis

The highlight of this thesis is the characterization of DOM by complementary high resolution organic structural spectroscopy (optical spectroscopy, 12T FT-ICR MS, 500 and 800 MHz NMR spectroscopy). With these highly resolving techniques, the compositional information of DOM can be revealed in great detail, especially after the sample complexity has been reduced by SPE. In order to make the best of the data information about DOM structures, complementary analysis is highly needed (Hertkorn et al. 2007). Mainly two directions of the structure-related complementary analysis can be addressed further.

1. Association of the three complementary aspects of structural information. The complex DOM samples produce data-rich spectra and complementary analysis will reveal critical

hidden relationships necessary for understanding of DOM structures and functions. For example, certain functional groups related to sp^2-hybridized carbon are related to the specific fluorescence peaks and are positioned in specific sections of mass spectra-derived van Krevelen diagrams and NMR spectra.

2. Correlation of these structure-related DOM characteristics with multiple connected data sets such as environmental parameters, biological activities and genetic fingerprints (Lucas et al 2016, Osterholtz et al. 2016, Traving et al. 2016). Recent endeavours of combining data from experimental conditions, spectroscopic characterization, metagenomics and metatranscriptomics in the field of metabolomics can be adapted to environmental samples to reveal the functioning of "the boundless carbon cycle" (Battin 2009).

8.5 References

Battin, T.J., Luyssaert, S., Kaplan, L.A., Aufdenkampe, A.K., Richter, A. and Tranvik, L.J. (2009) The boundless carbon cycle. Nat Geosci 2(9), 598-600.

Flerus, R., Koch, B.P., Schmitt-Kopplin, P., Witt, M. and Kattner, G. (2011) Molecular level investigation of reactions between dissolved organic matter and extraction solvents using FT-ICR MS. Mar Chem 124(1-4), 100-107.

Hertkorn, N., Ruecker, C., Meringer, M., Gugisch, R., Frommberger, M., Perdue, E.M., Witt, M. and Schmitt-Kopplin, P. (2007). High-precision frequency measurements: indispensable tools at the core of the molecular-level analysis of complex systems. Anal Bioanal Chem 389(5), 1311-1327.

Li, Y., Harir, M., Lucio, M., Kanawati, B., Smirnov, K., Flerus, R., Koch, B.P., Schmitt-Kopplin, P. and Hertkorn, N. (2016a) Proposed Guidelines for Solid Phase Extraction of Suwannee River Dissolved Organic Matter. Anal Chem 88(13), 6680-6688.

Li, Y., Harir, M., Lucio, M., Gonsior, M., Koch, B. P., Schmitt-Kopplin, P., Hertkorn, N. (2016b) Comprehensive structure-selective characterization of dissolved organic matter by reducing molecular complexity and increasing analytical dimensions. Water Res 106, 477-487.

Lucus, J., Koester, I., Wichels, A., Niggemann, J., Dittmar, T., Callies, U., Wiltshire, K.H. and Gerdts G. (2016). Short-term dynamics of North Sea bacterioplankton – dissolved organic matter coherence on molecular level. Front Microbiol 7, 321.

McIntyre, C. and McRae, C. (2005) Proposed guidelines for sample preparation and ESI-MS analysis of humic substances to avoid self-esterification. Org Geochem 36(4), 543-553.

Murphy, K.R., Stedmon, C.A., Graeber, D. and Bro, R. (2013) Fluorescence spectroscopy and multi-way techniques. PARAFAC. Anal Meth 5(23), 6557.

Osterholz, H., Singer, G., Wemheuer, B., Daniel, R., Simon, M., Niggemann, J. and Dittmar, T. (2016) Deciphering associations between dissolved organic molecules and bacterial communities in a pelagic marine system. ISME J 10(7), 1717-1730.

Traving, S.J., Bentzon-Tilia, M., Knudsen-Leerbeck, H., Mantikci, M., Hansen, J.L.S., Stedmon, C.A., Sørensen, H., Markager, S. and Riemann, L. (2016) Coupling bacterioplankton populations and environment to community function in coastal temperate waters. Front Microbiol 7, 1533.

Zhang, F., Harir, M., Moritz, F., Zhang, J., Witting, M., Wu, Y., Schmitt-Kopplin, P., Fekete, A., Gaspar, A. and Hertkorn, N. (2014) Molecular and structural characterization of dissolved organic matter during and post cyanobacterial bloom in Taihu by combination of NMR spectroscopy and FTICR mass spectrometry. Water Res 57, 280-294.

9 Appendix

9.1   Appendix 1: Supplementary Information for Chapter 6

Supplementary Information for

Chapter 6

Published as: *Yan Li, Mourad Harir, Jenny Uhl, Basem Kanawati, Marianna Lucio, Kirill Smirnov, Boris P. Koch, Philippe Schmitt-Kopplin, Norbert Hertkorn (2016). How Representative are dissolved organic matter (DOM) extracts? A comprehensive study of sorbent selectivity for DOM isolation. Water Research. Under revision. (Electronic supplementary material, published online). Reproduced with permission from Water Research. © Copyright Elsevier.*

Table S1. Properties of SPE sorbents

sorbent	category	functional group	Size (mg)	carbon loading (%)	mean pore size (Å)	particle size (μm) and shape	end-capped
2OH	polar	diol/silica based	100	6.8	60	40, irregular	no
C1	very weakly non-polar	methyl/silica based	100	4.1	60	40, irregular	yes
C2	weakly non-polar	ethyl/silica based	100	5.6	60	40& 120, irregular	yes
C8	moderately non-polar	octyl/silica based	100	12.2	60	40& 120, irregular	yes
C18	strongly non-polar	trifunctional octadecyl/silica based	100	17.4	60	40 & 120, irregular	yes
C18OH	moderately non-polar, significant polar interactions	octadecyl/silica based	100	14.9	150	40 & 120, irregular	no
CBA	mid-polar, weak cation exchange	carboxylic acid/silica based	100	7.4	60	40, irregular	yes
CH	moderately non-polar	cyclohexyl/silica based	100	9.6	60	40 & 120, irregular	yes
CN-E	medium polar, weak non-polar	cyanopropyl/silica based	100	8.1	60	40-120, irregular	yes
CN-U	medium polar, weak non-polar	cyanopropyl/silica based	100	7.8	60	40-120, irregular	no
DPA-6S	reversed phase (polar)	polyamide/polymer	100	n.a.		50-160	-
ENV	non-polar	styrene divinybenzene/polymer	100	n.a.	450	125, spherical	-
HLB	non-polar	divinylbenzene/polymer, N-vinylpyrrolidone	60	n.a.	80	30	-
MAX	mixed mode, strong anion exchange	divinylbenzene, CH_2NR_3, poly(divinylbenzene-co-N-vinylpyrrolidone)	60	n.a.	80	30	-
MCX	mixed mode, strong cation exchange	divinylbenzene, sulfonic acid group, poly(divinylbenzene-co-N-vinylpyrrolidone)	60	n.a.	80	30	-
NH2	polar, weak anion exchange	aminopropyl/silica based	100	6.7	60	40, irregular	no
PH	moderately non-polar	phenyl/silica based	100	10.7	60	40-120, irregular	yes
PPL	non-polar	functionalized styrene divinybenzene	100	n.a.	150	125, spherical	yes
SAX	strong anion exchange	trimethylaminopropyl/silica based	100	7.5	60	40, irregular	no
SCX	strong cation exchange	benzenesulfonic acid/silica based	100	10.9	60	40-120, irregular	no
SI	strongly polar	native silica/silica based	100	n.a.	60	40, irregular	no
Strata™-X-C	mixed mode, strong cation exchange	sulfonic acid/polymer	100	n.a.	n.a.	33	-
WAX	mixed mode, weak anion exchange	divinylbenzene	60	n.a.	80	30	-
WCX	mixed mode, weak cation exchange	divinylbenzene,	60	n.a.	80	30	-

161

**Table S2.** Counts of mass peaks as computed from FT-ICR MS data of SR DOM extracts for singly charged ions.

SPE cartridges	CHO	CHOS	CHNO	CHNOS	Σ (*)	H_a [%]	C_a [%]	O_a [%]	N_a [%]	S_a [%]	H/C ratio	O/C ratio	average intensity	DBE_a	$(DBE/C)_a$	$(m/z)_a$
2OH	191	41	19	8	258	7.68	65.35	22.25	0.80	3.92	1.41	0.26	4471606	6.3	0.30	355.0
C1	920	46	79	13	1058	6.31	61.14	31.60	0.19	0.76	1.24	0.39	6244875	8.2	0.40	394.3
C2	887	56	95	11	1049	6.29	61.17	31.57	0.17	0.79	1.23	0.39	7082693	8.2	0.40	394.0
C8	1209	97	277	12	1595	5.76	59.02	34.53	0.21	0.48	1.17	0.44	8568421	8.5	0.44	393.0
C18	1368	142	373	11	1894	5.50	58.15	35.65	0.23	0.46	1.14	0.46	9701574	8.8	0.46	395.7
C18OH	1349	115	364	9	1837	5.49	57.88	35.92	0.25	0.45	1.14	0.47	9273357	8.6	0.46	390.0
CBA	1031	70	116	7	1224	6.20	60.84	32.11	0.16	0.70	1.22	0.40	6773088	8.3	0.41	395.4
CH	1191	84	244	9	1528	5.76	59.01	34.49	0.20	0.54	1.17	0.44	8455181	8.6	0.44	394.6
CN-E	660	36	25	11	732	6.63	63.08	28.74	0.23	1.31	1.26	0.34	4238305	8.1	0.39	388.9
CN-U	524	30	26	16	596	7.07	62.69	27.25	0.49	2.50	1.35	0.33	3664798	6.8	0.34	368.4
DPA-6S	1073	105	129	4	1311	5.74	58.32	34.82	0.56	0.55	1.18	0.45	7984887	8.8	0.46	391.7
ENV	1227	125	260	8	1620	5.50	58.21	35.62	0.21	0.46	1.13	0.46	8584892	9.3	0.49	388.8
HLB	1336	154	350	12	1852	5.42	57.57	36.32	0.22	0.47	1.13	0.47	9787625	8.7	0.46	388.1
MAX	1242	114	341	9	1706	5.55	57.62	36.12	0.23	0.48	1.16	0.47	10413927	8.4	0.45	387.6
MCX	1151	89	233	10	1483	5.88	59.26	34.04	0.20	0.62	1.19	0.43	8623018	8.3	0.43	388.5
NH2	31	32	13	5	81	8.43	67.28	19.20	1.19	3.90	1.50	0.21	2802192	5.3	0.26	341.3
PH	1135	89	235	8	1467	6.12	60.21	32.67	0.20	0.80	1.22	0.41	8323500	8.2	0.41	393.2
PPL	1335	179	366	9	1898	5.47	57.75	36.02	0.25	0.51	1.14	0.47	9201721	8.7	0.46	392.6
SAX	403	40	32	18	493	7.06	62.47	27.05	0.63	2.79	1.36	0.32	3715928	6.6	0.34	363.2
SCX	187	34	8	10	239	7.31	63.44	22.90	1.09	5.26	1.38	0.27	9151084	6.2	0.34	340.5
SI	367	43	24	9	443	7.25	62.91	26.40	0.53	2.90	1.38	0.31	3571828	6.5	0.33	364.9
Strata XC	1140	76	214	12	1442	5.97	59.82	33.41	0.23	0.57	1.20	0.42	7614210	8.2	0.43	384.6
WAX	1275	129	331	10	1745	5.40	57.18	36.74	0.23	0.45	1.13	0.48	9678118	8.6	0.46	390.2
WCX	1171	80	244	6	1501	5.89	59.15	34.17	0.22	0.57	1.20	0.43	8337589	8.2	0.43	387.4

(*) total number of assigned mass peaks

Table S3. Counts of mass peaks as computed from FT-ICR MS data of NS DOM extracts for singly charged ions.

| SPE cartridges	CHO	CHOS	CHNO	CHNOS	Σ (*)	H_a [%]	C_a [%]	O_a [%]	N_a [%]	S_a [%]	H/C ratio	O/C ratio	average intensity	DBE_a	$(DBE/C)_a$	$(m/z)_a$
2OH	132	72	64	18	286	8.57	64.94	20.28	1.56	4.65	1.58	0.23	5246668	4.5	0.22	341.1
C1	718	92	123	27	960	7.40	64.12	26.17	0.80	1.50	1.38	0.31	4774477	6.7	0.32	369.2
C2	900	127	303	19	1349	6.63	61.32	30.84	0.47	0.73	1.30	0.38	6077560	7.6	0.37	389.9
C8	1254	399	949	42	2644	6.14	58.98	33.03	0.95	0.91	1.25	0.42	8571800	7.8	0.41	386.7
C18	1274	458	1036	47	2815	6.01	58.47	33.58	1.00	0.93	1.23	0.43	9139953	7.8	0.42	386.8
C18OH	1309	435	993	38	2284	6.12	58.85	33.11	0.99	0.94	1.25	0.42	8528194	7.7	0.41	383.3
CBA	714	101	104	21	940	7.13	62.54	28.29	0.51	1.53	1.37	0.34	4755935	6.9	0.33	382.2
CH	1178	350	830	37	2395	6.16	59.31	32.95	0.80	0.78	1.25	0.42	8322768	7.9	0.41	391.4
CN-E	291	67	77	27	462	8.29	62.88	22.89	1.48	4.46	1.58	0.27	4442221	4.5	0.22	345.7
CN-U	280	87	68	21	456	8.35	62.11	23.47	1.10	4.97	1.61	0.28	4543800	4.0	0.20	342.3
DPA-6S	370	67	94	21	552	7.37	62.63	25.29	2.30	2.40	1.41	0.30	3656535	6.2	0.32	364.3
ENV	1169	390	929	35	2523	5.85	58.04	34.15	1.12	0.84	1.21	0.44	7642038	8.0	0.43	384.5
HLB	1231	461	1068	47	2807	5.74	57.50	34.53	1.26	0.97	1.20	0.45	8740834	8.0	0.44	382.6
MAX	1205	244	930	36	2415	5.91	58.66	33.91	0.91	0.61	1.21	0.43	8973866	8.1	0.43	384.9
MCX	1204	316	825	31	2376	6.05	58.93	33.31	0.87	0.84	1.23	0.42	8243136	7.8	0.42	381.0
NH2	35	40	23	14	112	7.51	62.42	21.36	2.16	6.55	1.44	0.26	3987440	5.9	0.30	358.0
PH	880	146	393	38	1457	6.49	61.34	30.58	0.75	0.84	1.27	0.37	5832630	7.8	0.39	386.8
PPL	1228	468	1121	69	2886	5.65	57.01	34.98	1.45	0.92	1.19	0.46	8391180	8.1	0.44	382.6
SAX	192	57	62	21	332	8.24	65.03	21.74	1.45	3.54	1.52	0.25	4110567	5.2	0.25	349.6
SCX	486	142	88	27	743	10.42	72.61	14.29	0.49	2.19	1.72	0.15	18280711	3.1	0.16	308.1
SI	45	28	36	23	132	7.48	60.18	23.29	2.57	6.48	1.49	0.29	3523599	5.7	0.28	360.9
Strata XC	1200	239	696	26	2161	6.30	60.31	31.77	0.84	0.79	1.25	0.40	7380022	7.6	0.40	373.4
WAX	889	127	523	26	1565	6.02	59.06	33.25	0.88	0.79	1.22	0.42	6139175	7.9	0.42	379.4
WCX	1201	331	824	30	2386	6.05	59.17	33.10	0.85	0.82	1.23	0.42	8356873	7.9	0.42	381.9

(*) total number of assigned mass peaks
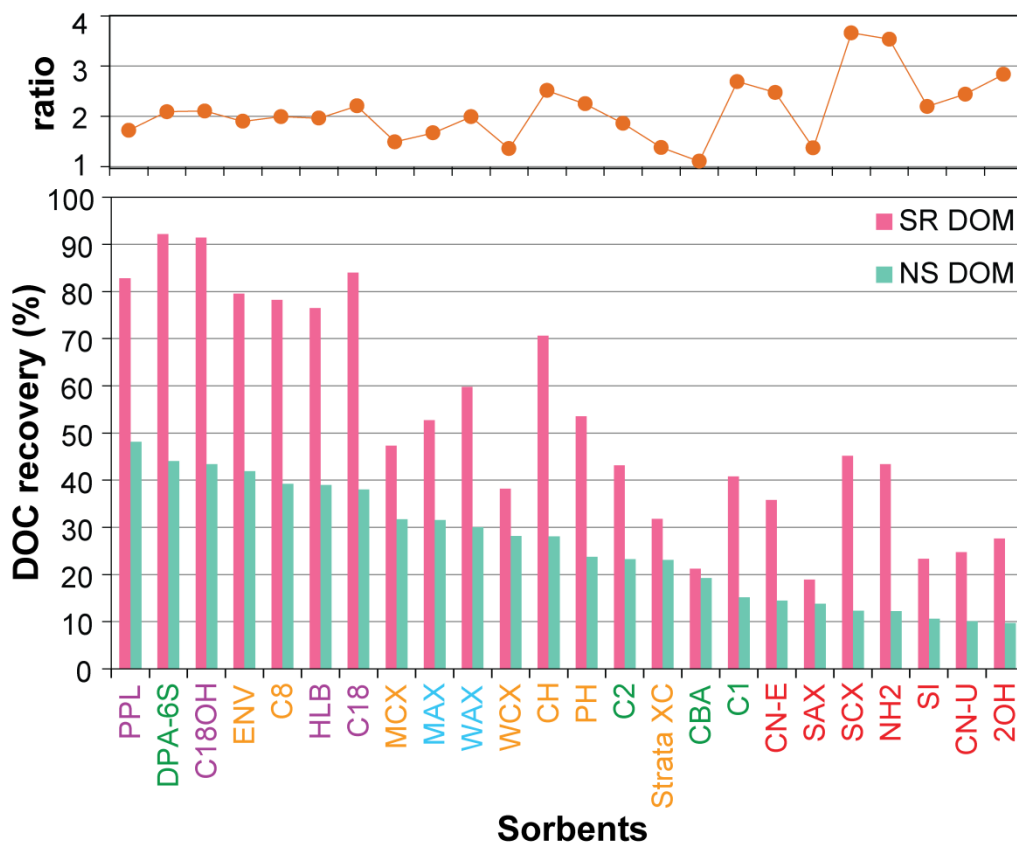
Figure S1. DOC recoveries of DOM extracts obtained with 24 commercially available sorbents. The ratio was calculated with DOC recovery of SR DOM/ DOC recovery of NS DOM. Purple: non-polar; blue: mixed mode with anion exchange; orange: moderately non-polar and mixed mode with cation exchange; green: weakly non-polar and mid-polar; red: polar and strong ion exchange.

Table S4. ^{1}H NMR (800 MHz, CD$_3$OD, 283K) section integrals of SR DOM and NS DOM.

| δ(^{1}H) [ppm]	key substructures	SR DOM	NS DOM
10.0 - 7.0 ppm	C$_{ar}$**H**	5.1	3.2
7.0 - 5.1 ppm	=C**H**, O$_2$C**H**	5.6	3.0
4.9 - 3.1 ppm	OC**H**	25.8	27.2
3.1 - 1.9 ppm	OCC**H**	33.3	28.8
1.9 - 0.5 ppm	CCC**H**	30.2	37.8
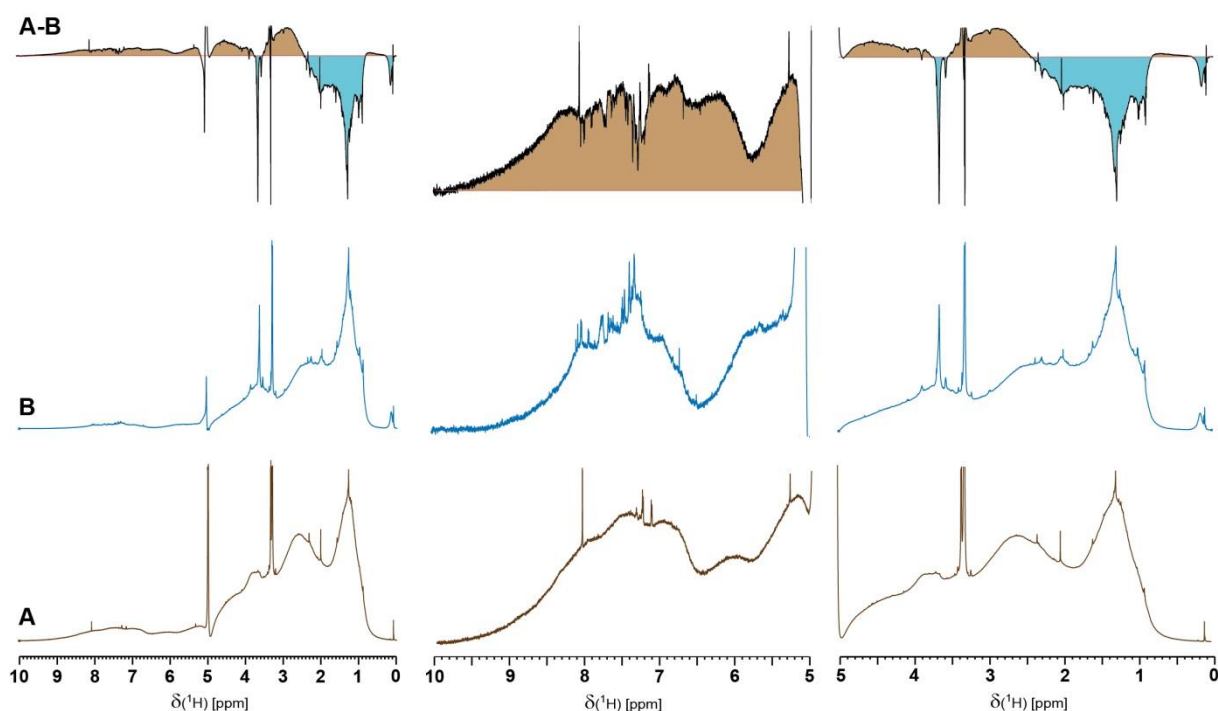
Figure S2. ^{1}H NMR spectra (800 MHz, CD$_3$OD, 283K) of (panel A) Suwannee River DOM (SR DOM) and (panel B) North Sea DOM (NS DOM), together with (panel A-B) manual difference NMR spectrum [up (brown color): SR DOM > NS DOM; down (blue color) NS DOM > SR DOM].

As shown by NMR section integrals (Table S4) and difference NMR spectra, NS DOM showed higher aliphaticity than SR DOM whereas unsaturated chemical environments (C$_{sp2}$**H**) were comparatively less abundant in NS DOM. This referred to all chemical environments in the chemical shift range $\delta_H \sim$ 10 – 5 ppm, i.e. aromatic and olefin protons as well as O$_2$C**H** units. Non-functionalized ($\delta_H <$ 1.9 ppm) as well as aliphatic carboxylic acids ($\delta_H \sim$ 2.1-2.4 ppm) were comparatively more common in NS DOM, whereas typical CRAM ($\delta_H >$ 2.4 ppm) were more prevalent in SR DOM, indicating more abundant aromatic carboxylic acids. The rather sharp NMR resonance at $\delta_H \sim$ 3.7 ppm in NS DOM may have resulted from scavenging of reactive CHOS compounds by methanol, forming aliphatic methyl esters.
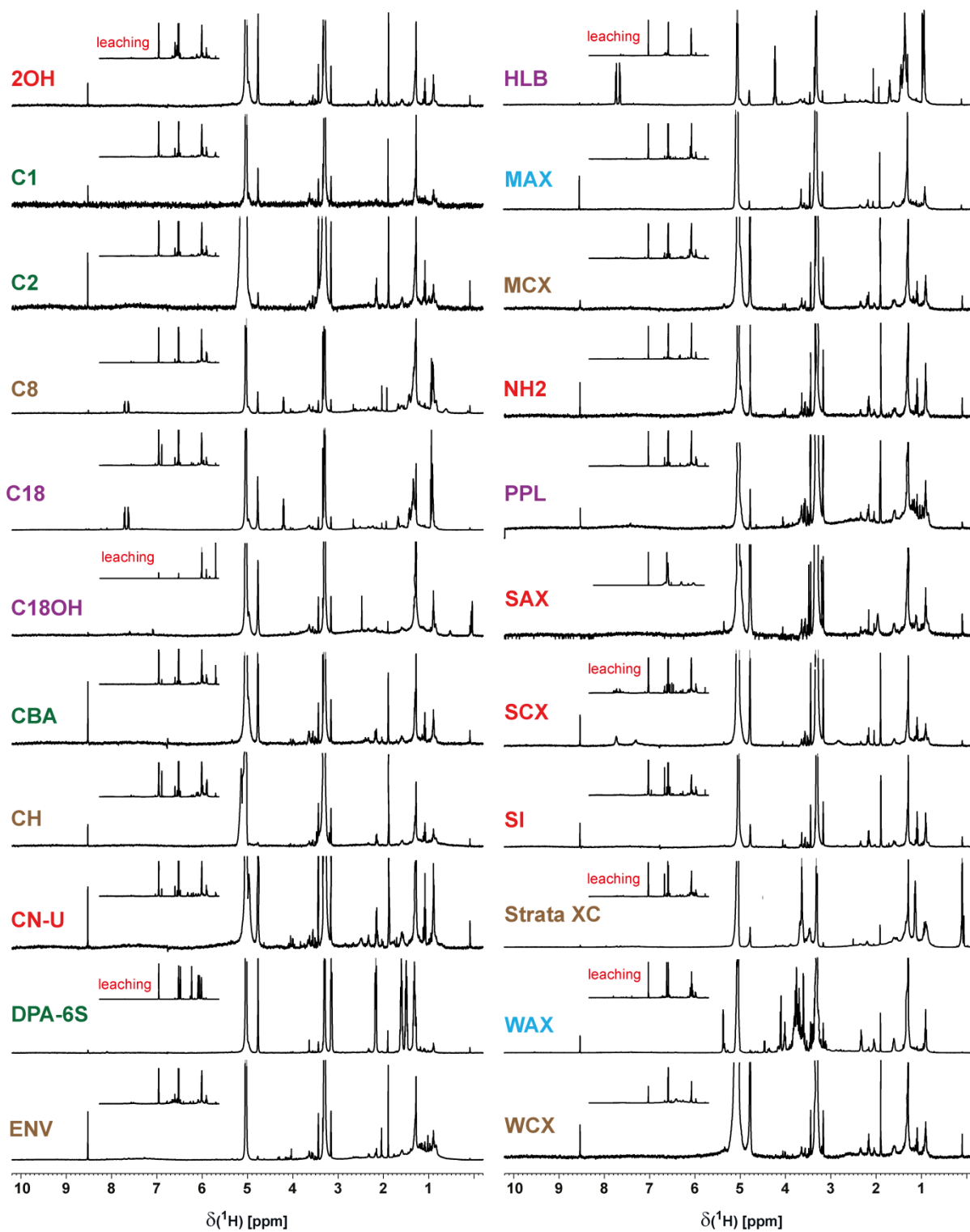
Figure S3. ^{1}H NMR spectra (500 MHz, CD$_3$OD) of SR SPE-DOM extracts obtained with different cartridges. The spectra of blanks were shown on the left of each extract.
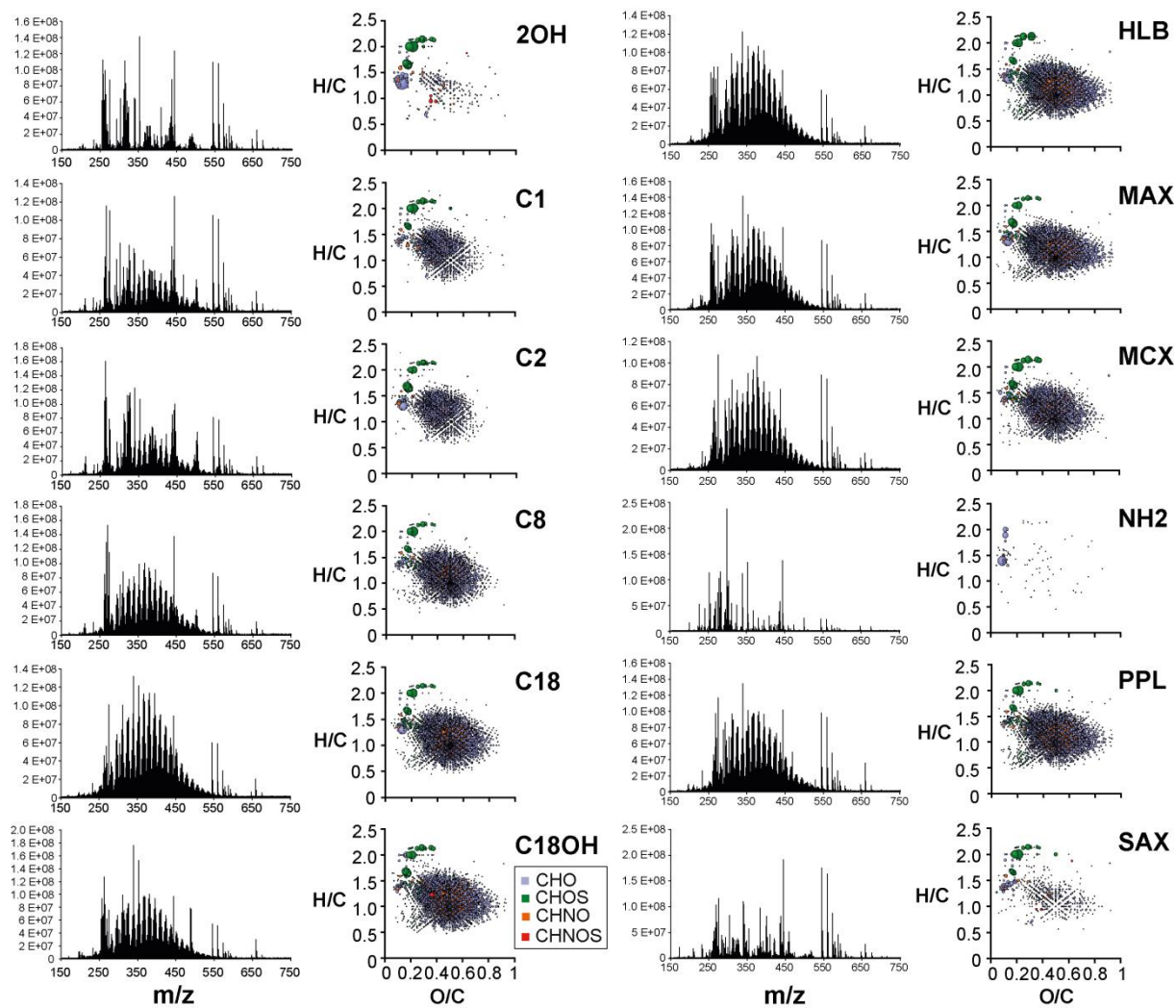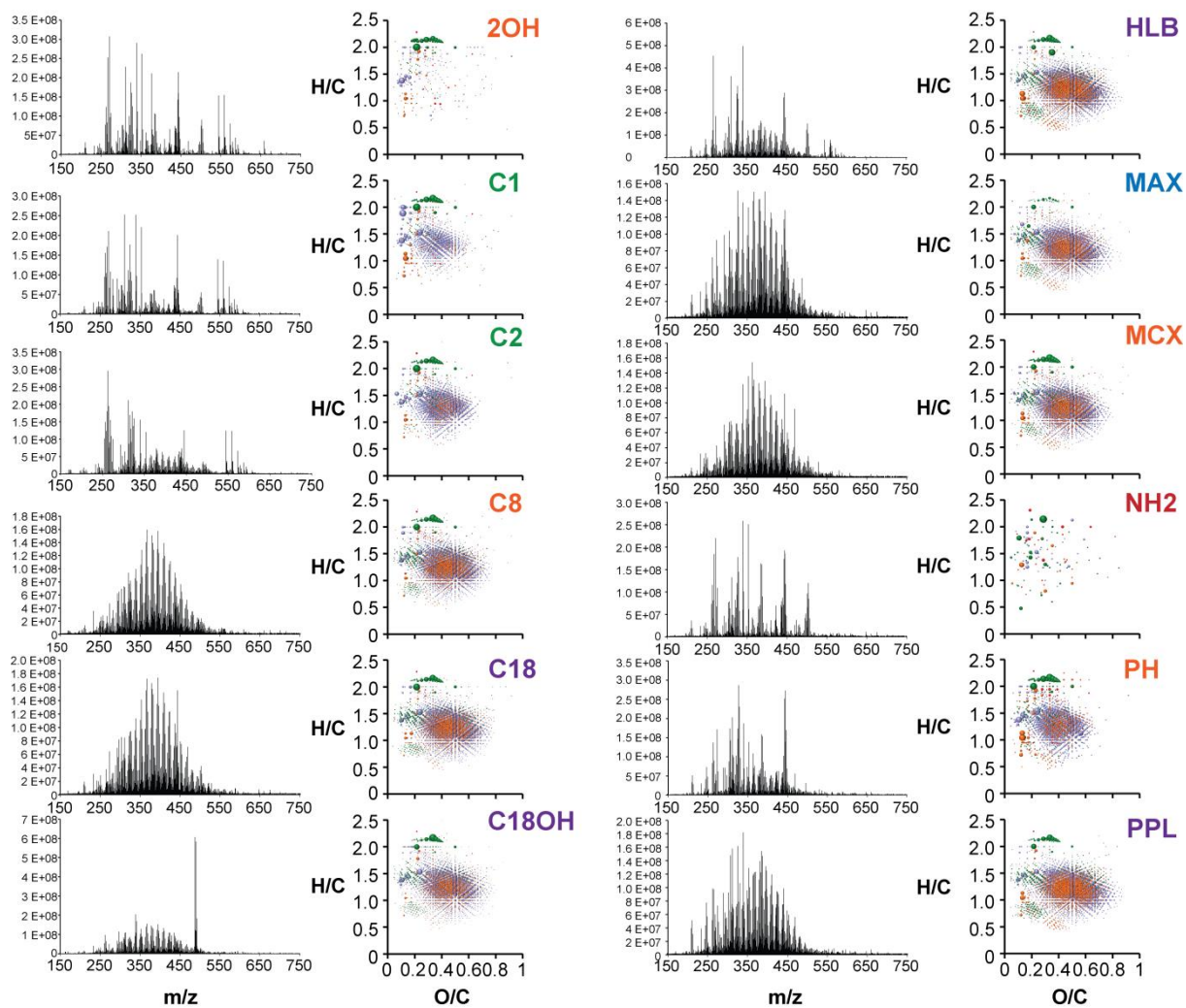
Figure S4. Negative ESI FT-ICR mass spectra (left) and (right) van Krevelen diagrams of SR SPE-DOM extracts obtained with different cartridges. Purple: non-polar; blue: mixed mode with anion exchange; orange: moderately non-polar and mixed mode with cation exchange; green: weakly non-polar and mid-polar; red: polar and strong ion exchange.
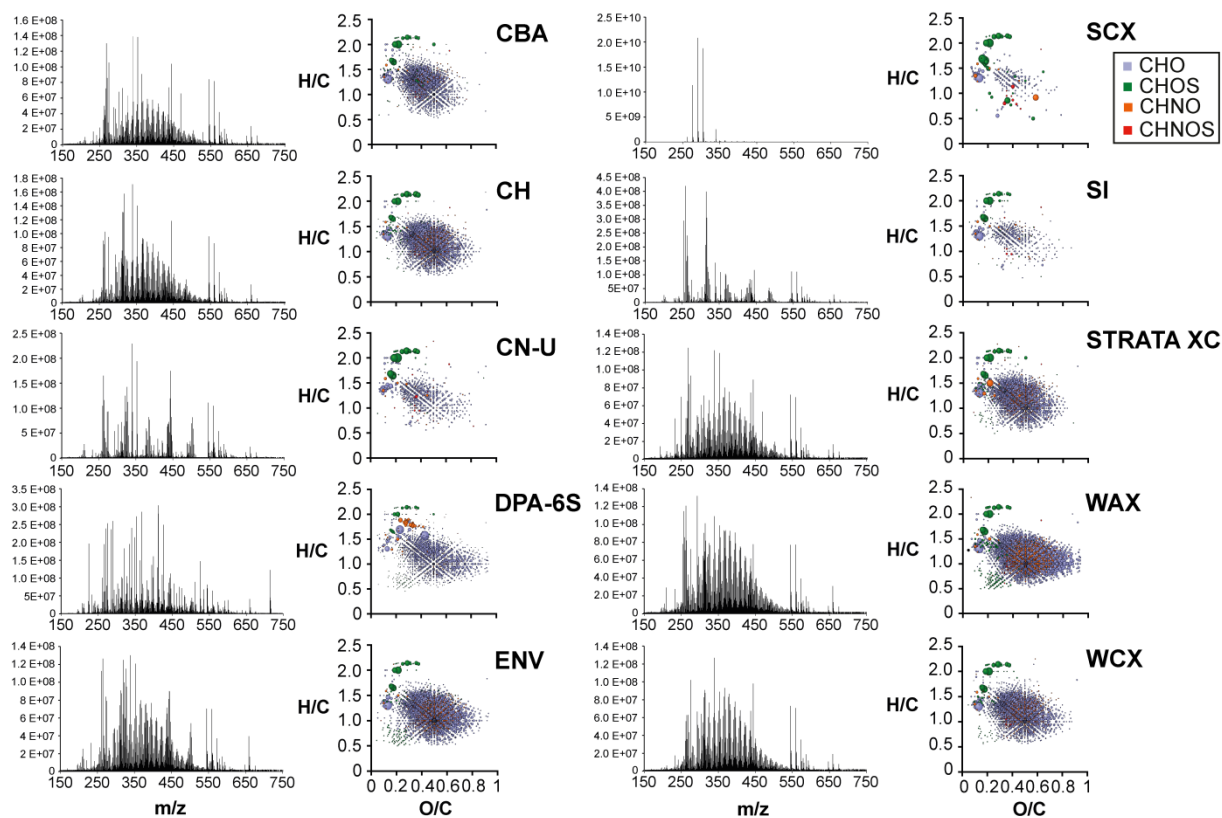
Figure S5. Negative ESI FT-ICR mass spectra (left) and (right) van Krevelen diagrams of SR SPE-DOM extracts obtained with different cartridges. Purple: non-polar; blue: mixed mode with anion exchange; orange: moderately non-polar and mixed mode with cation exchange; green: weekly non-polar and mid-polar; red: polar and strong ion exchange.
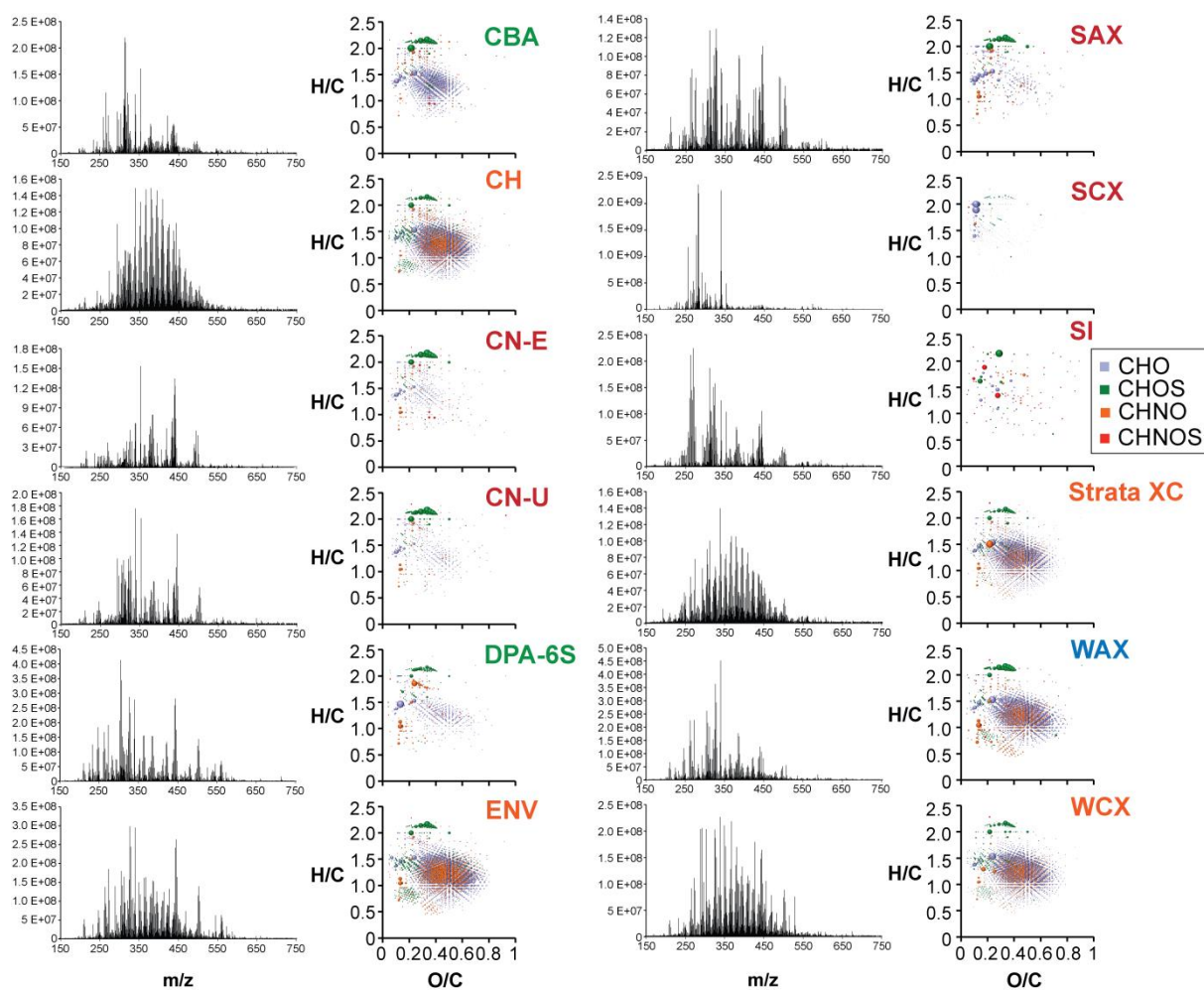
Figure S6. Negative ESI FT-ICR mass spectra (left) and (right) van Krevelen diagrams of NS SPE-DOM extracts obtained with different cartridges. Purple: non-polar; blue: mixed mode with anion exchange; orange: moderately non-polar and mixed mode with cation exchange; green: weakly non-polar and mid-polar; red: polar and strong ion exchange.
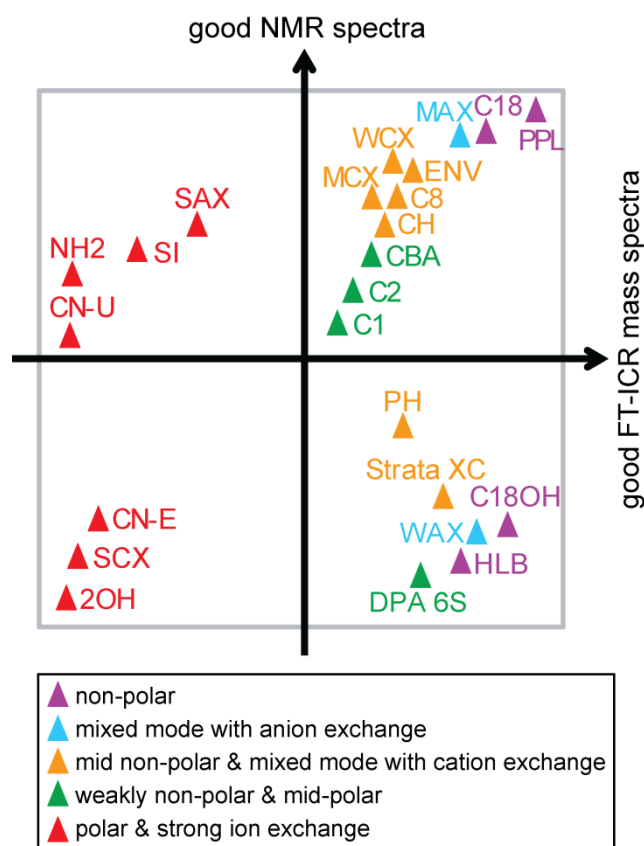
Figure S7. Negative ESI FT-ICR mass spectra (left) and (right) van Krevelen diagrams of NS SPE-DOM extracts obtained with different cartridges. Purple: non-polar; blue: mixed mode with anion exchange; orange: moderately non-polar and mixed mode with cation exchange; green: weekly non-polar and mid-polar; red: polar and strong ion exchange.

Figure S8. Quality assessment of solid-phase extraction (SPE) as deduced from FT-ICR mass spectra (horizontal axis: count of assigned molecular formulas and absence of obvious leachate molecules) and NMR spectra (vertical axis: proportions of leachate molecules). The first quadrant presents SPE sorbents with both satisfactory FT-ICR mass spectra and NMR spectra; the second quadrant presents the sorbents with few signals in FT-ICR mass spectra and virtual absence of leaching behavior in NMR spectra; the third quadrant presents sorbents with FT-ICR mass spectra and NMR spectra dominated by leachate molecules; the fourth quadrant presents the sorbents with inconspicuous FT-ICR mass spectra but leaching behavior in NMR spectra.

171

9.2   Appendix 2: Author contributions to Chapter 6

Yan Li, Mourad Harir, Philippe Schmitt-Kopplin and Norbert Hertkorn designed the experiment;

Jenny Uhl conducted the experiment, measured on FT-ICR MS. Yan Li analysed the FT-ICR mass spectra with the help of Mourad Harir and Basem Kanawati, and Yan Li measured on NMR with the help of Norbert Hertkorn;

Marianna Lucio and Kirill Smirnov helped to evaluate the data;

Boris P. Koch measured DOC and gave great inputs on paper correction;

Yan Li wrote the paper together with Mourad Harir and Norbert Hertkorn with great contributions from Boris P. Koch and Philippe Schmitt-Kopplin.

9.3 Appendix 3: Author contributions to Chapter 7

Yan Li, Mourad Harir, Philippe Schmitt-Kopplin and Norbert Hertkorn designed the experiment;

Yan Li conducted the experiment, measured on FT-ICR MS with the help of Mourad Harir and on NMR with the help of Norbert Hertkorn;

Michael Gonsior measured on fluorescence spectroscopy;

Boris P. Koch measured DOC and gave insightful inputs;

Yan Li wrote the paper together with Mourad Harir and Norbert Hertkorn with great contributions from Boris P. Koch and Philippe Schmitt-Kopplin.

10 Curriculum Vitae

Persönliche Daten	
Name	Yan Li
Geschlecht	Weiblich
Staatsangehörigkeit	Chinesisch
Geburtsdatum	26. Juni 1987
Geburtsort	Changzhou, Jiangsu, VR China
E-Mail	liyan6280890@gmail.com
Telefonnummer	017661432448
Anschrift	Kaulbachstr. 25 80539, München Deutschland
Aktuelle Beschäftigung	Doktorandin

Ausbildung	
09. 2012 – 12.2016	Doktorandin am Helmholtz Zentrum München (betreut durch Dr. Norbert Hertkorn) und an der Technischen Universität München (Doktor-Vater: Prof. Dr. Philippe Schmitt-Kopplin), finanziert durch ein Stipendium des China Scholarship Council Doktorarbeit: „Comprehensive characterization of dissolved organic matter by using chemical fractionation and high resolution organic structural spectroscopy"
09. 2009 - 03. 2012	Studium der Pharmazeutischen Ingenieurwissenschaften zur Erlangung des Diploms (MS) an der "East China University of Science and Technology (ECUST), Shanghai"
09. 2011 - 01 2012	Diplomarbeit: „Catalytic wet air oxidation of selected antibiotics in water and wastewater" (ECUST)
06. 2010 - 09. 2010	Forschungsaufenthalt am Institut für Ökologische Chemie, Helmholtz Zentrum München, Neuherberg, Deutschland
09. 2005 - 06. 2009	Studium der Pharmazeutischen Ingenieur an der Changzhou University, Jiangsu, China zur Erlangung von Bachelor of Science

Forschungsinteressen
Umfassende Charakterisierung von natürlicher organischer Materie (NOM) mittels hochauflösender chemischer Fraktionierung und organischer Strukturspektroskopie, wie Massenspektrometrie, NMR und Fluoreszenz-Spektroskopie. Aufklärung von NOM-Prozessierung in verschiedenen Ökosystemen; Erweiterung durch Einbeziehung von stabilen und Radioisotopen ist höchst wünschenswert.

Wissenschaftliches Profil
• Trennmethoden: Festphasenextraktion (SPE), Flüssigkeitschromatographie (GC), Größenausschlußchromatographie (SEC)
• Massenspektrometrie: LC-MS, GC-MS and FT-ICR MS
• Hochauflösende NMR Spectroskopie: ^1H, ^{13}C, DEPT ^{13}C, 2D NMR (JRES, COSY, TOCSY, HSQC, DEPT HSQC)
• Statistische Datenauswertung komplementärer komplexer Daten
Fähigkeiten
• Sprachen: Chinesisch (Muttersprache), Englisch (fließend), Deutsch (B1)
• Software: R, MATLAB
Preise und Auszeichnungen
2014 Reisestipendium zum Tagungsbesuch 17th International Humic Substances Society (IHSS) Konferenz, Ioannina, Griechenland
Publikationen
• <u>Yan Li</u>, Mourad Harir, Marianna Lucio, Basem Kanawati, Kirill Smirnov, Ruth Flerus, Boris P. Koch, Philippe Schmitt-Kopplin, Norbert Hertkorn (2016). Proposed guidelines for solid phase extraction of Suwannee River dissolved organic matter. *Analytical Chemistry* (88), 6680-6688.
• <u>Yan Li</u>, Mourad Harir, Marianna Lucio, Michael Gonsior, Boris P. Koch, Philippe Schmitt-Kopplin, Norbert Hertkorn (2016). Comprehensive structure-selective characterization of dissolved organic matter by reducing molecular complexity and increasing analytical dimensions. *Water Research* (106), 477-487.
• Chloé Roullier-Gall, Daniel Hemmler, Michael Gonsior, <u>Yan Li</u>, Maria, Nikolantonaki, Alissa Aron, Christian Coelho, Philippe Schmitt-Kopplin, Regis Gougeon (2017). Sulfites and the wine sulfur metabolome. *Food Chemistry* (237), 106-113.
• <u>Yan Li</u>, Mourad Harir, Jenny Uhl, Basem Kanawati, Boris P. Koch, Philippe Schmitt-Kopplin, Norbert Hertkorn (2017). How Representative are dissolved organic matter (DOM) extracts? A comprehensive study of sorbent selectivity for DOM isolation. *Water Research* (116), 316-323.
• <u>Yan Li</u>, Mourad Harir, Basem Kanawati, Michael Gonsior, Boris P. Koch, Philippe Schmitt-Kopplin, Norbert Hertkorn (2017). Insight into dissolved organic matter composition and structure by phase-optimized solid phase extraction (POP SPE). *Analytical Chemistry*. Wird eingereicht.
• <u>Yan Li</u>, Feifang Zhang, Xinmiao Liang, Ayfer Yediler (2013). Chemical and toxicological evaluation of an emerging pollutant (enrofloxacin) by catalytic wet air oxidation and ozonation in aqueous solution. *Chemosphere* (90), 284-291.
• Hongyue Guo, Changhu Chu, <u>Yan Li</u>, Bingcheng Yang, Xinmiao Liang (2011). A novel silica based click lysine anion exchanger for ion exchange chromatography. *Analyst*, 136, 5302-5307.
• <u>Yan Li</u>, Jiangping Gu, Kejun Zhang, Qing Du, Feifang Zhang, Xinmiao Liang (2011). Catalytic wet oxidation of formaldehyde by Cu/TiO_2. *Technology of Wastewater Treatment* (In Chinese).
• Xinmiao Liang, Feifang Zhang, Yapu Li, <u>Yan Li</u> (2011). Catalytic Hydrodebromination of DecaBDE (BDE-209) in ethanol over Pd/TiO_2 catalyst. 201110329369.3. (Patent)

Konferenzen
• Poster: Proposed Guidelines for Solid Phase Extraction (SPE) of Suwannee River Dissolved Organic Matter (SR DOM), 2015, ASLO Aquatic Science Meeting, Granada, Spanien.
• Weiterbildungskurs: Parallel Factor Analysis (PARAFAC), 2015, NOM6 (6th Specialist Conference on Natural Organic Matter in Drinking Water), Malmö, Schweden.
• Vortrag: Study of pH Effect on Solid Phase Extraction (SPE) of Suwannee River Dissolved Organic Matter (SR DOM), 2014, International Humic Substances Society (IHSS), 17. Internationale Konferenz: Natural Organic Matter: Structure, Dynamics, Innovative Applications, Ioannina, Griechenland.
• Poster: Study of pH Effect on Solid Phase Extraction (SPE) of Suwannee River Dissolved Organic Matter (SR DOM), 2014, International Humic Substances Society (IHSS), 17. Internationale Konferenz: Natural Organic Matter: Structure, Dynamics, Innovative Applications, Ioannina, Griechenland.

Zusätzliche wissenschaftliche Erfahrung		
•	06. 2016	Laboraustausch, Prof. Dr. Rudolf Jaffe, Florida International University (Miami) *Größenausschlußchromatographie von DOM*
•	05. 2016	User Summer School in National High Magnetic Field Lab (Tallahassee)
•	02. 2016	Laboraustausch, Dr. Peter Herzsprung, Helmholtz Zentrum für Umweltforschung (UFZ Magdeburg) *Fluoreszenz-Spektroskopie von DOM inclusive Auswerteverfahren*
•	10. 2015	Laboraustausch, Prof. Dr. Boris Koch, Alfred-Wegener-Institut (AWI) Bremerhaven, Helmholtz Zentrum für Polar und Meeresforschung, *Fraktionierung von Meerwasser-DOM*
•	05. 2014	Laborbesuch, Prof. Dr. Stefan Peiffer, Universität Bayreuth, *Umfassende Charakterisierung von DOM in Moorgebieten assoziiert mit Fe- und S-bezogenen Redoxgradienten*